August, 1981

LIDS-TH-1129

Research Supported By:

NASA Grant NGL-22-009-124
DOE Contract DE-AC01-78RA03395

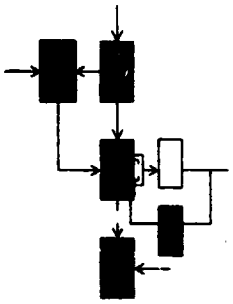

ON REGULATORS WITH A PRESCRIBED DEGREE OF STABILITY

Peng-Teng Peter Ng

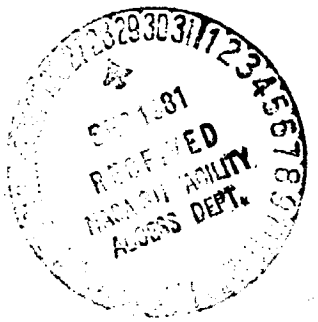

Laboratory for Information and Decision Systems

MASSACHUSETTS INSTITUTE OF TECHNOLOGY, CAMBRIDGE, MASSACHUSETTS

ON REGULATORS WITH A PRESCRIBED DEGREE OF STABILITY

by

PENG-TENG PETER NG

B.S. Massachusetts Institute of Technology
(1979)

SUBMITTED IN PARTIAL FULFILLMENT
OF THE REQUIREMENTS FOR THE
DEGREE OF

MASTER OF SCIENCE

at the

MASSACHUSETTS INSTITUTE OF TECHNOLOGY

July 1981

Signature of Author _____
Department of Electrical Engineering and
Computer Science, July 31, 1981

Certified by Michael Athans
Michael Athans
Thesis Supervisor

Certified by _____
Bernard C. Levy
Thesis Supervisor

Accepted by _____
Arthur C. Smith
Chairman, Departmental Committee on Graduate Students

ON REGULATORS WITH A PRESCRIBED DEGREE OF STABILITY

by

PENG-TENG PETER NG

Submitted to the Department of Electrical Engineering and Computer Science on July 31, 1981 in partial fulfillment of the requirements for the Degree of Master of Science

ABSTRACT

Several important aspects of the Regulator with a Prescribed Degree of Stability (RPDS) methodology and its applications are considered. The solution of the time-varying RPDS problem as well as the characterization of RPDS closed-loop eigenstructure properties are obtained. Based on the asymptotic behavior of RPDS root-loci, a novel one-step algorithm for designing Regulators with Prescribed Damping Ratio (RPDR) is developed. The robustness properties of RPDS are characterized in terms of the properties of the return difference and the inverse return difference matrices for the RPDS state feedback loop. This class of regulators is found to possess excellent multi-loop margins with respect to stability and degree of stability properties. The ability of RPDS design to tolerate changing operating conditions and unmodelled dynamics are also illustrated with a multi-terminal DC/AC power system example. The output feedback realization of RPDS requires the use of Linear-Quadratic-Gaussian (LQG) methodology. Several interesting issues that arise in the application of robustness recovery procedures to the design of RPDS based LQG compensators are also examined.

Thesis Supervisor: Dr. Michael Athans

Title: Professor of Systems Science and Engineering

Thesis Supervisor: Dr. Bernard C. Levy

Title: Assistant Professor of Electrical Engineering

ACKNOWLEDGEMENTS

It is my pleasure to express my sincere gratitude to Professors Michael Athans and Bernard C. Levy for their supervision of this thesis. Professor Athan's patience in training me to become a creative researcher is most appreciated - not to mention his tolerance of my undisciplined working habits. Professor Levy deserves special thanks for his enthusiasm in my education. The many hours that he spent with me in going through the technical details of my research is gratefully acknowledged. My appreciation also goes to my fellow graduate students at L.I.D.S. for their contribution to my learning experience during the past two years. Norman A. Lehtomaki is to be thanked for teaching me many facts about robustness theory. I am also indebted to Sherman M. Chan for his timely help in my programming effort.

Beyond the technical support, my graduate education was very much enriched by personal interactions with my fellow Christian brothers and sisters --- too many to mention by name. In particular, I wish to mention Chris Law, Alex Hui, Ser-Aik Quek, Ching Lau, Gloria Chyen and Juliet Wong for their warm friendship, understanding and moral supports.

Last but not the least, I wish to say thanks to all members of my family, particularly my parents, Mr. and Mrs. Ng Tee-Peng. Without their unfailing encouragement, the completion of this work would have been impossible.

This research was conducted at the M.I.T. Laboratory for Information and Decision Systems with support provided by the U.S. Department of Energy under

DEDICATION TO MY GRANDMOTHER

Madam Wong Yu-Yook

and in remembrance of my grandfather

Mr. Yap Lee-Poh

TABLE OF CONTENTS

LIST OF FIGURES

CHAPTER I

INTRODUCTION

1.1 Thesis Motivation

A linear time-invariant (LTI) system of the form

$$\dot{\underline{x}}(t) = \underline{A}\,\underline{x}(t) \tag{1.1}$$

is said to have a degree of stability α if all the poles of $\underline{A}$ are located to the left of the line $\sigma = -\alpha$ (where α is real and positive) in the left-half complex plane (see Figure 1.1). The Regulator with a Prescribed Degree of Stability (RPDS) problem is one of determining the weighting matrices $\underline{Q}$ and $\underline{R}$ in the cost functional of a Linear Quadratic (LQ) regulator problem.

$$\min_{\underline{u}(t)} \lim_{t_1 \to \infty} \int_{t_o}^{t_1} [\underline{x}^T(t)\,\underline{Q}\,\underline{x}(t) + \underline{u}^T(t)\,\underline{R}\,\underline{u}(t)]dt \tag{1.2}$$

subject to the dynamic constraint

$$\dot{\underline{x}}(t) = \underline{A}\,\underline{x}(t) + \underline{B}\,\underline{u}(t) \tag{1.3}$$

so that the resulting state feedback design has a prescribed degree of stability.

The RPDS problem for LTI systems was first formulated and solved by Anderson and Moore [An 1]; their work is one of the many attempts to combine the poleplacement techniques and LQ methodology in some useful fashion. Other major contributions in this area include the asymptotic LQ poleplacement technique of Harvey and Stein [Ha 1] and the sequential poleplacement method of Solheim [So 1]. Both of these methods address

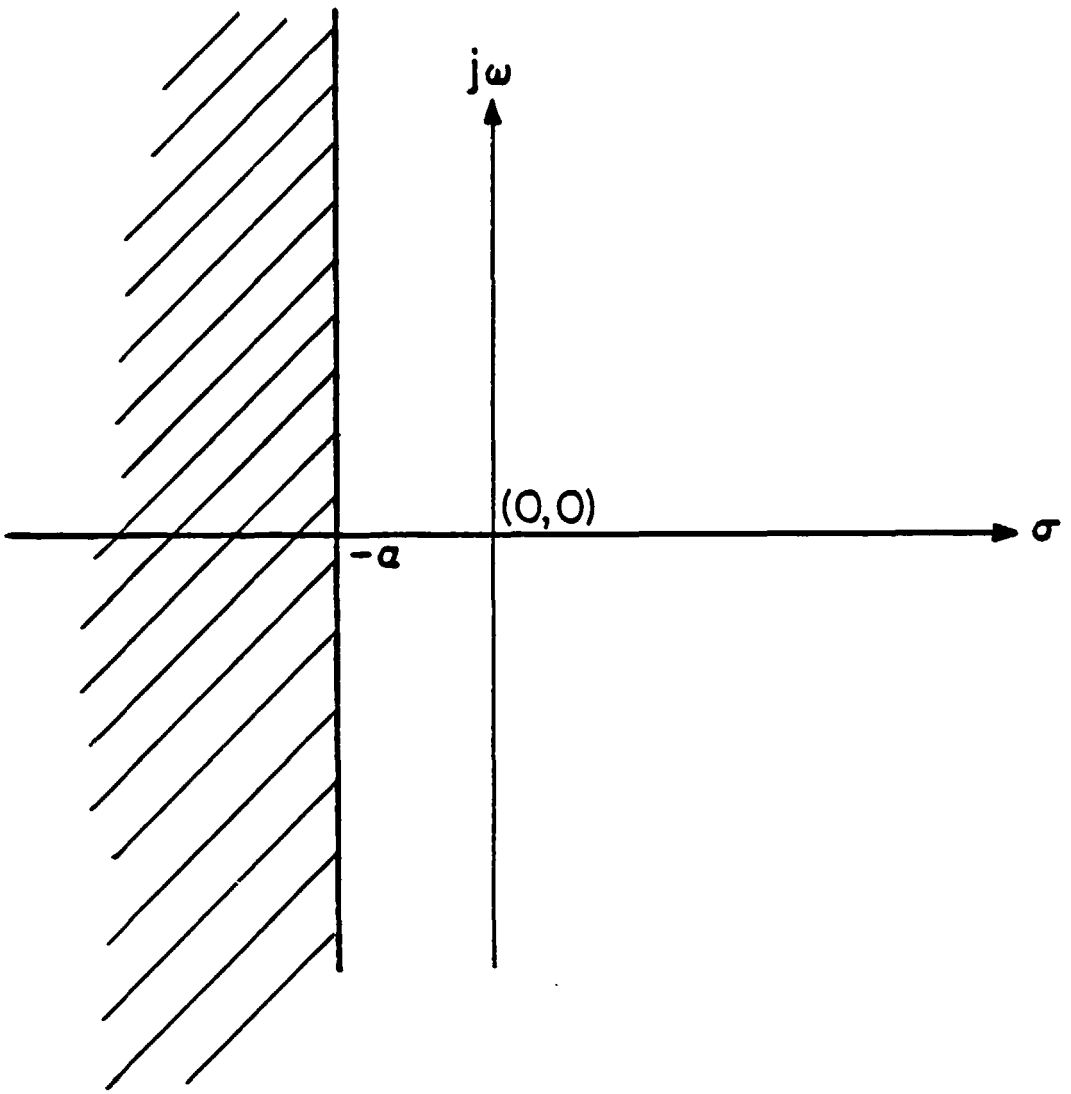

FIG. 1.1 Region (shaded) of Allowable Closed-Loop Poles for a RPDS Design with Stability Factor Equals to α . ($\alpha > 0$)

the problem of finding the appropriate $\underline{Q}$ and $\underline{R}$ matrices that correspond to a prescribed set of eigenvalues.

The RPDS problem is useful from the application point of view. In many engineering problems of interest, the exact position of the closed-loop poles may be of secondary importance. As a result, the designers are interested only in locating all the closed-loop poles in some regions of the left-half complex plane.

One such example which motivates the research in this thesis is the design of a state feedback law for a reduced order model of a m-terminal DC/AC power system([Gr 1], [Ch 1]). This is the preliminary stage of design for a decentralized output feedback control scheme. A standard power system model of this type, with n aggregated areas, has (2n-2) modes of iterarea oscillations[1]. Such modes are usually poorly damped in the absence of compensation. The two remaining modes are real. The one located at the origin is the clock error mode. The one located slightly to the left of the origin is the average frequency mode. For physical reasons, it is desirable for both of these modes to remain unchanged under state feedback. This could be trivially accomplished in the LQ design by making such modes unobservable in the cost functional.[2] The primary design objective is to find a state feedback control law that results in sufficient damping for the (2n-2) oscillatory modes. One natural way to specify the damping criterion is simply to require all the

---

[1] See Figure 5.1 of Section 5.1 for an example of such pole configuration

[2] A detailed discussion of such a poleplacement technique is given in Section 5.2

closed-loop poles to lie to the left of some line $\sigma = -\alpha$ in the complex plane. This class of problem can be effectively handled using non-asymptotic LQ poleplacement techniques such as RPDS and Solheim's method [So 1]. With respect to the computational requirements, RPDS is the simpler of the two methods. In every design iteration using RPDS method, one needs to solve a Riccati equation and an eigenvalue problem. In the case of Solheim's method, one may have to solve as many as n Riccati equations and n eigenvalue problems for each iteration. Although the above mentioned design objective can also be handled by asymptotic techniques such as Harvey/Stein's method [Ha 1] with relative ease; the use of which in the multiterminal DC/AC power system is however inappropriate. From an engineering point of view, it is undesirable to speed up some of the oscillatory modes as required by the asymptotic poleplacement method in order to allow the poles of the remaining modes to approach their specified locations.

Despite the potential usefulness of RPDS as evidenced in the above discussion, research on this class of regulators has been largely overlooked in the literature. Apart from a few brief remarks found in the original work of Anderson and Moore [An 1], little is known to date about the relation between the prescribed degree of stability and the feedback properties of a RPDS system. This is partly a result of the lack of appropriate tools for effective analysis of multivariable feedback systems. It is only recently, in the context of studying the robustness properties of controllers derived using Linear-Quadratic-Guassian (LQG) technique that an appropriate formulation has emerged ([Le 1], [Do 4]). One major objective of this thesis is therefore to analyze the feedback

properties of RPDS with special emphasis on robustness properties.

Another important problem of interest here is the possible application of RPDS to the design of LQ regulators with specifications other than prescribed degree of stability. One such example is the design of regulators with prescribed damping ratio (RPDR). This class of LQ regulators has all its poles lying inside a convex cone centered at the origin and symmetric about the negative real axis (see Fig. 1.2). Such designs are of potential application in the power system example mentioned above.

It is hoped that the new insights on properties of RPDS obtained in this thesis will help the control system designers to better appreciate the benefits that they may expect from this class of regulators.

1.2 Thesis Organization

This thesis is organized as follows:

In Chapter II we first formulate and solve the generalized RPDS problem for linear time-varying systems. A precise notion of degree of stability that applies to all finite dimensional linear system is introduced for this purpose. We then specialize these results to the time-invariant case which was the original form of RPDS problem addressed by Anderson and Moore. Extension of RPDS techniques to the dual problem of designing a Kalman Bucy filter with a prescribed degree of stability (FPDS) is also considered, and interpretations of the FPDS design procedure in the context of estimation are given.

In Chapter III, the eigenstructure properties of time-invariant RPDS are examined. We first derive some sensitivity formulas for the closed-

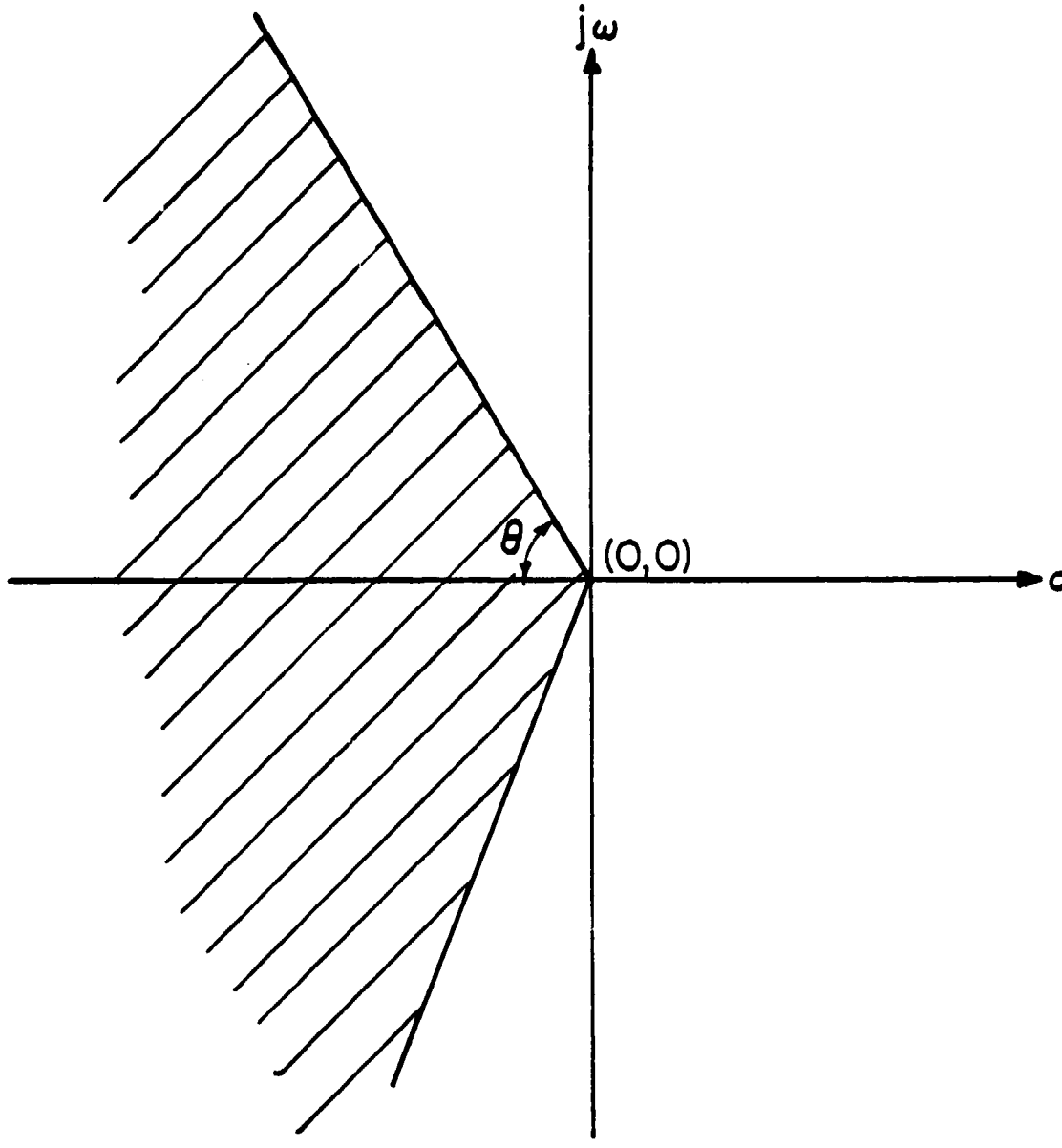

FIG. 1.2 Region (shaded) of Allowable Closed-Loop Poles for a Regulator with a Prescribed Damping Ratio $\cos\theta$ $(0 < \theta < \frac{\pi}{2})$

loop poles with respect to the stability factor α . This is followed by a study of the behavior of RPDS root-loci as the relative weight between the state and control weightings varies. It turns out that this problem can be formulated in a fashion similar to the conventional LQ root-locus problem [Kw 1]. The control weighting matrix is chosen to be of the form $\rho\underline{R}$. The relative weight between the state and control weightings can be adjusted by varying the scalar ρ . We are particularly interested in the asymptotic behavior of the root-loci as $\rho(\rho > 0)$ becomes very large or close to 0. Based on the asymptotic properties of the RPDS root-loci as ρ approaches infinity, a novel algorithm for solving the regulator with prescribed damping ratio problem is derived.

The robustness properties of RPDS are discussed in Chapter IV. Adopting the framework developed in [Do 2] and [Le 1], we use the minimum singular value of the return difference and the inverse return difference matrices as basic robustness measures for multiple-input multiple-output (MIMO) feedback systems. The dependence of the robustness properties on the stability factor α is analyzed by using the frequency domain inequalities for the RPDS return difference and inverse return difference matrices. The dual robustness problem for FPDS is next formulated, and the FPDS robustness properties are interpreted in the context of estimation.

In Chapter V, we consider an example where the RPDS technique is used to design a state feedback control law for a reduced order model of a multi-terminal DC/AC power system. Besides validating theorems and conjectures stated in previous chapters, the results obtained here also reveal several desirable features of RPDS designs not predicted by the theorems developed in this thesis. This provides considerable justification

for the use of RPDS methodology in power systems control.

Since full state feedback can never be realized in real life, we are thus motivated to study the feedback properties of RPDS based LQG compensators in which the feedback gain is designed by using the RPDS technique and where a KBF is used to provide the state estimates. This problem is considered in Chapter VI. LQG compensators are known to possess no guaranteed uncertainty tolerance in general [Do 4]. As a result, we only focus our discussion in this thesis on the class of RPDS based LQG compensators that are designed with the robustness recovery procedures ([Do 1] and [Kw 1]). Such procedures allow one to approximate the state feedback transfer matrix (and consequently their robustness properties) with the LQG loop-transfer matrix in a systematic manner. Several difficulties encountered in attempts to combine the RPDS technique and robustness recovery methods in designing LQG compensators are illustrated with numerical examples.

Chapter 7 consists of conclusions and suggested directions for future research.

1.3 Contributions of This Thesis

The major contributions of this research are:

(1) Formulation and solution of the time-varying RPDS problem.

(2) Development of a simple procedure for studying the asymptotic behavior of the RPDS root-loci.

(3) Development of a novel algorithm for solving the regulator with prescribed damping ratio problem.

(4) Clarifying the robustness properties of RPDS

(5) Uncovering some potential problems that one may encounter in combining the RPDS technique with robustness recovery methods in designing LQG compensators.

1.4 Notation

SISO	single-input single-output
MIMO	multiple-input multiple-output
LQ	liner-quadratic
LQG	linear-quadratic Guassian
KBF	Kalman Bucy filter
RPDS	regulators with a prescribed degree of stability
FPDS	Kalman Bucy filter with a prescribed degree of stability
LTI	linear time-invariant
$\underline{T}(s)$	loop transfer matrix
$\underline{T}_\alpha(s)$	loop transfer matrix for RPDS with a degree of stability α
$\underline{F}_\alpha(s)$	loop transfer matrix for FPDS with a degree of stability α
$\underline{L}(s)$	multiplicative perturbation of $\underline{T}(s)$ or $\underline{T}_\alpha(s)$
$\lambda(\underline{A})$	an eigenvalue of $\underline{A}$
$\underline{A}^H$	complex conjugate transpose of $\underline{A}$
$\sigma_{max}(\underline{A})$	maximum singular value of $\underline{A} \triangleq \lambda_{max}^{\frac{1}{2}}(\underline{A}^H \underline{A})$
$\sigma_{min}(\underline{A})$	minumum singular value of $\underline{A} \triangleq \lambda_{min}^{\frac{1}{2}}(\underline{A}^H \underline{A})$
$\triangleq$	defined as
$\underline{A} > \underline{B}$	$\underline{A} - \underline{B}$ is a positive definite matrix
$\underline{A} \geq \underline{B}$	$\underline{A} - \underline{B}$ is a positive semi-definite matrix
$\underline{I}$	Identity matrix

CHAPTER II

THE REGULATOR WITH A PRESCRIBED DEGREE OF STABILITY PROBLEM AND ITS DUAL

2.1 Introduction

In this chapter, we formulate and solve the RPDS problem for finite dimensional linear system. By 'linear systems' we mean a pair of equations of the form

$$\dot{\underline{x}}(t) = \underline{A}(t)\,\underline{x}(t) + \underline{B}(t)\,\underline{u}(t) \tag{2.1}$$

$$\underline{y}(t) = \underline{C}(t)\,\underline{x}(t) \tag{2.2}$$

We make an assumption at this point that is to hold throughout this chapter. The elements of the matrix $\underline{A}(t)$ are continuous and bounded functions of time defined on $-\infty < t < \infty$. The elements of the matrices $\underline{B}(t)$ and $\underline{C}(t)$ are piecewise continuous and bounded functions defined on $-\infty<t<\infty$.

The formulation and solution of the time-varying RPDS problem is given in section 2.3. In order to study this problem, a precise definition for 'degree of stability' that applies to both time-varying and time-invariant systems is introduced. The time-invariant version of the RPDS problem studied by Anderson and Moore [An 1] becomes a special case of our formulation.

The problem of designing Kalman Bucy Filter with a prescribed degree of stability (FPDS) is considered in Section 2.4. In view of the dual nature between the Kalman Bucy Filter problem and the LQ regulator problem, the design techniques for RPDS can be readily applied to FPDS. Several

interpretations of the formulation and solution of the FPDS problem are given.

2.2 Degree of Stability for Linear Systems

The concept of 'Degree of Stability' for linear time-invariant (LTI) systems is directly related to the system pole locations.

Definition 2.1 An autonomous system $\dot{\underline{x}}(t) = \underline{A}\,\underline{x}(t)$ is said to possess a degree of stability α, for some real positive constant α, if all the eigenvalues of $\underline{A}$ are located to the left of the line $\sigma = -\alpha$ in the left-half complex plane.

Intuitively speaking, a LTI system with a degree of stability α will attenuate any given initial state perturbation at a rate faster than or equal to $e^{-\alpha t}$. To motivate the extension of such concepts to the time-varying case, let us first recall the following definition of exponential stability for finite dimensional linear system.

Definition 2.2 ([Br 1]), Section 29)

The system $\dot{\underline{x}}(t) = \underline{A}(t)\,\underline{x}(t)$ is said to be exponentially stable if there exists some positive constants γ and λ, such that for all t and t_o in the half plane $t \geq t_o$, we have

$$|\underline{\phi}(t,t_o)| \leq \gamma e^{-\lambda(t-t_o)} \tag{2.3}$$

where

$$\dot{\underline{\phi}}(t,t_o) = \underline{A}(t)\,\underline{\phi}(t,t_o) \tag{2.4}$$

and

$$\underline{\phi}(t_o,t_o) = \underline{I} \tag{2.5}$$

It is well known that the exponential stability of LTI systems can be easily established by checking the pole locations of the system matrix. The following theorem clarifies the relationship between the poles of a LTI system $\dot{\underline{x}}(t) = \underline{A}\,\underline{x}(t)$ and the induced norm[1] of the respective transition matrix $e^{\underline{A}t}$.

Theorem 2.1 Consider the autonomous system

$$\dot{\underline{x}}(t) = \underline{A}\,\underline{x}(t) \tag{2.6}$$

Let α be some given positive constant. Then

$$\max_i \left(\mathrm{Re}(\lambda_i(\underline{A}))\right) < -\alpha \tag{2.7}$$

if and only if there exists a positive constant γ such that

$$\|e^{\underline{A}(t-t_o)}\| < \gamma\, e^{-\alpha(t-t_o)} \qquad \text{for all } t \geq t_o \tag{2.8}$$

Proof: Sufficiency: Suppose that (2.8) is true for some positive γ and a given α. Observe that $e^{\max_i R_e(\lambda_i(\underline{A}))\,(t-t_o)}$ is the spectral radius of $e^{\underline{A}(t-t_o)}$. Using the fact that the spectral radius of a matrix is always less than or equal to its spectral norm, we get

$$\begin{aligned} & e^{\max_i R_e(\lambda_i(\underline{A})\,(t-t_o))} \\ \leq\ & \|e^{\underline{A}(t-t_o)}\| \\ <\ & \gamma e^{-\alpha(t-t_o)} . \end{aligned} \tag{2.9}$$

Since the inequality (2.9) holds if and only if

---

[1] All the vector norms considered here are the Euclidean norm. The corresponding induced norm is the 2-matrix norm (See(De 1]).

$$\max_i \ \mathrm{Re}(\lambda_i(\underline{A})) < -\alpha \quad , \tag{2.10}$$

this completes the proof of sufficiency.

Necessity: Suppose that $\max_i(\mathrm{Re}(\lambda_i(\underline{A})) < -\alpha$. We can find a similarity transformation that reduces $\underline{A}$ to its Jordan form $\underline{A}_j = \underline{P}\,\underline{A}\,\underline{P}^{-1}$ ([B 1] Section 12). For system in Jordan Form, the transition matrix is block diagonal with each of the nonzero element being one of the three forms

$$t^k e^{\sigma t} \cos \omega t, \quad t^k e^{\sigma t} \sin \omega t \quad \text{or} \quad t^k e^{\lambda t} \tag{2.11}$$

where $\sigma \pm j\omega$ and λ are eigenvalues of $\underline{A}$. It follows from our assumption on the eigenvalues of $\underline{A}$ that each element of $e^{\underline{A}jt}$ approaches 0 at a rate faster than $e^{-\alpha t}$ as t approaches infinity.

This in turn implies the existence of some positive constant $\hat{\gamma}$ such that

$$|| e^{\underline{A}_j(t-t_o)} || \leq \hat{\gamma} e^{-\alpha(t-t_o)} \tag{2.12}$$

Since $\underline{A} = \underline{P}^{-1} A_j \underline{P}$, it follows that

$$\begin{aligned} &||e^{\underline{A}(t-t_o)}|| \\ &\quad ||\underline{P}^{-1} e^{\underline{A}_j(t-t_o)} \underline{P}|| \\ &\leq \ ||\underline{P}^{-1}||\ ||e^{\underline{A}_j(t-t_o)}||\ ||\underline{P}|| \\ &\leq \ \hat{\gamma}\ ||\underline{P}^{-1}||\ ||\underline{P}||\ e^{-\alpha(t-t_o)} \quad . \end{aligned} \tag{2.13}$$

This completes the proof of necessity.

Corollary 2.1 The autonomous system (2.6) has a degree of stability α if and only if there exists a positive constant γ such that for all $t \geq t_o$

$$||e^{\underline{A}(t-t_o)}|| \leq \gamma\, e^{-\alpha(t-t_o)} \tag{2.14}$$

Proof: This is a trivial consequence of Definition 2.1 and Theorem 2.1.

It seems natural from the result of Corollary 2.1 that we should define the stability of a linear system $\dot{\underline{x}}(t) = \underline{A}(t)\,\underline{x}(t)$ in terms of the norm of its transition matrix.

Definition 2.3

A linear system $\dot{\underline{x}}(t) = \underline{A}(t)\,\underline{x}(t)$ is said to have a degree of stability α if there exists some positive constants γ such that for all $t \geq t_o$,

$$||\underline{\phi}(t,t_o)|| \leq \gamma\, e^{-\alpha(t-t_o)} \tag{2.15}$$

The following theorem characterizes the degree of stability using Lyapunov's Direct Method.

Theorem 2.2 Let $V(\underline{x}(t),t)$ be a Lyapunov function of the form $V(\underline{x}(t),t) = \underline{x}^T(t)\,\underline{Q}\,\underline{x}(t)$ for $\dot{\underline{x}}(t) = \underline{A}(t)\,\underline{x}(t)$ on the whole state space. If for some constant $\varepsilon > 0$,

$$\underline{Q}(t) \geq \varepsilon\,\underline{I} \qquad \text{for all } t \geq t_o, \tag{2.16}$$

then the system described by $\dot{\underline{x}}(t) = \underline{A}(t)\,\underline{x}(t)$ has a degree of stability α if for all $t \geq t_o$,

$$\dot{V}(\underline{x}(t),t) \leq -2\alpha\, V(\underline{x}(t),t) \tag{2.17}$$

Proof: It follows from (2.17) that $V(\underline{x}(t),t)$ is bounded above by $e^{-2\alpha(t-t_o)}\, V(\underline{x}(t_o)t_o)$. Since $V(\underline{x}(t),t) \geq \epsilon\, ||\underline{x}(t)||^2$ this means that

$$||\underline{x}(t)|| \leq \left(\frac{1}{\epsilon}\, V(\underline{x}(t_o),t_o)\right)^{\frac{1}{2}} e^{-\alpha(t-t_o)} \tag{2.18}$$

Dividing both sides of (2.18) by $||\underline{x}(t_o)||$ and taking the supremum on the right, we obtain

$$\frac{||\underline{x}(t)||}{||\underline{x}(t_o)||} \leq \left(\frac{1}{\epsilon}\, \lambda\max\, (\underline{Q}(t_o))\right)^{\frac{1}{2}} e^{-\alpha(t-t_o)} \tag{2.19}$$

Now, by taking the supremum on the left side of (2.19), we obtain

$$||\underline{\phi}(t,t_o)|| \leq \left(\frac{1}{\epsilon}\, \lambda\max\, (\underline{Q}(t_o))\right)^{\frac{1}{2}} e^{-\alpha(t-t_o)} \tag{2.20}$$

which establishes the degree of stability.

Remark In situations such as designing feedback laws with optimal control methods where a Lyapunov function is available, Theorem 2.2 provides a convenient mean of evaluating the degree of stability for a feedback design. This point will be made clear in Theorem 2.4.

2.3 Formulation and Solution of the Continuous Time RPDS Problem

In this section, we formulate the RPDS problem for finite dimensional linear systems. Although the RPDS problem studied by Anderson and Moore is a special case of that considered in this thesis, their solution of time-invariant problem extends readily to time-varying case.

2.2.1 The RPDS Problem Statement

Consider the following LQ regulator problem

$$\min_{\underline{u}(t)} \quad J = \lim_{t_1 \to \infty} \int_{t_o}^{t_1} \underline{x}^T(t)\, \underline{Q}(t)\, \underline{x}(t) + \underline{u}^T(t)\, \underline{R}(t)\, \underline{u}(t)\, dt \tag{2.21}$$

subject to the dynamic constraint

$$\dot{\underline{x}}(t) = \underline{A}(t)\, \underline{x}(t) + \underline{B}(t)\, \underline{u}(t) \tag{2.22}$$

$$\underline{x}(t_o) = \underline{x}_o \tag{2.23}$$

where $(\underline{A}(t), \underline{B}(t))$ is uniformly completely controllable.

The RPDS problem is to find the appropriate weighting matrices $\underline{Q}(t)$ and $\underline{R}(t)$ such that the steady state control law that minimizes the cost functional (2.21) has a degree of stability α.

2.2.2 Solution of the RPDS Problem

The solution of the RPDS problem is given in the following theorem.

Theorem 2.3 Consider the deterministic LQ regulator problem in Section 2.2.1. The weighting matrices are chosen as

$$\underline{Q}(t) = \tilde{\underline{Q}}\, e^{2\alpha t} \tag{2.24}$$

$$\underline{R}(t) = \tilde{\underline{R}}\, e^{2\alpha t} \tag{2.25}$$

where $\tilde{\underline{Q}}(t)\, e^{2\alpha t}$ and $\tilde{\underline{R}}(t)\, e^{2\alpha t}$ are piecewise continuous and bounded on $[t_o, \infty]$ with

$$\tilde{\underline{Q}}(t) \geq \beta_1 \underline{I} \quad \text{and} \quad \tilde{\underline{R}}(t) \geq \beta_2 \underline{I} \qquad \text{for all } t \tag{2.26}$$

where β_1 and β_2 are some positive constants. Furthermore, $(\underline{Q}(t)^{\frac{1}{2}}, \underline{A}(t))$ is uniformly completely reconstructable. Then the solution $\tilde{\underline{K}}_\alpha(t)$ of the Riccati equation

$$-\dot{\underline{K}}_\alpha(t) = (\underline{A}(t) + \alpha\, \underline{I})^T\, \tilde{\underline{K}}_\alpha(t) + \tilde{\underline{K}}_\alpha(t)\, (\underline{A}(t) + \alpha\, \underline{I}) + \underline{Q}(t)$$
$$- \tilde{\underline{K}}_\alpha(t)\, \underline{B}(t)\, \underline{R}^{-1}(t)\, \underline{B}^T(t)\, \tilde{\underline{K}}_\alpha(t) \qquad (2.27)$$

with terminal condition $\tilde{\underline{K}}_\alpha(t_1) = \underline{K}_1$ converges to $\underline{K}_\alpha(t)$ as t_1 approaches ∞ for any $\underline{K}_1 \geq \underline{0}$ and the steady state optimal control law given by

$$\underline{u}(t) = -\underline{R}^{-1}(t)\, \underline{B}^T(t)\, \underline{K}_\alpha(t)\, \underline{x}(t) \qquad (2.28)$$

has a degree of stability α.

Proof: The assumptions on $\underline{A}(t)$, $\underline{B}(t)$, $\underline{Q}(t)$ and $\underline{R}(t)$ relating to continuity, boundedness, uniform complete controllability and uniform complete reconstructability guarantee the existence of an exponentially stable steady state optimal control law that minimizes the given cost functional. To establish the degree of stability of the control law, we introduce the following transformations

$$\tilde{\underline{x}}(t) \triangleq e^{\alpha(t-t_o)}\, \underline{x}(t) \qquad (2.29)$$

$$\tilde{\underline{u}}(t) \triangleq e^{\alpha(t-t_o)}\, \underline{u}(t) \qquad (2.30)$$

Then, $\tilde{\underline{x}}(t)$ and $\tilde{\underline{u}}(t)$ are related dynamically by

$$\dot{\tilde{\underline{x}}}(t) = \frac{d}{dt}\, (e^{\alpha(t-t_o)}\, \underline{x}(t)) \qquad (2.31)$$

$$= (\underline{A}(t) + \alpha\, \underline{I})\, \tilde{\underline{x}}(t) + \underline{B}(t)\, \tilde{\underline{u}}(t) \qquad (2.32)$$

The initial condition of $\tilde{\underline{x}}(t)$ is given by

$$\tilde{\underline{x}}(t_o) = \underline{x}_o \tag{2.33}$$

The cost functional J in (2.21) can now be written as

$$J = \lim_{t_1 \to \infty} \int_{t_o}^{t_1} [\tilde{\underline{x}}(t)^T \tilde{Q}(t) \tilde{\underline{x}}(t) + \tilde{\underline{u}}^T(t) \underline{R}(t) \tilde{\underline{u}}(t)]dt \tag{2.34}$$

Observe the strong connection between the transformed LQ regulator problem described by (2.32) and (2.34) and the original problem described by (2.21) and (2.22). Suppose that $\underline{u}^*(t)$ is the optimal control at time t for the original problem, then $\tilde{\underline{u}}^*(t) = e^{\alpha t} \underline{u}^*(t)$ is the value of the optimal control at time t for the transformed problem. The resulting value of the state $\tilde{\underline{x}}^*(t)$ is given by $\tilde{\underline{x}}^*(t) = e^{\alpha t} \underline{x}^*(t)$, provided that $\tilde{\underline{x}}^*(t_o) = e^{\alpha t_o} \underline{x}^*(t_o)$. Thus, a feedback control law obtained for the transformed problem readily yields a feedback control law for the original problem. Moreover, the resulting minimum value of the cost functional is the same for each problem.

Our next step is to study the transformed LQ regulator problem

$$\min_{\underline{u}(t)} J = \lim_{t_1 \to \infty} \int_{t_o}^{t_1} \left[\tilde{\underline{x}}^T(t) \tilde{Q}(t) \tilde{\underline{x}}(t) + \tilde{\underline{u}}^T(t) \tilde{R}(t) \tilde{\underline{u}}(t)\right]dt \tag{2.35}$$

subject to dynamic constraint

$$\dot{\tilde{\underline{x}}}(t) = (\underline{A}(t) + \alpha \underline{I}) \tilde{\underline{x}}(t) + \underline{B}(t) \tilde{\underline{u}}(t) \quad ; \quad \tilde{\underline{x}}(t_o) = \underline{x}_o \tag{2.36}$$

We need to check all the technical conditions that ensure the existence of an exponentially stable steady state optimal control law for the above optimization problem. It is trivial to see that $\underline{A}(t) + \alpha \underline{I}$ is bounded and continuous. Moreover, the piecewise continuity and

boundedness of $\underline{B}(t)$, $\tilde{\underline{Q}}(t)$ and $\tilde{\underline{R}}(t)$ follows from the assumption of the original LQ regulator problem. To guarantee the existence of an exponentially stable steady state control law, we also require the uniform complete reconstructability of $(\underline{Q}^{\frac{1}{2}}(t), \underline{A}(t) + \alpha \underline{I})$. The uniform complete controllability of $(\underline{A}(t) + \alpha \underline{I}, \underline{B}(t))$ follows from that of $(\underline{A}(t), \underline{B}(t))$ by observing the equivalence of the following four statements.[1]

(i) $(\underline{A}(t), \underline{B}(t))$ is uniformly completely controllable

(ii.) There exists some positive numbers $\sigma, \gamma_o, \gamma_1, \beta_o, \beta_1$ such that

$$\text{(a)}\quad \gamma_o \underline{I} \leq \int_{t_o}^{t_o+\sigma} \left[\underline{\phi}(t_o+\sigma,\tau)\underline{B}(\tau)\ \underline{B}^T(\tau)\ \phi^T(t_o+\sigma,\tau)\right]d\tau \leq \gamma_1 \underline{I} \tag{2.37}$$

$$\text{(b)}\quad \beta_o \underline{I} \leq \underline{\phi}(t_o,t_o+\sigma)\left[\int_{t_o}^{t_o+\sigma} \left[\underline{\phi}(t_o+\sigma,\tau)\ \underline{B}(\tau)\ \underline{B}^T(\tau)\ \underline{\phi}^T(t_o+\sigma,\tau)\right]d\tau\right]$$
$$\underline{\phi}^T(t_o,t_o+\sigma) \leq \beta_1 \underline{I} \qquad \text{for all } t_o \tag{2.38}$$

(iii) There exist some positive real numbers σ, γ_o, γ_1, β_o, β_1 such that

$$\text{(a)}\ \gamma_o \underline{I} \leq \int_{t_o}^{t_o+\sigma} \left[e^{\alpha(t_o+\sigma-\tau)}\underline{\phi}(t_o+\sigma,\tau)\ \underline{B}(\tau)\ \underline{B}^T(\tau)\ \phi^T(t_o+\sigma,\tau)\right.$$
$$\left. e^{\alpha(t_o+\sigma-\tau)}\right]d\tau \leq e^{2\alpha\sigma}\gamma_1 \underline{I} \qquad \text{for all } t_o \tag{2.39}$$

---

[1] Readers are referred to Chapter I of [Kw 1] for a detailed discussion on uniform complete controllability and uniform complete observability

$$\text{(b)}\quad e^{-2\alpha\sigma}\,\beta_o\,\underline{I} \le e^{-\alpha\sigma}\,\underline{\phi}(t_o,t_o+\sigma)\left[\int_{t_o}^{t_o+\sigma}\left[\underline{\phi}(t_o+\sigma,\tau)e^{\alpha(t_o+\sigma-\tau)}\,\underline{B}(\tau)\,\underline{B}^T(\tau)\,\underline{\phi}^T(t_o+\sigma,\tau)\,e^{\alpha(t_o+\sigma-\tau)}\right]d\tau\right]$$

$$\underline{\phi}^T(t_o,t_o+\sigma)\,e^{-\alpha\sigma} \le \beta_1\,\underline{I} \qquad \text{for all } t_o \tag{2.40}$$

(iv) $(\underline{A}(t)+\alpha\,\underline{I},\underline{B}(t))$ is uniformly completely controllable.

The equivalence between (iii) and (iv) follows from the observation that $\underline{\phi}(t,t_o)\,e^{\alpha(t-t_o)}$ is the state transition matrix of the system described by (2.32).

By duality, the uniform complete reconstructability of $(\underline{Q}^{\frac{1}{2}}(t),\,\underline{A}(t))$ also implies the uniform complete reconstructability of $(\underline{Q}^{\frac{1}{2}}(t),\underline{A}(t)+\alpha I)$.

Thus, it follows from Theorem 3.6 of [Kw 1] that $\tilde{\underline{K}}_\alpha(t)$, the solution of the Riccati Equation (2.27) with terminal condition $\tilde{\underline{K}}_\alpha(t_1)=\underline{K}_1$, converges to $\underline{K}_\alpha(t)$ as $t_1\to\infty$ for any $\underline{K}_1\ge 0$. Moreover, $\underline{K}_\alpha(t)$ is also a solution of (2.27). The resulting steady state optimal control law is given by

$$\tilde{\underline{u}}(t) = -\tilde{\underline{R}}^{-1}(t)\,\underline{B}^T(t)\,\underline{K}_\alpha(t)\,\tilde{\underline{x}}(t) \tag{2.41}$$

It follows from the uniform complete observability of $(\underline{Q}^{\frac{1}{2}}(t),\,\underline{A}(t)+\alpha I)$ that the closed-loop system

$$\dot{\tilde{\underline{x}}}(t) = (\underline{A}(t)+\alpha\underline{I}-\underline{B}(t)\,\tilde{\underline{R}}^{-1}(t)\,\underline{B}^T(t)\,\underline{K}_\alpha(t))\tilde{\underline{x}}(t) \tag{2.42}$$

is exponentially stable. Applying the feedback law (2.41) to the original system (2.22), we get

$$\dot{\underline{x}}(t) = (\underline{A}(t)-\underline{B}(t)\,\tilde{\underline{R}}^{-1}(t)\,\underline{B}^T(t)\,\underline{K}_\alpha(t))\underline{x}(t) \tag{2.43}$$

Let $\underline{\phi}_{c\alpha}(t,t_o)$ and $\underline{\phi}_c(t,t_o)$ be the state transition matrices of systems (2.42) and (2.43) respectively. Since system (2.42) is exponentially stable, there exists some positive constants λ and γ such that for all $t \geq t_o$, we have

$$||\underline{\phi}_{c\alpha}(t,t_o)|| \leq \gamma\, e^{-\lambda(t-t_o)} \tag{2.44}$$

Since $\underline{\phi}_c(t,t_o)\, e^{\alpha(t-t_o)} = \underline{\phi}_{c\alpha}(t,t_o)$, this means that

$$\begin{aligned} ||\underline{\phi}_c(t,t_o)|| &= ||\underline{\phi}_{c\alpha}(t,t_o)||\, e^{-\alpha(t-t_o)} \\ &\leq \gamma e^{-\lambda(t-t_o)}\, e^{-\alpha(t-t_o)} \end{aligned} \tag{2.45}$$

which establishes the prescribed degree of stability of system (2.43) and this completes the proof.

Remark The proof of the above theorem is parallel to that given by Anderson and Moore [An 1] for the time-invariant version of the theorem. It is also possible to prove Theorem 2.3 without resorting to a transformed LQ regulator problem. Consider the Riccati equation of the minimization problem defined in the statement of the theorem

$$\begin{aligned} \dot{\tilde{\underline{K}}}(t) = &-\tilde{\underline{K}}(t)\, \underline{A}(t) - \underline{A}^T(t)\, \tilde{\underline{K}}(t) + e^{-2\alpha t}\, \tilde{\underline{K}}(t)\, \underline{B}(t)\, \tilde{\underline{R}}(t)^{-1}\, \underline{B}(t)^T\, \tilde{\underline{K}}(t) \\ &- \tilde{\underline{Q}}(t)\, e^{2\alpha t} \end{aligned} \tag{2.46}$$

Let us postulate a solution of the form

$$\tilde{\underline{K}}(t) = \hat{\underline{K}}_\alpha(t)\, e^{2\alpha t} \tag{2.47}$$

where $\hat{\underline{K}}_\alpha(t)$ is some positive definite matrix function. Substituting (2.47) into (2.46), we obtain

$$-\dot{\hat{\underline{K}}}_\alpha(t) = \hat{\underline{K}}_\alpha(t)\ (\underline{A}(t) + \alpha \underline{I}) + (\underline{A}(t) + \alpha \underline{I})^T \hat{\underline{K}}_\alpha(t) + \tilde{\underline{Q}}(t)$$

$$- \hat{\underline{K}}_\alpha(t)\ \underline{B}(t)\ \tilde{\underline{R}}^{-1}(t)\ \underline{B}^T(t)\ \hat{\underline{K}}_\alpha(t) \qquad (2.48)$$

which is the same Riccati equation as (2.27) obtained from the transformed LQ problem. If we further assume that the boundary conditions at t_1 for equations (2.48) and (2.27) match, then $\tilde{\underline{K}}(t) = \tilde{\underline{K}}_\alpha(t)\ e^{2\alpha t}$ for (t_o, t_1) where $\tilde{\underline{K}}_\alpha(t)$ is the positive definition solution of (2.27). As t_1 approaches ∞, we have $\tilde{\underline{K}}_\alpha(t)$ approaches $\underline{K}_\alpha(t)$ for any $\tilde{\underline{K}}_\alpha(t_1) = \underline{K}_1 \geq \underline{0}$. Hence $\tilde{\underline{K}}(t)$ approaches $\underline{K}_\alpha(t)\ e^{2\alpha t}$ for $\tilde{\underline{K}}\ (t_1) = \tilde{\underline{K}}_1\ e^{2\alpha t_1} \geq \underline{0}$. It follows that the feedback control law is given by

$$\underline{u}(t) = -(\tilde{\underline{R}}(t)\ e^{2\alpha t})^{-1}\ \underline{B}^T(t)\ \underline{K}_\alpha(t)\ e^{2\alpha t}\ \underline{x}(t)$$

$$= -\tilde{\underline{R}}^{-1}(t)\ \underline{B}^T(t)\ \underline{K}_\alpha(t)\ \underline{x}(t) \qquad (2.49)$$

which agrees with that given in Theorem 2.3 and this establishes our claim.

An alternate way to verify the degree of stability for the closed-loop system

$$\dot{\underline{x}}(t) = (\underline{A}(t) - \underline{B}(t)\ \tilde{\underline{R}}^{-1}(t)\ \underline{B}^T(t)\ \underline{K}_\alpha(t))\ \underline{x}(t) \qquad (2.50)$$

is to use the result of Theorem 2.2. The following theorem identifies the Lyapunov function required for such purpose.

Theorem 2.4 $V(\underline{x}(t), t) = \underline{x}^T(t)\ \underline{K}_\alpha(t)\ \underline{x}(t)$ is a Lyapunov function for the closed-loop system (2.50) with the property that $\dot{V}(\underline{x}(t), t) \leq -2\alpha\ V(\underline{x}(t), t)$.

Proof: To show that $V(\underline{x}(t),t)$ is a Lyapunov function, we have to establish the following:

(i) $V(\underline{x}(t),t)$ is once differentiable with respect to time

(ii) There exists some positive constants π_1 , π_2 and β such that

$$\pi_1|\underline{x}|^2 \leq V(\underline{x},t) \leq \pi_2 |\underline{x}|^2 \tag{2.51}$$

and

$$\left|\frac{\partial V(\underline{x},t)}{\partial t}\right| \leq \beta|\underline{x}|^2 , \qquad \text{for all } t \geq t_o \tag{2.52}$$

(iii) $\dot{V}(\underline{x}(t),t) < 0$ along the trajectory of

$$\dot{\underline{x}}(t) = (\underline{A}(t) - \underline{B}(t)\, \tilde{\underline{R}}^{-1}(t)\, \underline{B}^T(t)\, \underline{K}_\alpha(t))\, \underline{x}(t)$$

for all $t \geq t_o$ (2.53)

For any given $\underline{x} \in R^n$, $\frac{\partial V}{\partial t}(\underline{x},t) = \underline{x}^T \dot{\underline{K}}_\alpha(t)\, \underline{x}$. Since $\underline{K}_\alpha(t)$ is the steady state solution of the Riccati equation (2.27), it follows that $V(\underline{x},t)$ is once differentiable with respect to t. By Theorem 3.4 of [Kw 1], we have

$$V(\underline{x},t) = \lim_{t_1 \to \infty} \underline{x}^T \left[\int_{t_o}^{t_1} \left[\underline{\phi}_\alpha^T(\tau,t)\, [\tilde{\underline{Q}}(\tau) + \underline{K}_\alpha(\tau)\, \underline{B}(\tau)\, \tilde{\underline{R}}^{-1}_{(\tau)}\, \underline{B}^T(\tau)\, \underline{K}_\alpha(\tau)] \right. \right.$$

$$\left. \left. \underline{\phi}_\alpha(\tau,t) \right] d\tau \right] \underline{x} \tag{2.54}$$

where

$$\frac{d}{d\tau}\, \underline{\phi}_\alpha(\tau,t) = (\underline{A}(\tau) + \alpha\underline{I} - \underline{B}(\tau)\, \tilde{\underline{R}}^{-1}(\tau)\, \underline{B}^T(\tau)\, \underline{K}_\alpha(\tau))\, \underline{\phi}_\alpha(\tau,t) \tag{2.55}$$

Since $\dot{\underline{x}}(t) = (\underline{A}(t) + \alpha\underline{I} - \underline{B}(t)\, \tilde{\underline{R}}^{-1}(t)\, \underline{B}^T(t)\, \underline{K}_\alpha(t))\, \underline{x}(t)$ is exponentially stable by problem definition, and $[\tilde{\underline{Q}}(t) + \underline{K}_\alpha(t)\, \underline{B}(t)\, \tilde{\underline{R}}^{-1}(t)\, \underline{B}^T(t)\, \underline{K}_\alpha(t)\ ]$ is a bounded positive definite

matrix function by the properties of the time-varying Riccati equations, it then follows from Theorem 6 in section 3.1 of [Br 1] that there exists constants π_1 and π_2 such that for all t and $\underline{x} \in R^n$,

$$0 < \pi_1 |\underline{x}|^2 \leq V(\underline{x},t) \leq \pi_2 |\underline{x}|^2 \tag{2.56}$$

To show the boundedness of $\left|\frac{\partial V}{\partial t}(\underline{x},t)\right|$, take the norm on both sides of the Riccati equation (2.27) and obtain

$$||\dot{\underline{K}}_\alpha(t)|| \leq 2(\alpha + ||\underline{A}(t)||)\ ||\underline{K}_\alpha(t)|| + ||\tilde{\underline{Q}}(t)|| + ||\underline{K}_\alpha(t)||^2\ ||\underline{B}(t)||^2 / \sigma\min(\tilde{\underline{R}}(t)) \quad \text{for all } t \geq t_o \tag{2.57}$$

Since all the matrices on the right hand side of the above inequality are bounded from above and since $\tilde{\underline{R}}(t)$ is also bounded from below as assumed in Theorem 2.3, it follows that there exists a constant β such that

$$\left|\frac{\partial V}{\partial t}(\underline{x},t)\right| \leq ||\dot{\underline{K}}_\alpha(t)||\ |\underline{x}|^2 \triangleq \beta |\underline{x}|^2 \tag{2.58}$$

To compute the derivative $V(\underline{x}(t),t)$ along the trajectory of $\dot{\underline{x}}(t) = (\underline{A}(t) + \alpha\underline{I} - \underline{B}(t)\ \tilde{\underline{R}}^{-1}(t)\ \underline{B}^T(t)\ \underline{K}_\alpha(t))\ \underline{x}(t)$, observe that

$$\dot{V}(\underline{x}(t),t) = \underline{x}^T(t)\ [\underline{K}_\alpha(t)\ \underline{A}(t) - \underline{K}_\alpha(t)\ \underline{B}(t)\ \underline{R}^{-1}(t)\ \underline{B}^T(t)\ \underline{K}_\alpha(t) + \underline{A}^T(t)\ \underline{K}_\alpha(t) - \underline{K}_\alpha(t)\ \underline{B}(t)\ \underline{R}^{-1}(t)\ \underline{B}^T(t)\ \underline{K}_\alpha(t) + \dot{\underline{K}}_\alpha(t)]\ \underline{x}(t) \tag{2.59}$$

$$= \underline{x}^T(t)\ [-2\ \underline{K}_\alpha(t) - \tilde{\underline{Q}}(t) - \underline{K}_\alpha(t)\ \underline{B}(t)\ \tilde{\underline{R}}^{-1}(t)\ \underline{B}^T(t)\ \underline{K}_\alpha(t)]\ \underline{x}(t) \tag{2.60}$$

$$\leq -2\alpha[\underline{x}^T(t)\ \underline{K}_\alpha(t)\ \underline{x}(t)] \tag{2.61}$$

$$= -2\alpha\ V(\underline{x}(t),t) < 0 \tag{2.62}$$

In going from (2.59) to (2.60), we used the Riccati equation (2.27). The inequality (2.61) is obtained by observing that the matrix function $(\tilde{Q}(t) + K_\alpha(t)\, B(t)\, \tilde{R}^{-1}(t)\, B^T(t)\, K_\alpha(t))$ is positive semi-definite for all $t \geq t_o$. Inequality (2.62) follows from the positive definiteness of $V(x,t)$ and the assumption that α is positive. Hence $V(x,t)$ is a Lyapunov function for $\dot{x}(t) = (A(t) - B(t)\, \tilde{R}^{-1}(t)\, B^T(t)\, K_\alpha(t))x(t)$ with the property $\dot{V}(x(t),t) \leq -2\alpha\, V(x(t),t)$ and this completes the proof.

Remark By Theorem 2.2, the condition $\dot{V}(x(t),t) \leq -2\alpha V(x(t),t)$ implies that the system $\dot{x}(t) = (A(t) - B(t)\, \tilde{R}^{-1}(t)\, B^T(t)\, K_\alpha(t))x(t)$ has a degree of stability α. This agrees with the result given in the proof of Theorem 2.3.

Remark The result of this theorem is not new. The LTI version of Theorem 2.4 was used by Anderson and Moore [An 1] to establish the asymptotic stability of LQ regulators. Safonov has employed the same type of Lyapunov function to induce conic sectors that were used to analyze the stability robustness of LQ regulators.

If the matrices $A(t)$, $B(t)$, $\tilde{Q}(t)$ and $\tilde{R}(t)$ in Theorem 2.3 are time-invariant, then the resulting state feedback control law is also time-invariant. Observe that the cost functional is still time-varying because it includes the factor $e^{2\alpha t}$. That the feedback law should be constant in this case is not at all obvious. The proof of this fact simply follows from that of Theorem 2.3. Applying the transformation (2.29) and (2.30) to the cost functional

$$J = \lim_{t_1 \to \infty} \int_{t_o}^{t_1} e^{2\alpha(t-t_o)} \left[\underline{x}^T(t)\, \tilde{\underline{Q}}\, \underline{x}(t) + \underline{u}^T(t)\, \tilde{\underline{R}}\, \underline{u}(t) \right] dt \qquad (2.63)$$

and the dynamic constraint

$$\dot{\underline{x}}(t) = \underline{A}\, \underline{x}(t) + \underline{B}\, \underline{u}(t) \qquad (2.64)$$

we get

$$J = \lim_{t_1 \to \infty} \int_{t_o}^{t_1} \left[\tilde{\underline{x}}(t)^T\, \tilde{\underline{Q}}\, \tilde{\underline{x}}(t) + \tilde{\underline{u}}^T(t)\, \tilde{\underline{R}}\, \tilde{\underline{u}}(t) \right] dt \qquad (2.65)$$

and

$$\dot{\tilde{\underline{x}}}(t) = (\underline{A} + \alpha \underline{I})\, \tilde{\underline{x}}(t) + \underline{B}\, \tilde{\underline{u}}(t) \qquad (2.66)$$

respectively.

Since the transformed minimization problem is time-invariant, the resulting feedback law for this problem is of the form

$$\tilde{\underline{u}}(t) = -\tilde{\underline{R}}^{-1}\, \underline{B}^T\, \underline{K}_\alpha\, \tilde{\underline{x}}(t) \qquad (2.67)$$

where $\underline{K}_\alpha$ is the unique positive definite solution to the algebraic Riccati equation

$$\underline{K}_\alpha\, (\underline{A} + \alpha \underline{I}) + (\underline{A} + \alpha \underline{I})^T\, \underline{K}_\alpha - \underline{K}_\alpha\, \underline{B}\, \tilde{\underline{R}}^{-1}\, \underline{B}^T\, \underline{K}_\alpha + \tilde{\underline{Q}} = \underline{0} \qquad (2.68)$$

The controllability of $(\underline{A} + \alpha \underline{I}, \underline{B})$, which is implied by that of $(\underline{A}, \underline{B})$, ensures the existence of $\underline{K}_\alpha$. The stability of the control law (2.67) follows from the observability of $(\tilde{\underline{Q}}^{1/2}, \underline{A} + \alpha \underline{I})$ which is implied by that of $(\tilde{\underline{Q}}^{1/2}, \underline{A})$. Reversing the transformation (2.29) and (2.30) we obtain the optimal control law for the original problem

$$\underline{u}(t) = -e^{-\alpha(t-t_o)}\, \tilde{\underline{R}}^{-1}\, \underline{B}^T\, \underline{K}_\alpha\, e^{\alpha(t-t_o)}\, \underline{x}(t)$$

$$= -\tilde{\underline{R}}^{-1}\, \underline{B}^T\, \underline{K}_\alpha\, \underline{x}(t) \qquad (2.69)$$

which is time-invariant. That the closed-loop system $\dot{\underline{x}}(t) = (\underline{A} - \underline{B}\,\underline{R}^{-1}\,\underline{B}^T\,\underline{K}_\alpha)\,\underline{x}(t)$ has a degree of stability α follows from the stability of $\dot{\tilde{\underline{x}}}(t) = (\underline{A} + \alpha I - \underline{B}\,\underline{R}^{-1}\,\underline{B}^T\,\underline{K}_\alpha)\,\tilde{\underline{x}}(t)$. In terms of the closed-loop eigenvalues, we have

$$\mathrm{Re}(\lambda_i(\underline{A} + \alpha I - \underline{B}\,\tilde{\underline{R}}^{-1}\,\underline{B}^T\,\underline{K}_\alpha)) < 0$$

which in turn implies that

$$\mathrm{Re}\,(\lambda_i(\underline{A} - \underline{B}\,\tilde{\underline{R}}^{-1}\,\underline{B}^T\,\underline{K}_\alpha)) < -\alpha \quad . \tag{2.70}$$

and this establishes the degree of stability of the feedback law (2.67).

We summarize the results of the above discussion in the following theorem

Theorem 2.5 Consider the LQ regulator problem

$$\min_{\substack{\underline{u}(t) \\ t \geq t_o}} J = \lim_{t_1 \to \infty} \int_{t_o}^{t_1} \left[\underline{x}^T(t)\,\underline{Q}(t)\,\underline{x}(t) + \underline{u}^T(t)\,\underline{R}(t)\,\underline{u}(t)\right] dt \tag{2.71}$$

subject to the dynamic constraint

$$\underline{\dot{x}}(t) = \underline{A}\,\underline{x}(t) + \underline{B}\,\underline{u}(t) \tag{2.72}$$

where $(\underline{A}, \underline{B})$ is controllable.

The weighting matrices are chosen as

$$\underline{Q}(t) = \tilde{\underline{Q}}\,e^{2\alpha t} \text{ and } \underline{R}(t) = \tilde{\underline{R}}\,e^{2\alpha t} \tag{2.73}$$

where $\tilde{\underline{Q}} \geq 0$ and $\tilde{\underline{R}} > 0$.

Furthermore, supposed that $(\tilde{\underline{Q}}^{1/2}, \underline{A})$ is observable. Then the optimal control law for the given LQ regulator problem is given by

$$u(t) = -\underline{R}^{-1} \underline{B}^T \underline{K}_\alpha \underline{x}(t) \tag{2.74}$$

where $\underline{K}_\alpha$ is the unique positive definite solution of the algebraic Riccati equation

$$\underline{K}_\alpha(\underline{A} + \alpha I) + (\underline{A} + \alpha I)^T \underline{K}_\alpha + \underline{Q} - \underline{K}_\alpha \underline{B} \underline{R}^{-1} \underline{B}^T \underline{K}_\alpha = \underline{0} \tag{2.75}$$

Moreover, the closed-loop system

$$\dot{\underline{x}}(t) = (\underline{A} - \underline{B} \underline{R}^{-1} \underline{B}^T \underline{K}_\alpha) \underline{x}(t) \tag{2.76}$$

has a degree of stability at least α.

In view of the time-invariant control law that results from the minimization problem considered in Theorem 2.5, one might suspect the possibility of constructing a cost functional with time-invariant matrices $\underline{Q}$ and $\underline{R}$ such that the control law obtained from minimizing the cost functional is the same as that derived in the preceding theorem with $\tilde{\underline{Q}} e^{2\alpha t}$ and $\tilde{\underline{R}} e^{2\alpha t}$. Pairs of weighting matrices $\underline{Q}$, $\underline{R}$ with the above mentioned properties do indeed exist. The following corollary to Theorem 2.5 shows how such matrices may be chosen.

Corollary 2.5 If $\underline{Q}(t)$ and $\underline{R}(t)$ in Theorem 2.5 are chosen to be

$$\underline{Q}(t) = \tilde{\underline{Q}} + 2\alpha \underline{K}_\alpha \tag{2.77}$$

and

$$\underline{R}(t) = \tilde{\underline{R}} \tag{2.78}$$

respectively, where $\underline{K}_\alpha$ is the unique positive definite solution of the algebraic Riccati equation (2.75), then the resulting optimal feedback law is given by

$$\underline{u}(t) = -\tilde{\underline{R}}^{-1} \underline{B}^T \underline{K}_\alpha \underline{x}(t) \tag{2.79}$$

and the closed-loop system $\dot{\underline{x}}(t) = (\underline{A} - \underline{B}\,\underline{R}^{-1}\,\underline{B}^T\,\underline{K}_\alpha)\,\underline{x}(t)$ has a degree of stability at least α.

Proof: Note that $(\underline{A}, \underline{B})$ is controllable by assumption and that $((\tilde{\underline{Q}} + 2\alpha\,\underline{K}_\alpha)^{1/2}, \underline{A})$ is observable as a result of $\underline{K}_\alpha > 0$.

It follows that the algebraic Riccati equation

$$\underline{K}\,\underline{A} + \underline{A}^T\,\underline{K} + (\tilde{\underline{Q}} + 2\alpha\,\underline{K}_\alpha) - \underline{K}\,\underline{B}\,\tilde{\underline{R}}^{-1}\,\underline{B}^T\,\underline{K} = \underline{0} \qquad (2.80)$$

associated with the given minimization problem has a unique positive definite solution. Comparing (2.68) with (2.80), it is clear that $\underline{K}_\alpha$, which is the solution of (2.68) is also a solution of (2.80). This completes the proof.

Remark While constant matrices $\underline{Q}$ and $\underline{R}$ can be chosen such that the associated regulator problem leads to a closed-loop system with degree of stability α, it does not seem possible for us to obtain such matrices without first solving a LQ regulator problem with weighting matrices of the form $\tilde{\underline{Q}}\,e^{2\alpha t}$ and $\tilde{\underline{R}}\,e^{2\alpha t}$.

Remark It is clear from the preceding corollary that RPDS for LTI systems is just a particular class of LQ regulator with a very special choice of weighting matrices. This is an important observation for it implies that all the feedback properties of LQ regulators are shared by RPDS.

2.4 Kalman-Bucy Filter with a Prescribed Degree of Stability (FPDS)

In this section, we turn to the problem of designing a Kalman-Bucy filter with a prescribed degree of stability. By stability of a filter, we refer to the stability of the estimation error dynamics. Mathemati-

cally, this is a problem dual to the RPDS problem considered in the last section. To make clear the connection between the regulator problem and the filter problem, we consider a linear system of the following type

$$\dot{\underline{x}}(t) = \underline{A}(t)\,\underline{x}(t) + \underline{\zeta}(t) \tag{2.81}$$

$$\underline{y}(t) = \underline{C}(t)\,\underline{x}(t) + \underline{\theta}(t) \tag{2.82}$$

where $\underline{\zeta}(t)$ and $\underline{\theta}(t)$ are uncorrelated zero mean white noises with spectral intensity $\underline{\Xi}(t)$ and $\underline{\Theta}(t)$ respectively. We wish to obtain a linear estimate of $\underline{x}(t)$ given $\underline{y}(\tau)$, $-\infty \leq \tau < t$, such that the mean square estimation error is minimized. Under the assumption that ,

(i) $\underline{A}(t)$ is continuous and bounded, $\underline{C}(t)$, $\underline{\Xi}(t)$ and $\underline{\Theta}(t)$ are piecewise continuous and bounded for all t (2.83)

(ii) $\underline{\Xi}(t) \geq \beta_1 \underline{I}$ and $\underline{\Theta}(t) > \beta_2 \underline{I}$ for all t where β_1 and β_2 are some positive real constants (2.84)

(iii) $(\underline{C}(t), \underline{A}(t))$ is uniformly completely reconstructable and $(\underline{A}(t), \underline{\Xi}^{1/2}(t))$ is uniformly completely controllable (2.85)

it is well known (see Chapter 4 of [Kw 1]) that the optimal linear state estimate $\hat{\underline{x}}(t)$ is pecified by

$$\dot{\hat{\underline{x}}}(t) = \underline{A}(t)\,\hat{\underline{x}}(t) + \underline{\Sigma}(t)\,\underline{C}(t)\,\underline{\Theta}(t)^{-1}\,(\underline{y}(t) - \underline{C}(t)\,\hat{\underline{x}}(t)) \tag{2.86}$$

where $\underline{\Sigma}(t)$ is the steady state solution of the Riccati equation.

$$\dot{\tilde{\underline{\Sigma}}}(t) = \underline{A}(t)\,\tilde{\underline{\Sigma}}(t) + \tilde{\underline{\Sigma}}(t)\,\underline{A}^{T}(t) + \underline{\Xi}(t) - \tilde{\underline{\Sigma}}(t)\,\underline{C}^{T}(t)\,\underline{\Xi}^{-1}(t)\,\underline{C}(t)\,\tilde{\underline{\Sigma}}(t) \tag{2.87}$$

as t_o approaches $-\infty$ for any initial condition $\underline{\Sigma}_o > 0$. Moreover, the state estimate error dynamics specified by

$$\dot{\underline{e}}(t) = (\underline{A}(t) - \underline{H}(t)\,\underline{C}\,(t))\underline{e}(t) \tag{2.88}$$

where $\underline{e}(t) = \hat{\underline{x}}(t) - \underline{x}(t)$ is the state estimation error and where $\underline{H}(t) = \underline{\Sigma}(t)\,\underline{C}^T(t)\,\underline{\Theta}(t)^{-1}$, the filter gain, is asymptotically stable. Given an initial estimation error, the rate of decay of $\underline{e}(t)$ is determined by that of $\underline{\phi}_F(t,t_o)$ where

$$\dot{\underline{\phi}}_F(t,t_o) = (\underline{A}(t) - \underline{H}(t)\,\underline{C}(t))\,\underline{\phi}_F(t,t_o) \tag{2.89}$$

The decay rate of $||\underline{\phi}_F(t,t_o)||$ is in turn dependent on the noise intensity matrices $\underline{\Xi}(t)$ and $\underline{\Theta}(t)$.

In some applications, one may require a state estimate error dynamics that is faster than the one specified by the noise characteristics given by the physical systems. This can be accomplished by making appropriate adjustment of $\underline{\Xi}(t)$ and $\underline{\Theta}(t)$ in the filter design equation (2.87) so that for a given positive constant α, there exists some positive γ such that $||\underline{\phi}_F(t,t_o)|| \leq \gamma\, e^{-\alpha(t-t_o)}$ for all $t \geq t_o$. We call a filter with such property a KBF with degree of stability α. In view of the dual relationship between the KBF and the LQ regulator problem, the technique for designing RPDS discussed in the previous section is readily applicable to the design of FPDS. This is illustrated by the following theorem.

Since the duality between the LQ regulator problem and the KBF problem is well known, we will omit all the dual proofs in this section, and simply formulate the dual problems and state the corresponding

results. Special emphasis will, however, be given to result interpretetions that are unique to estimation problems.

Theorem 2.6 Consider the linear dynamical system described by the equation pair (2.81) and (2.82). Suppose that $\underline{\zeta}(t)$ and $\underline{\theta}(t)$ are zero mean, uncorrelated white noises of spectral intensity $\underline{\Xi}(t)\, e^{-2\alpha t}$ and $\underline{\Theta}(t)\, e^{-2\alpha t}$ respectively, and that α is some positive constant. The matrices $\underline{\Xi}(t)$ and $\underline{\Theta}(t)$ are assumed to be bounded and piecewise continuous with $\underline{\Xi}(t) \geq \beta_1 I$ and $\underline{\Theta}(t) \geq \beta_2 I$ for all t where β_1 and β_2 are positive constants. Furthermore, suppose that $(\underline{C}(t), \underline{A}(t))$ is uniformly completely reconstructable and that $(\underline{A}(t), \underline{\Xi}^{1/2}(t))$ is uniformly completely controllable. Then the KBF gain $\underline{H}_\alpha(t)$ obtained from solving the linear least square estimate of $\underline{x}(t)$ given $\underline{y}(\tau)$, $-\infty < \tau < t$, is

$$\tilde{\underline{H}}_\alpha(t) = \underline{\Sigma}_\alpha(t)\, \underline{C}^T(t)\, \underline{\Theta}^{-1}(t) \tag{2.90}$$

where $\underline{\Sigma}_\alpha(t)$ is the steady state solution of the Riccati equation

$$\begin{aligned}\dot{\tilde{\underline{\Sigma}}}_\alpha(t) &= \tilde{\underline{\Sigma}}_\alpha(t)\, (\underline{A}(t) + \alpha I)^T + (\underline{A}(t) + \alpha I)\, \tilde{\underline{\Sigma}}_\alpha(t) + \underline{\Xi}(t) \\ &\quad - \tilde{\underline{\Sigma}}_\alpha(t)\, \underline{C}^T(t)\, \underline{\Theta}^{-1}(t)\, \underline{C}(t)\, \tilde{\underline{\Sigma}}_\alpha(t)\end{aligned} \tag{2.91}$$

as t_o approaches $-\infty$ for any $\underline{\Sigma}_\alpha(t_o) \geq 0$.

Moreover, the state estimate error dynamics has a degree of stability of at least α .

As we specialize the results of Theorem 2.6 to the time-invariant case by setting $\underline{A}(t), \underline{B}(t), \underline{\Xi}(t)$ and $\underline{\Theta}(t)$ equal to some constant matrices $\underline{A}$, $\underline{B}$, $\underline{\Xi}, \underline{\Theta}$ that satisfy the required controllability, observability and positive definiteness conditions, the KBF gain obtained above is also

time-invariant. A precise statement of the results is stated in the following theorem which is the exact dual of Theorem 2.5.

Theorem 2.7 Consider the linear dynamical system

$$\dot{\underline{x}}(t) = \underline{A}\,\underline{x}(t) + \underline{\zeta}(t) \tag{2.92}$$

$$\underline{y}(t) = \underline{C}\,\underline{x}(t) + \underline{\theta}(t) \tag{2.93}$$

Suppose that $\underline{\theta}(t)$ and $\underline{\zeta}(t)$ are zero mean white noise with spectral intensity matrices $\underline{\Theta}e^{-2\alpha t}$ and $\underline{\Xi}e^{-2\alpha t}$ respectively and α being some positive constant. The matrices $\underline{\Theta}$ and $\underline{\Xi}$ are assume to satisfy

$$\underline{\Theta} > 0 \text{ and } \underline{\Xi} \geq 0 \tag{2.94}$$

and $(\underline{A}, \underline{\Xi}^{1/2})$ is controllable. Furthermore, suppose that $\left(\underline{C}, \underline{A}\right)$ is observable. Then the KBF gain $\underline{H}_\alpha$ obtained from solving the linear least square estimate of $\underline{x}(t)$ given $\underline{y}(\tau)$ $-\infty < \tau < t$ is given by

$$\underline{H}_\alpha = \underline{\Sigma}_\alpha\, \underline{C}^T \underline{\Theta}^{-1} \tag{2.95}$$

where $\underline{\Sigma}_\alpha$ is the unique positive definite solution of the algebraic Riccati equation

$$(\underline{A} + \alpha I)\, \underline{\Sigma}_\alpha + \underline{\Sigma}_\alpha (\underline{A} + \alpha I)^T + \underline{\Xi}\ \underline{\Sigma}_\alpha\, \underline{C}^T\, \underline{\Theta}^{-1}\, \underline{C}\, \underline{\Sigma}_\alpha = 0 \tag{2.96}$$

Moreover, the estimation error dynamics described by

$$\dot{\underline{e}}(t) = (\underline{A} - \underline{H}_\alpha\, \underline{C})\, \underline{e}(t) \tag{2.97}$$

has a degree of stability α .

Remark Observe that both noises specified in Theorem 2.7 have spectral intensity matrices that decay exponentially with time. The resulting

FPDS will therefore give more emphasis to the recent data in view of its greater accuracy. This has the desirable effect of enhancing the filter's tolerance of modelling errors. In the classical Weighted Least Square approach to estimation, the same effect of giving more emphasis to recent data is achieved by penalizing the recent estimation errors more than the old ones [Sc 1].

We now state the dual of Corollary 2.5.

Corollary 2.7 If $\underline{\Xi}(t)$ and $\underline{\Theta}(t)$ in Theorem 2.7 are chosen to be

$$\underline{\Xi}(t) = \underline{\Xi} + 2_{\alpha}\, \underline{\Sigma}_{\alpha} \quad \text{and} \quad \underline{\theta}(t) = \underline{\Theta} \tag{2.98}$$

respectively, where $\underline{\Sigma}_{\alpha}$ is the unique positive definite solution of the algebraic Riccati equation (2.96) then the resulting KBF gain is given by

$$\underline{H}_{\alpha} = \underline{\Sigma}_{\alpha}\, \underline{C}^{T}\, \underline{\Theta}^{-1} \tag{2.99}$$

and the error dynamics of the filter

$$\dot{\underline{e}}(t) = (\underline{A} - \underline{H}_{\alpha}\, \underline{C})\, \underline{e}(t) \tag{2.100}$$

has a degree of stability at least α.

Remark It is clear from Corollary 2.7 that one needs to introduce a very special choice of process noise in order to design a KBF with a prescribed degree of stability. One common approach to speed up the filter error dynamics is to use an observation noise with spectral intensity matrix of the form $\rho\underline{\Theta}(\rho > 0)$. The value of ρ is then decreased toward zero until a satisfactory design is obtained. Intuitively, decreasing the value of ρ will improve the speed of the state

reconstruction since less attention is now paid to the filtering of observation noise. However, this procedure does not always lead to improvement of error dynamics. Consider the case where $\underline{\zeta}(t)$ is of the form $\underline{\zeta}(t) = \underline{F}\tilde{\underline{\zeta}}(t)$ with $\underline{F}$ having the same dimension as $\underline{C}^T$ and $\tilde{\underline{\zeta}}(t)$ being a zero mean white noise. Let the spectral intensity of $\tilde{\underline{\zeta}}(t)$ be $\tilde{\underline{\Xi}}$ where $\tilde{\underline{\Xi}}$ is positive definite. The spectral intensity of $\underline{\zeta}(t)$ is then given by $\underline{\Xi} = \underline{F}\,\hat{\underline{\Xi}}\,\underline{F}^T$. Then, as ρ approaches 0, the p filter poles will approach the p values $\hat{\nu}_i$ where

$$\hat{\nu}_i = \begin{cases} \nu_i & \text{if } \mathrm{Re}(\nu_i) \leq 0 \\ -\mathrm{Re}(\nu_i) + j\ \mathrm{Im}(\nu_i) & \text{if } \mathrm{Re}(\nu_i) > 0, \end{cases} \qquad i = 1,2,\ldots,p \tag{2.101}$$

and ν_i's are the values of s (complex) that give rise to rank deficiency of the matrix

$$\begin{bmatrix} sI - \underline{A} & \underline{\Xi}^{1/2} \\ \underline{C} & \underline{0} \end{bmatrix}$$

It is possible that some of the ν_i's may be located very close to $j\omega$-axis. The filter poles driven toward such ν_i's as ρ approaches 0 will result in poor error decay for certain initial values of the filter error.

There are however situations where a filter designed with the latter procedure is preferable to one designed using the method suggested in Theorem 2.3. If the observation noise intensity $\rho\,\underline{\Theta}$ is small compared with the process noise intensity $\underline{\Xi}$, and if $(\underline{C}, \underline{A}, \underline{\Xi}^{1/2})$ constitutes a minimum phase system, it can be shown that

$$\lim_{\rho \to 0} E\left\{ (\hat{\underline{x}}(t) - \underline{x}(t)^T (\hat{\underline{x}}(t) - \underline{x}(t)) \right\} = 0 \qquad (2.102)$$

In this limiting case, the structure of the system to be observed is so exploited that the estimate error $\underline{e}(t)$ cannot be driven into the subspace spanned by the eigenvectors of those filter poles that are located in the neighborhood of the $j\omega$-axis. Employing a FPDS with an arbitrarily large degree of stability in such situations may in fact give rise to a large error covariance.

2.5 Concluding Remarks

We have studied in this chapter the extension of the RPDS method to the linear time-varying systems. Given an appropriate definition of 'degree of stability' for such systems, the exponential weighting technique developed by Anderson and Moore for solving the time-invariant RPDS problem is readily applicable to the time-varying case.

We also obtain a characterization of the degree of stability in terms of Lyapunov function. This is a natural generalization of the known results in Laypunov stability theory and is useful for establishing the degree of stability of feedback laws which are designed using RPDS technique .

The formulation and solution of the time-varying FPDS problem follows dually from that of RPDS. For the time-invariant case, the FPDS solution admits interpretation of interest to design of fast response filters. It is not possible in general to speed up the filter dynamics by simply scaling up the process noise. The solutions to the FPDS problem specify a class of spectral intensity of the process noise that is useful for such purpose.

CHAPTER III

EIGENSTRUCTURE PROPERTIES OF THE TIME-INVARIANT REGULATORS WITH A PRESCRIBED DEGREE OF STABILITY

3.1 Introduction

This chapter explores several important eigenstructure properties of time-invariant RPDS and their potential applications.

Some equations are obtained for the derivatives of the RPDS closed-loop eigenvalues with respect to the stability factor α. These equations are useful for the purpose of recomputing the closed-loop eigenvalues given a small change of α.

Equations that describe the asymptotic behavior of RPDS root-loci are also derived. Specifically, we consider a cost functional of the form

$$J = \lim_{t_1 \to +\infty} \int_0^{t_1} e^{2\alpha t} [\underline{x}^T(t)\ \underline{Q}\ \underline{x}(t) + \underline{u}^T(t)\ \rho \underline{R}\ \underline{u}(t)]dt; \quad \rho > 0 \tag{3.1}$$

and examine the various branches of the loci traced by the closed-loop eigenvalues as ρ varies.

To close this chapter, we employ the asymptotic property of RPDS poles as ρ approaches infinity to obtain a novel solution of the Regulator with Prescribed Damping Ratio (RPDR) problem.

3.2 Properties of the Solution of the RPDS Algebraic Riccati Equation

In this section, we state two lemmas that will be used extensively

in the remainder of this chapter and in the next one. Both lemmas address the behavior of the matrix $\underline{K}_\alpha$, which is the unique positive definite solution of the RPDS algebraic Riccati equation (2.68) in Theorem 2.5, with respect to the increment of the stability factor α.

Lemma 3.1 Let $\underline{K}_{\alpha_1}$ and $\underline{K}_{\alpha_2}$ be the unique positive definite solutions of the algebraic Riccati equations

$$\underline{K}_{\alpha_1}(\underline{A} + \alpha_1\underline{I}) + (\underline{A} + \alpha_1\underline{I})^T \underline{K}_{\alpha_1} + \underline{Q} - \underline{K}_{\alpha_1} \underline{B}\,\underline{R}^{-1}\,\underline{B}^T \underline{K}_{\alpha_1} = \underline{0} \tag{3.2}$$

$$\underline{K}_{\alpha_2}(\underline{A} + \alpha_2\underline{I}) + (A + \alpha_2\underline{I})^T \underline{K}_{\alpha_2} + \underline{Q} - \underline{K}_{\alpha_2} \underline{B}\,\underline{R}^{-1}\,\underline{B}^T \underline{K}_{\alpha_2} = \underline{0} \tag{3.3}$$

respectively.

The following conditions

(i) $\underline{Q} \geq \underline{0}$ and $\underline{R} > \underline{0}$ (3.4)

(ii) $(\underline{A}, \underline{B})$ controllable (3.5)

(iii) $(\underline{Q}^{1/2}, \underline{A})$ observable (3.6)

that are sufficient to guarantee the existence of $\underline{K}_{\alpha_1}$ and $\underline{K}_{\alpha_2}$ are assumed to be satisfied. Then one has $\underline{K}_{\alpha_1} > \underline{K}_{\alpha_2}$ if $\alpha_1 > \alpha_2$.

Proof: Let $\Delta\underline{K} = \underline{K}_{\alpha_1} - \underline{K}_{\alpha_2}$. We need to show that $\Delta\underline{K}$ is positive definite if $\alpha_1 > \alpha_2$. Substitute $\underline{K}_{\alpha_1} = \underline{K}_{\alpha_2} + \Delta\underline{K}$ into (3.2) to obtain

$$(\underline{K}_{\alpha_2} + \Delta\underline{K})(\underline{A} + \alpha_1\underline{I}) + (\underline{A} + \alpha_1\underline{I})^T (\underline{K}_{\alpha_2} + \Delta\underline{K}) + \underline{Q}$$

$$- (\underline{K}_{\alpha_2} + \Delta\underline{K})\,\underline{B}\,\underline{R}^{-1}\,\underline{B}^T(\underline{K}_{\alpha_2} + \Delta\underline{K}) = \underline{0} \tag{3.7}$$

Rearranging the terms in (3.7), we obtain

$$\Delta K(\underline{A} - \underline{B}\,\underline{R}^{-1}\,\underline{B}^T\,\underline{K}_{\alpha_2} + (\alpha_1 - \alpha_2)\underline{I}) + (\underline{A} - \underline{B}\,\underline{R}^{-1}\,\underline{B}^T\,\underline{K}_{\alpha_2} + (\alpha_1 - \alpha_2)\underline{I})^T\,\Delta\underline{K}$$

$$- \Delta\underline{K}\,\underline{B}\,\underline{R}^{-1}\,\underline{B}^T\,\Delta\underline{K} + 2(\alpha_1 - \alpha_2)\underline{K}_{\alpha_2} = \underline{0} \qquad (3.8)$$

Observe that (3.8) is an algebraic Riccati equation in $\Delta\underline{K}$. To find out if there exists a unique positive definite solution $\Delta\underline{K}$ for (3.8), we need to check the controllability of $(\underline{A} + (\alpha_1 - \alpha_2)\underline{I} - \underline{B}\,\underline{R}^{-1}\,\underline{B}^T\,\underline{K}_{\alpha_2}, \underline{B})$ and the observability of $([2(\alpha_1 - \alpha_2)\underline{K}_{\alpha_2}]^{1/2}, \underline{A} - \underline{B}\,\underline{R}^{-1}\,\underline{B}^T\,\underline{K}_{\alpha_2} + (\alpha_1 - \alpha_2)\underline{I})$

The controllability of $(\underline{A} - \underline{B}\,\underline{R}^{-1}\,\underline{B}^T\,\underline{K}_{\alpha_2} + (\alpha_1 - \alpha_2)\underline{I}, \underline{B})$ is implied by the controllability of $(\underline{A} + (\alpha_1 - \alpha_2)\underline{I}, \underline{B})$, since controllability is not affected under state feedback. The controllability of the latter in turn follows from that of $(\underline{A}, \underline{B})$ as shown in the proof of Theorem 2.3. Since the controllability of $(\underline{A}, \underline{B})$ is assumed in the original problem statement, this proves the controllability of $(\underline{A} + (\alpha_1 - \alpha_2)\underline{I} - \underline{B}\,\underline{R}^{-1}\,\underline{B}^T\,\underline{K}_{\alpha_2}, \underline{B})$. The observability of $([2(\alpha_1 - \alpha_2)\underline{K}_{\alpha_2}]^{1/2}, \underline{A} - \underline{B}\,R^{-1}\,\underline{B}^T\,\underline{K}_{\alpha_2} + (\alpha_1 - \alpha_2)\underline{I})$ follows from the positive definiteness of $\underline{K}_{\alpha_2}$.

In order to prove the positive definiteness of $\Delta\underline{K}$, we need to demonstrate the stability of the matrix (see Theorem 3.7 [Kw 1])

$$\tilde{\underline{A}} \triangleq \underline{A} - \underline{B}\,\underline{R}^{-1}\,\underline{B}^T\,\underline{K}_{\alpha_2} + (\alpha_1 - \alpha_2)\underline{I} - \underline{B}\,\underline{R}^{-1}\,\underline{B}^T\,\Delta\underline{K} \qquad (3.9)$$

By definition of $\Delta\underline{K}$, we can rewrite $\tilde{\underline{A}}$ as

$$\tilde{\underline{A}} = \underline{A} - \underline{B}\,\underline{R}^{-1}\,\underline{B}^T\,\underline{K}_{\alpha_1} + (\alpha_1 - \alpha_2)\underline{I} \qquad (3.10)$$

Since $\underline{A} - \underline{B}\,\underline{R}^{-1}\,\underline{B}^T\,\underline{K}_{\alpha_1} + \alpha_1\underline{I}$ is stable by definition and $\alpha_2 > 0$, the stability of $\tilde{\underline{A}}$ follows immediately and this completes the proof.

Remark: Lemma 3.1 establishes the fact that $\underline{K}_\alpha$ is an increasing function of α. We shall make extensive use of this result in our study of the RRDS robustness properties in Chapter 4.

Lemma 3.2 Let $\underline{K}_\alpha$ be the unique positive definite solution of the algebraic Riccati equation

$$\underline{K}_\alpha(\underline{A} + \alpha\underline{I}) + (\underline{A} + \alpha\underline{I})^T\,\underline{K}_\alpha - \underline{K}_\alpha\,\underline{B}\,\underline{R}^{-1}\,\underline{B}^T\,\underline{K}_\alpha + \underline{Q} = \underline{0} \tag{3.11}$$

The following conditions

$$\text{(i)}\quad \underline{Q} \geq 0 \quad \text{and} \quad \underline{R} > \underline{0} \tag{3.12}$$

$$\text{(ii)}\quad (\underline{A}, \underline{B}) \text{ controllable} \tag{3.13}$$

$$\text{(iii)}\quad (\underline{Q}^{1/2}, \underline{A}) \text{ observable} \tag{3.14}$$

that are sufficient to guarantee the existence of $\underline{K}_\alpha$ are assumed to be satisfied. Then the derivative matrix $\dfrac{\partial \underline{K}_\alpha}{\partial \alpha}$ is positive definite for all values of α.

Proof: Differentiating the left side of (3.11) with respect to α, we obtain

$$\frac{\partial \underline{K}_\alpha}{d\alpha}\,(\underline{A} + \alpha\underline{I}) + (\underline{A} + \alpha\underline{I})^T\,\frac{\partial \underline{K}_\alpha}{\partial \alpha} + 2\,\underline{K}_\alpha$$

$$- \frac{\partial \underline{K}_\alpha}{\partial \alpha}\,(\underline{B}\,\underline{R}^{-1}\,\underline{B}^T\,\underline{K}_\alpha) - (\underline{K}_\alpha\,\underline{B}\,\underline{R}^{-1}\,\underline{B}^T)\,\frac{\partial \underline{K}_\alpha}{\partial \alpha} + \underline{Q} = \underline{0}\,. \tag{3.15}$$

After rearranging terms, we obtain the following Lyapunov equation

$$\frac{\partial K_\alpha}{\partial \alpha}(A + \alpha I - B G_\alpha) + (A + \alpha I - B G_\alpha)^T \frac{\partial K_\alpha}{\partial \alpha} + (Q + 2 K_\alpha) = 0 \tag{3.16}$$

where $G_\alpha = R^{-1} B^T K_\alpha$ is the state feedback gain.

To show the existence of a positive definite solution $\frac{\partial K_\alpha}{\partial \alpha}$ to (3.16), we need to check the stability of $(A + \alpha I - B G_\alpha)$ (i.e. that all eigenvalues of $(A + \alpha I - B G_\alpha)$ have negative real part) and the positive definiteness of $(Q + 2 K_\alpha)$.

The stability of $(A + \alpha I - B G_\alpha)$ is a direct consequence of conditions (i), (ii) and (iii) (see Theorem 3.7 [Kw 1]). The positive definiteness of $(Q + 2 K_\alpha)$ simply follows from that of K_α. Since we have thus far made no reference to the sign of α, the matrix derivative $\frac{\partial K_\alpha}{\partial \alpha}$ is therefore positive definite for all values of α and this completes the proof.

3.3 Eigenvalue Sensitivity with Respect to the Stability Factor α.

In this section, we present two methods for finding $\frac{\partial \lambda_i}{\partial \alpha}$, the derivative of the RPDS poles with respect to the stability factor.

Lemma 3.3 For any value of α and for any distinct eigenvalue λ_i of $A - B R^{-1} B^T K_\alpha$, we have

$$\frac{\partial \lambda}{\partial \alpha} = \frac{-y_i^H B R^{-1} B^T \frac{\partial K_\alpha}{\partial \alpha} x_i}{y_i^H x_i} \tag{3.17}$$

where x_i and y_i are the right and left eigenvectors of $A - B R^{-1} B^T K_\alpha$ which are defined in the usual way by

$$(\underline{A} - \underline{B}\,\underline{R}^{-1}\,\underline{B}^{T}\,\underline{K}_{\alpha} - \lambda_i \underline{I})\,\underline{x}_i = \underline{0} \tag{3.18}$$

and

$$\underline{y}_i^{H}\,(\underline{A} - \underline{B}\,\underline{R}^{-1}\,\underline{B}^{T}\,\underline{K}_{\alpha} - \lambda_i \underline{I}) = \underline{0} \tag{3.19}$$

respectively.

Proof: First, we differentiate (3.18) with respect to α to obtain

$$\frac{\partial}{d\alpha}\,(\underline{A} - \underline{B}\,\underline{R}^{-1}\,\underline{B}^{T}\,\underline{K}_{\alpha} - \lambda_i \underline{I})\underline{x}_i + (\underline{A} - \underline{B}\,\underline{R}^{-1}\,\underline{B}^{T}\,\underline{K}_{\alpha} - \lambda_i \underline{I})\,\frac{\partial \underline{x}_i}{\partial \alpha} = \underline{0} \tag{3.20}$$

Multiplying both sides of the above equation by the left eigenvector $\underline{y}_i^{H}$ cancels the second term on the left hand side and one gets

$$\underline{y}_i^{H}\,\frac{\partial}{\partial \alpha}\,(\underline{A} - \underline{B}\,\underline{R}^{-1}\,\underline{B}^{T}\,\underline{K}_{\alpha} - \lambda_i \underline{I})\,\underline{x}_i = \underline{0} \tag{3.21}$$

By rearranging the terms, we obtain

$$\frac{\partial \lambda_i}{\partial \alpha} = \frac{\underline{y}_i^{H}\,\frac{\partial}{\partial \alpha}\,(\underline{A} - \underline{B}\,\underline{R}^{-1}\,\underline{B}^{T}\,K_{\alpha})\,\underline{x}_i}{\underline{y}_i^{H}\,\underline{x}_i} \tag{3.22}$$

$$= \frac{\underline{y}_i^{H}(-\underline{B}\,\underline{R}^{-1}\,\underline{B}^{T}\,\frac{\partial \underline{K}_{\alpha}}{\partial \alpha})\,\underline{x}_i}{\underline{y}_i^{H}\,\underline{x}_i} \tag{3.23}$$

The existence of $\frac{\partial \underline{K}_{\alpha}}{\partial \alpha}$ for an arbitrary real constant α follows from Lemma 3.2, and this completes the proof.

Remark: Lemma 3.3 is adapted from the standard result for finding $\frac{\partial \lambda_i}{\partial p}$ where λ_i is a closed-loop eigenvalue of the system matrix $(\underline{A} - \frac{1}{p}\,\underline{B}\,\underline{K}\,\underline{C})$ (see [Th 1] Chapter 3). The derivative $\frac{\partial \underline{K}_{\alpha}}{\partial \alpha}$ can be computed from a

Lyapunov equation of the form (3.16). An alternate way to compute $\frac{\partial \lambda_i}{\partial \alpha}$ is via the Hamiltonian system matrix we define now.

Definition 3.1 Consider a LQ regulator problem with cost functional

$$J = \int_0^\infty [\underline{x}(t)^T \underline{Q}\, \underline{x}(t) + \underline{u}^T(t)\, \underline{R}\, \underline{u}(t)]dt \tag{3.24}$$

and dynamic constraint

$$\dot{\underline{x}}(t) = \underline{A}\, \underline{x}(t) + \underline{B}\, \underline{u}(t) \tag{3.25}$$

Suppose that all the conditions required to guarantee the existence of a stable state feedback law minimizing J are satisfied, then the Hamiltonian system associated with the LQ regulator problem is given by

$$\dot{\underline{z}}(t) = \underline{Z}\, \underline{z}(t) \tag{3.26}$$

where

$$\underline{Z} = \begin{bmatrix} \underline{A} & -\underline{B}\, \underline{R}^{-1}\, \underline{B}^T \\ -\underline{Q} & -\underline{A}^T \end{bmatrix} \tag{3.27}$$

$$\underline{z}(t) = \begin{bmatrix} \underline{x}(t) \\ \underline{\xi}(t) \end{bmatrix} \tag{3.28}$$

The matrix $\underline{Z}$ is of interest because its eigenstructure describes the solution of the LQ regulator problem defined by (3.24) and (3.25) (see Chapter 3 of [Kw 1]). The eigenvalues of $\underline{Z}$ are symmetric about the $j\omega$-axis. Moreover, the eigenvalues in the left-half complex plane are exactly those closed-loop eigenvalues of the LQ regulator. If $[\underline{x}_1(t)^T, \underline{\xi}_1(t)^T]^T$ is a right eivenvector corresponding to a left-half plane eigenvalue of $\underline{Z}$, then $\underline{x}_1(t)$ is also a closed-loop right eigenvector

of the LQ regulator and

$$\underline{\xi}_1(t) = \underline{K}\,\underline{x}_1(t) \tag{3.29}$$

where $\underline{K}$ is the positive definite solution of the algebraic Riccati equation

$$\underline{K}\,\underline{A} + \underline{A}^T\,\underline{K} - \underline{K}\,\underline{B}\,\underline{R}^{-1}\,\underline{B}^T\,\underline{K} + \underline{Q} = \underline{0} \tag{3.30}$$

In order to compute $\frac{\partial \lambda_i}{\partial \alpha}$ for the RPDS problem solved in Theorem 2.5, we consider the following Hamiltonian system

$$\dot{\underline{z}}(t) = \underline{Z}_\alpha\,\underline{z}(t) \tag{3.31}$$

where

$$\underline{Z}_\alpha = \begin{bmatrix} \underline{A} + \alpha\underline{I} & -\underline{B}\,\underline{R}^{-1}\,\underline{B}^T \\ -\underline{Q} & -(\underline{A} + \alpha\underline{I})^T \end{bmatrix} \tag{3.32}$$

This system is obtained by considering the LQ regulator problem with cost functional

$$J = \lim_{t_1 \to \infty} \int_{t_o}^{t_1} [\underline{x}^T(t)\,\underline{Q}\,\underline{x}(t) + \underline{u}^T(t)\,\underline{R}\,\underline{u}(t)]dt \tag{3.33}$$

and dynamic constraint

$$\dot{\underline{x}}(t) = (\underline{A} + \alpha\underline{I})\,\underline{x}(t) + \underline{B}\,\underline{u}(t) \tag{3.34}$$

It follows from the proof of Theorem 2.3, and the property of Hamiltonian Systems, that the eigenvalues $\tilde{\lambda}_i$ of the matrix $(\underline{Z}_\alpha - \alpha I)$ positioned to the left of $\sigma = -\alpha$ are the closed loop eigenvalues of the RPDS obtained in Theorem 2.3. We can therefore obtain $\frac{\partial \lambda_i}{\partial \alpha}$ by computing $\frac{\partial \tilde{\lambda}_i}{\partial \alpha}$ for $\tilde{\lambda}_i = \lambda_i$. To determine $\frac{\partial \tilde{\lambda}_i}{\partial \alpha}$, simply use the following lemma which follows easily from the result of Lemma 3.3. The proof of which is omitted.

Lemma 3.4 For all values of $\alpha > 0$ and any distinct eigenvalue $\tilde{\lambda}_i$ of $\underline{Z}_\alpha$, we have

$$\frac{\partial \tilde{\lambda}_i}{\partial \alpha} = \frac{-2\, \underline{v}_i^H \underline{\zeta}_i}{\underline{w}_i^H \underline{x}_i + \underline{v}_i^H \underline{\zeta}_i} \tag{3.35}$$

where

$$[\tilde{\lambda}_i \underline{I} - \underline{Z}_\alpha + \alpha \underline{I}] \begin{bmatrix} \underline{x}_i \\ \underline{\zeta}_i \end{bmatrix} = \underline{0} \tag{3.36}$$

and

$$[\underline{w}_i^H \; \underline{v}_i^H] \; [\tilde{\lambda}_i \underline{I} - \underline{Z}_\alpha + \alpha \underline{I}] = \underline{0} \tag{3.37}$$

Remark If the right eigenvectors $[\underline{x}_i^T \; \underline{\zeta}_i^T]^T$ and the left eigenvectors $[\underline{w}_i^H \; \underline{v}_i^H]^T$ of $\underline{Z}_\alpha - \alpha \underline{I}$, are available as is the case when solving the algebraic Riccati equation using diagonalization method (see Chapter 3 of [Kw 1]), the computational effort required to obtain $\frac{\partial \lambda_i}{\partial \alpha}$ using (3.35) is negligible. This is a definite advantage over the method introduced in Leamma 2.3 which involves solving a nth order Lyapunov equation.

3.4 Asymptotic Behavior of RPDS Root-Loci

In this section, we examine the behavior of RPDS root-loci as the weight on the control vector goes to zero(or infinity). More precisely, the following problem is considered.

Given a LQ regulator problem with cost functional

$$J = \lim_{t_1 \to \infty} \int_0^{t_1} e^{2\alpha t} \, [\underline{x}(t)^T \, \underline{Q} \, \underline{x}(t) + \underline{u}^T(t) \, \rho \underline{R} \, \underline{u}(t)] dt; \qquad \rho > 0 \tag{3.38}$$

and dynamic constraint

$$\dot{\underline{x}}(t) = \underline{A} \, \underline{x}(t) + \underline{B} \, \underline{u}(t) \tag{3.39}$$

Our objective is to study the root-loci traced by the closed-loop regulator poles as ρ varies. We first consider the case of a single-input RPDS in section 3.4.1. Then we extend these results to the multiple-input case in section 3.4.2.

3.4.1 The Single-Input Case

Assume a state weighting matrix of the form

$$\underline{Q} = \underline{c}\,\underline{c}^T \tag{3.40}$$

where $(\underline{c}^T, \underline{A})$ is observable. If $\alpha = 0$, this reduces to a conventional optimal root-locus problem. Either the root-square locus method of Chang [Chg 1] or the root-locus method of Kwakernaak and Sivan [Kw 1] may be used for this purpose.

In order to adapt these techniques to cases where $\alpha > 0$, we will used the transformed LQ problem employed in the proof of Theorem 2.3. The cost functional and the dynamic constraints are given by

$$J = \lim_{t_1 \to \infty} \int_0^{t_1} [\tilde{\underline{x}}(t)\ \underline{Q}\ \tilde{\underline{x}}(t) + \tilde{\underline{u}}(t)\ \underline{R}\ \tilde{\underline{u}}(t)]dt \tag{3.41}$$

and

$$\dot{\tilde{\underline{x}}}(t) = (\underline{A} + \alpha \underline{I})\ \tilde{\underline{x}}(t) + \underline{B}\ \tilde{\underline{u}}(t) \tag{3.42}$$

respectively, where $\tilde{x}(t) = e^{\alpha t}\ \underline{x}(t)$ and $\tilde{\underline{u}}(t) = e^{\alpha t}\ \underline{u}(t)$. This transformed problem is in a form where conventional optimal root-loci techniques are applicable. Moreover, recall from our discussion of Theorem 2.4 that the closed-loop regulator poles of the original problem can be easily obtained by subtracting α from those of the transformed problem. We can therefore plot the optimal root-loci of RPDS as a functional of ρ in two steps.

Step 1: Plot the optimal root-locus of the transformed LQ regulator problem using conventional techniques.

Step 2: Shift the entire root loci to the left by $-\alpha$.

The following theorem summarizes the asymptotic properties of RPDS root-loci in the single-input case.

Theorem 3.1 Consider the LQ regulator problem with cost functional (3.41) and dynamic constraint (3.42) where u(t) is a scalar. Suppose that $(\underline{A}, \underline{b})$ is controllable and that $\underline{Q}$ has the form $\underline{Q} = \underline{c}\,\underline{c}^T$ where $(\underline{c}^T, \underline{A})$ is observable. Let the transfer function $\underline{c}^T(s\underline{I} - \underline{A})^{-1}\underline{b}$ be

$$\underline{c}^T (s\underline{I} - \underline{A})^{-1} \underline{b} = k \frac{\prod_{i=1}^{p} (s - \nu_i)}{\prod_{i=1}^{n} (s - \pi_i)} \quad ; \quad k \neq 0 \tag{3.43}$$

where ν_i's and π_i's are the zeroes and poles of the transfer function $\underline{c}^T(s\underline{I} - \underline{A})^{-1}\underline{b}$ respectively.

Then the following properties hold

(a) If ρ approaches 0, p of the n closed-loop poles of the RPDS asymptotically approach the number ν_i, i = 1,2.....p where

$$\hat{\nu}_i = \begin{cases} \nu_i & \text{if } \mathrm{Re}(\nu_i) \leq -\alpha \\ -\nu_i - 2\alpha & \text{if } \mathrm{Re}(\nu_i) > -\alpha \end{cases} \tag{3.45}$$

(b) As ρ approaches 0, the remaining n-p optimal closed-loop poles asymptotically approach straight lines which intersect at $(-\alpha, 0)$ and make angles with the negative real axis of magnitude

$$\begin{cases} \pm \ell \dfrac{\pi}{n-p} & \ell = 0,1,2,\ldots \dfrac{n-p-1}{2} \text{ if } n-p \text{ is odd} \\ \pm \dfrac{(\ell+\frac{1}{2})\pi}{n-p} & \ell = 0,1,2,\ldots \dfrac{n-p}{2} - 1 \text{ if } n-p \text{ is even} \end{cases} \tag{3.46}$$

These faraway closed-loop poles of RPDS are asymptotically at a distance $\omega_o = \left(\frac{k^2}{\rho}\right)^{\frac{1}{2(n-p)}}$ from $(-\alpha, 0)$. Moreover, k is independent of α.

(c) As ρ approaches ∞, then n closed-loop poles approach the numbers $\hat{\pi}_i$, $i = 1,2,3,\ldots n$ where

$$\hat{\pi}_i = \begin{cases} \pi_i & \text{if } Re(\pi_i) \leq -\alpha \\ -\pi_i - 2\alpha & \text{if } R_e(\pi_i) > -\alpha \end{cases} \tag{3.47}$$

Proof: When $\alpha = 0$, Theorem 3.1 reduces to Theorem 3.11 of [Kw 1]. The cases where $\alpha > 0$ trivially follow from the construction procedure of the RPDS root-loci described above.

The following example gives several root-loci plots obtained using the previous construction procedure.

Example 3.1 Consider the RPDS problem with cost functional given by

$$J = \lim_{t_1 \to \infty} \int_0^{t_1} e^{2\alpha t} \left[\underline{x}^T(t) \begin{bmatrix} 2 \\ 1 \end{bmatrix} [2 \quad 1] \, \underline{x}(t) \right] + \rho \, u^2(t) \Big] dt \tag{3.48}$$

subject to the dynamic constraint

$$\dot{\underline{x}}(t) = \begin{bmatrix} 0 & 1 \\ -3 & -4 \end{bmatrix} \underline{x}(t) + \begin{bmatrix} 0 \\ 1 \end{bmatrix} u(t) \qquad (3.49)$$

The transfer function $\underline{c}^T(s\underline{I} - \underline{A})^{-1}\,\underline{b}$ is given by $\frac{s+2}{(s+3)(s+4)}$. The loci of the closed-loop poles corresponding to RPDS design with values of α equal to 0,1,2.5 and 3.0 are plotted in Fig. 3.1 a,b,c and d respectively.

As expected, the RPDS root-loci lie to the left of the $\sigma = -\alpha$ line in all 4 cases. When the value of α is less than 2.0, one of the closed-loop pole is drawn to -2.0 with the remaining pole going off to infinity along the negative real axis. (Thus forming a first order Butterworth pattern). In cases where α is larger than 2.0, the finite poles approach $-2.0\alpha + 2.0$ asymptotically. (Property (a) of Theorem 3.1).

It is interesting to note that $-2.0\alpha + 2.0$ equals 3.0 when $\alpha = 2.5$. As a result, the open-loop pole located at -3.0 remains fixed as ρ varies (Fig.3.1c)

Property (a) of Theorem 3.1 has important design implications. Let us consider a LQ state feedback design configuration of the form depicted in Fig. 3.2 where the output matrix $\underline{c}^T$ in the figure is identical to the square root of the state weighting matrix $\underline{Q}$ in (3.48). If $\alpha = 0.0$ and if $\underline{c}^T(s\,\underline{I} - \underline{A})^{-1}\,\underline{b}$ is minimum phase, then by Theorem 3.1 the p finite closed-loop poles will asymptotically approach the p minimum phase zeroes of $\underline{c}^T(s\,\underline{I} - \underline{A})^{-1}\,\underline{b}$ as ρ approaches 0. These finite modes are therefore hidden from the output y(t). The remaining n-p visible modes form a Butterworth pattern which is known to give step response of small overshoot. In cases where $\alpha > 0$, the root-loci are constrained to lie to the left of $\sigma = -\alpha$. By property (a) of Theorem 3.1, the p finite modes will be hidden from the output only if the p minimum phase zeroes of

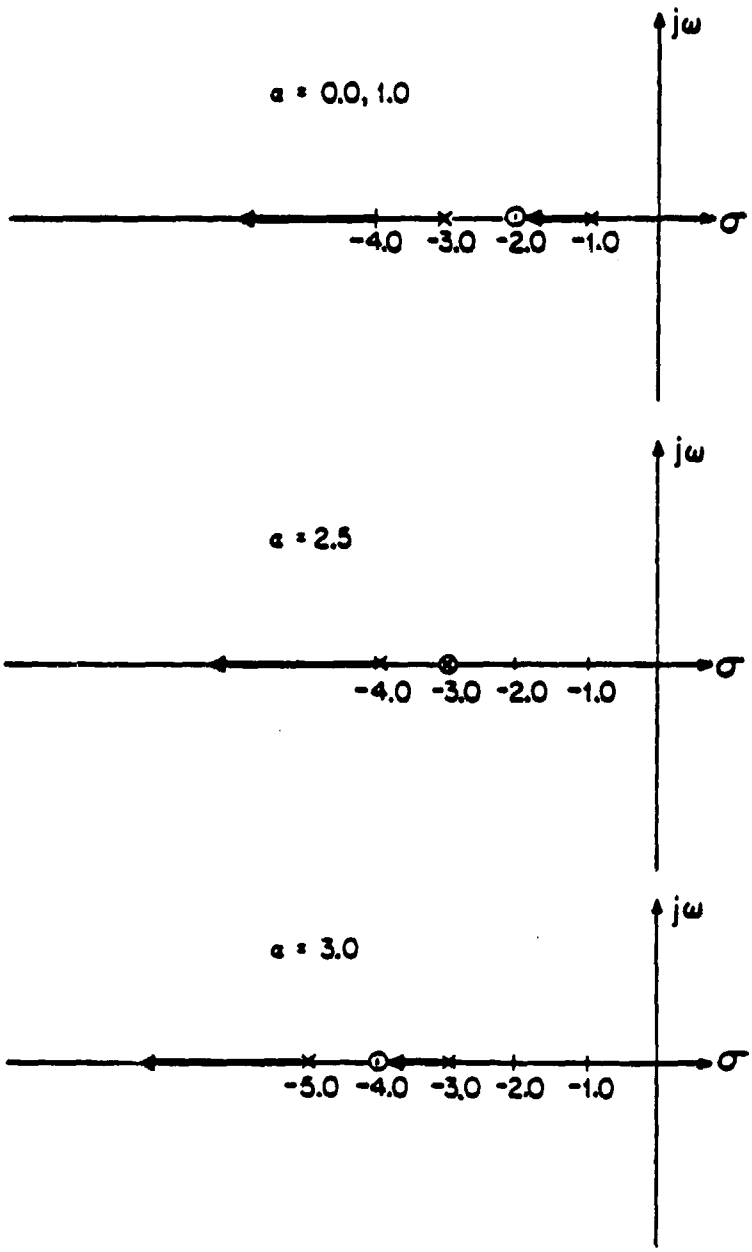

FIG. 3.1 Root-Loci of a Single-Input RPDS with Different Values of α

$\underline{c}^T(s\ \underline{I} - \underline{A})^{-1}\ \underline{b}$ are located to the left of $\sigma = -\alpha$.

In light of the above observation, one needs to exercise caution in using RPDS for state feedback design. If the finite optimal poles can be made 'reasonably' unobservable at an acceptable bandwidth, then the use of RPDS may not be desirable since it may introduce some slow modes in the observed output which would otherwise be absent. However, there may be situations where excessive bandwidth is required before some of the finite modes are made unobservable in the output. It is advantageous in such cases to consider the use of RPDS so that the finite modes that appear in the output are guaranteed to decay at a certain rate.

The following example demonstrates the relationship between the stability factor α and the observed output $y(t)$ as the weight on the control becomes vanishingly small.

Example 3.2 Consider a RPDS state feedback arrangement of the form shown in Fig. 3.2. The underlying system dynamics is specified by the differential equation (3.49) and the state variables $\underline{x}(t)$ are related by the observed output $y(t)$ by $y(t) = [2,1]\ \underline{x}(t)$. The RPDS state feedback gain $\underline{G}_\alpha$ is obtained by solving the RPDS problem described in Example 3.1 with α chosen to be 1.0 and 3.0 and the scaling factor ρ in (3.48) set to 10000.

An initial state perturbation equal to $[10,10]^T$ is applied. The resulting time simulation for the observed output $y(t)$ and the control $u(t)$ are plotted for the closed-loop RPDS systems with $\alpha = 1.0$ (Fig.3.3(a)) and $\alpha = 3.0$ (Fig. 3.3(b)).

Despite the presence of a slow mode near -2 (Recall from Example 3.1

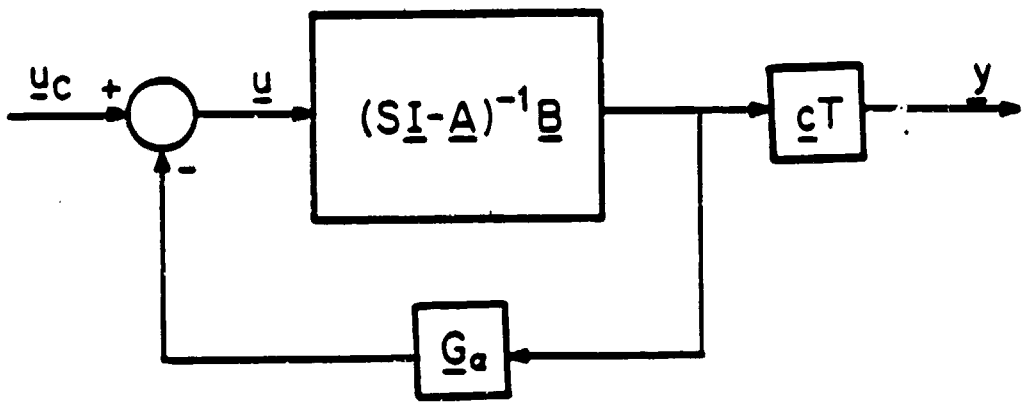

FIG. 3.2 RPDS State Feedback Configuration

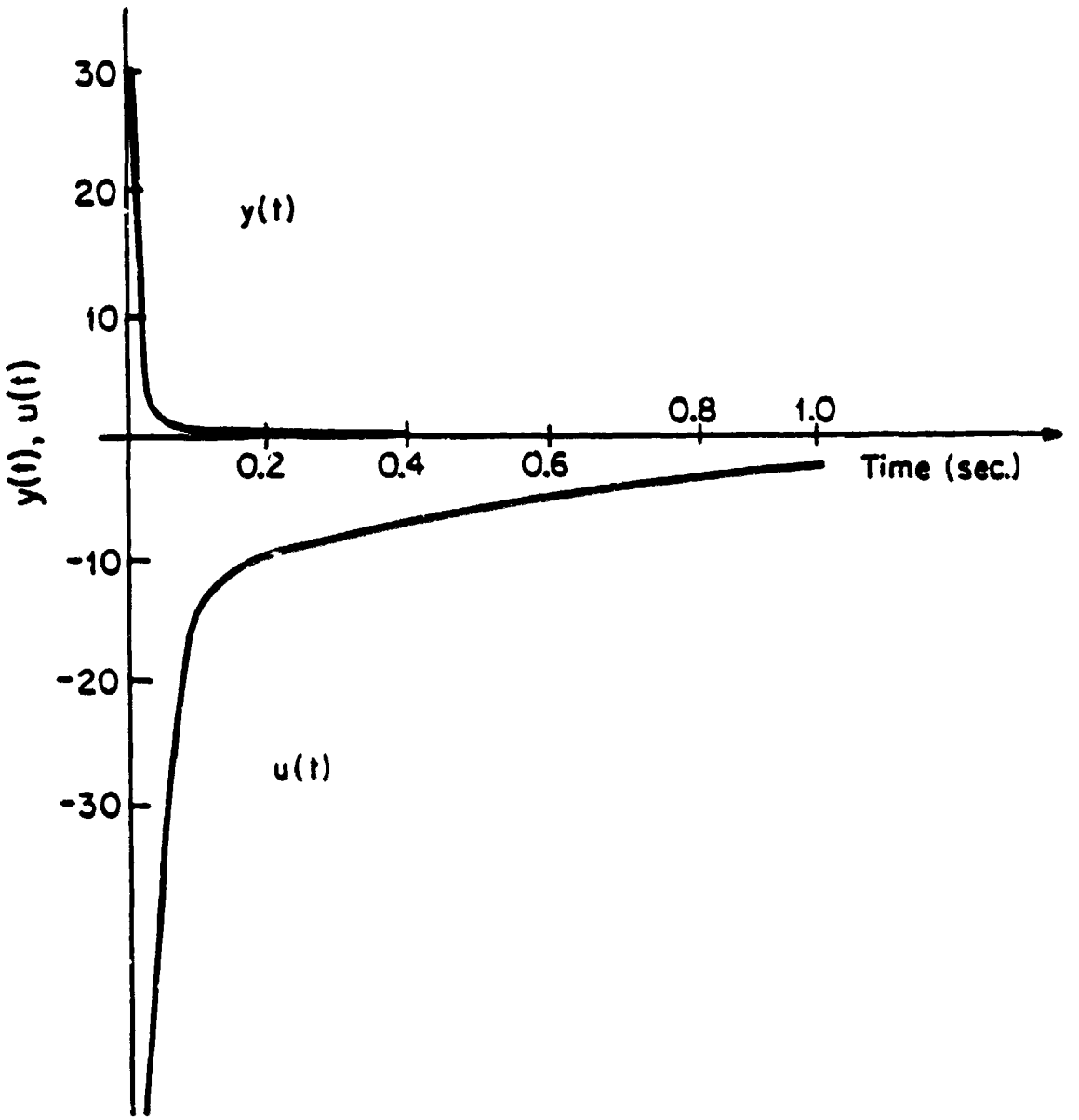

FIG. 3.3 (a) Time Response of a RPDS where the Slow Mode is Cancelled by the System Zero

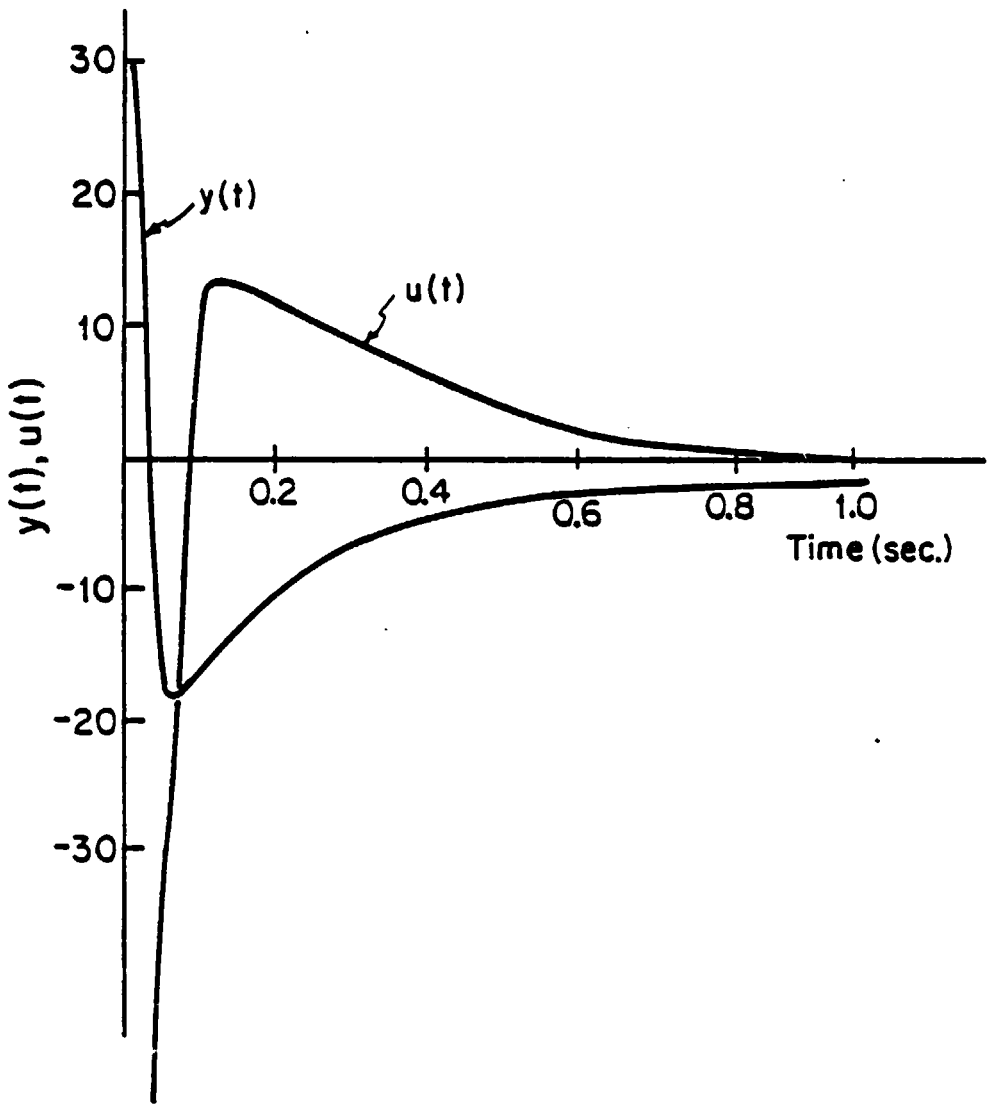

FIG. 3.3 (b) Time Response of a RPDS where the Slow Mode is not Cancelled by the System Zero

and Fig. 3.1), the RPDS design with $\alpha = 1.0$ is noted to decay rapidly. This is a result of the fact that the closed-loop eigenvalue near -2 is hidden from the output y(t) as a result of pole-zero cancellation. However, the same type of cancellation does not occur for the design with α equal to 3.0. In this case, all the closed-loop poles are constrained to lie to the left of $\sigma = -3.0$ line, thus preventing them from being hidden by the system zero at -2.0. This is evident from the slower decay observed in this case.

The presence of the slow mode is also responsible for the relatively long settling time of the feedback signal u(t) observed in both Figs.3.3(a) and (b).

3.4.2 The Multiple-Input Case

The procedure described for constructing the RPDS root-loci in the single-input case is equally applicable to the multiple-input case. The asymptotic behavior of the modes that stay finite as ρ approaches 0 are the same for both cases. However, the far-off closed-loop poles in the multiple-input case generally do not form a single Butterworth pattern, but group into several Butterworth configurations of different orders and different asymptotic raii. The exact detail of such patterns is not considered here. Interested readers may consult [St 1] and [Kw 2] for a thorough treatment of this subject. The corresponding multiple-input RPDS results are summarized in Theorem 3.2 and demonstrated in Example 3.3.

Theorem 3.2 Consider the LQ regulator problem with cost functional (3.38) and dynamical constraint (3.39). Suppose that ($\underline{A}$, $\underline{B}$) is controllable and

that $\underline{Q}$ is of the form $\underline{Q} = \underline{C}\,\underline{C}^T$ where $\underline{C}$ has the same rank as $\underline{B}$, and where $(\underline{C}^T, \underline{A})$ is observable. Let $\underline{H}(s)$ be the transfer function matrix

$$\underline{H}(s) = \underline{C}^T(S\,\underline{I} - \underline{A})^{-1}\,B \tag{3.50}$$

Suppose that $\phi(s) = \det(s\underline{I} - \underline{A})$ and write

$$\det\,(\underline{H}(s)) = \frac{\psi(s)}{\phi(s)} = k\,\frac{\prod_{i=1}^{p}(s - \nu_i)}{\prod_{i=1}^{n}(s - \pi_i)} \tag{3.51}$$

where $k \neq 0$ and where the π_i's are the poles of $\underline{A}$. Then the following facts hold.

(a) As ρ approaches 0, p of the optimal closed-loop poles approach the values $\tilde{\nu}_i$, $i = 1,2,\ldots\ p$ where

$$\tilde{\nu}_i = \begin{cases} \nu_i & \text{if } \mathrm{Re}(\nu_i) \leq -\alpha \\ -\nu_i - 2\alpha & \text{if } \mathrm{Re}(\nu_i) > -\alpha \end{cases} \tag{3.52}$$

The remaining closed-loop poles go to infinity and group into several Butterworth configurations of different orders and different radii.

(b) As ρ approaches ∞, the n closed-loop RPDS poles approach the numbers $\tilde{\pi}_i$, $i = 1,2,\ldots n$ where

$$\tilde{\pi}_i = \begin{cases} \pi_i & \text{if } \mathrm{Re}(\pi_i) \leq -\alpha \\ -\pi_i - 2\alpha & \text{if } \mathrm{Re}(\pi_i) > -\alpha \end{cases} \tag{3.53}$$

Proof: The results follow trivially from Theorem 3.12 of [Kw 1] and the root-loci construction procedure described above. The detail of the proof is omitted.

Example 3.3 Consider the following multiple-input RPDS problem

$$\min_{\underline{u}(t)} J = \lim_{t_1 \to \infty} \int_0^{t_1} e^{2\alpha t} [\underline{x}^T \underline{C} \underline{C}^T \underline{x}(t) + \underline{u}^T(t) \underline{u}(t)]dt \qquad (3.54)$$

where

$$\underline{C} = \begin{bmatrix} 0 & -5 & 2 & -2 \\ 8 & -14 & 0 & 2 \end{bmatrix}^T \qquad (3.55)$$

and subject to the dynamic constraint

$$\underline{\dot{x}}(t) = \begin{bmatrix} -6 & 7 & 1 & 13 \\ 0 & 1 & 0 & 2 \\ 4 & 7 & -6 & 8 \\ 0 & -1 & 0 & 2 \end{bmatrix} \underline{x}(t) + \begin{bmatrix} 0 & 1 \\ 1 & 0 \\ 2 & 0 \\ -2 & 0 \end{bmatrix} \underline{u}(t) \qquad (3.56)$$

It can be readily shown that the system zeroes for $[\underline{A}, \underline{B}, \underline{C}^T]$ are located at $-1.0 + j\,1.0$. The loci of the closed-loop poles corresponding to RPDS designs with values of α equal to 0.0, 0.5 and 2.0 are plotted in Figure 3.4 a,b,c respectively. In all three cases, the various branches of the loci stay in the half plane to the left of the $-\alpha$ line. Moreover, two of the four branches asymptotically approach infinity along the negative real axis, forming two first-order Butterworth patterns. The asymptotic behavior of the two remaining branches depends on the value of α. For α less than +1.0, these branches eventually arrive at

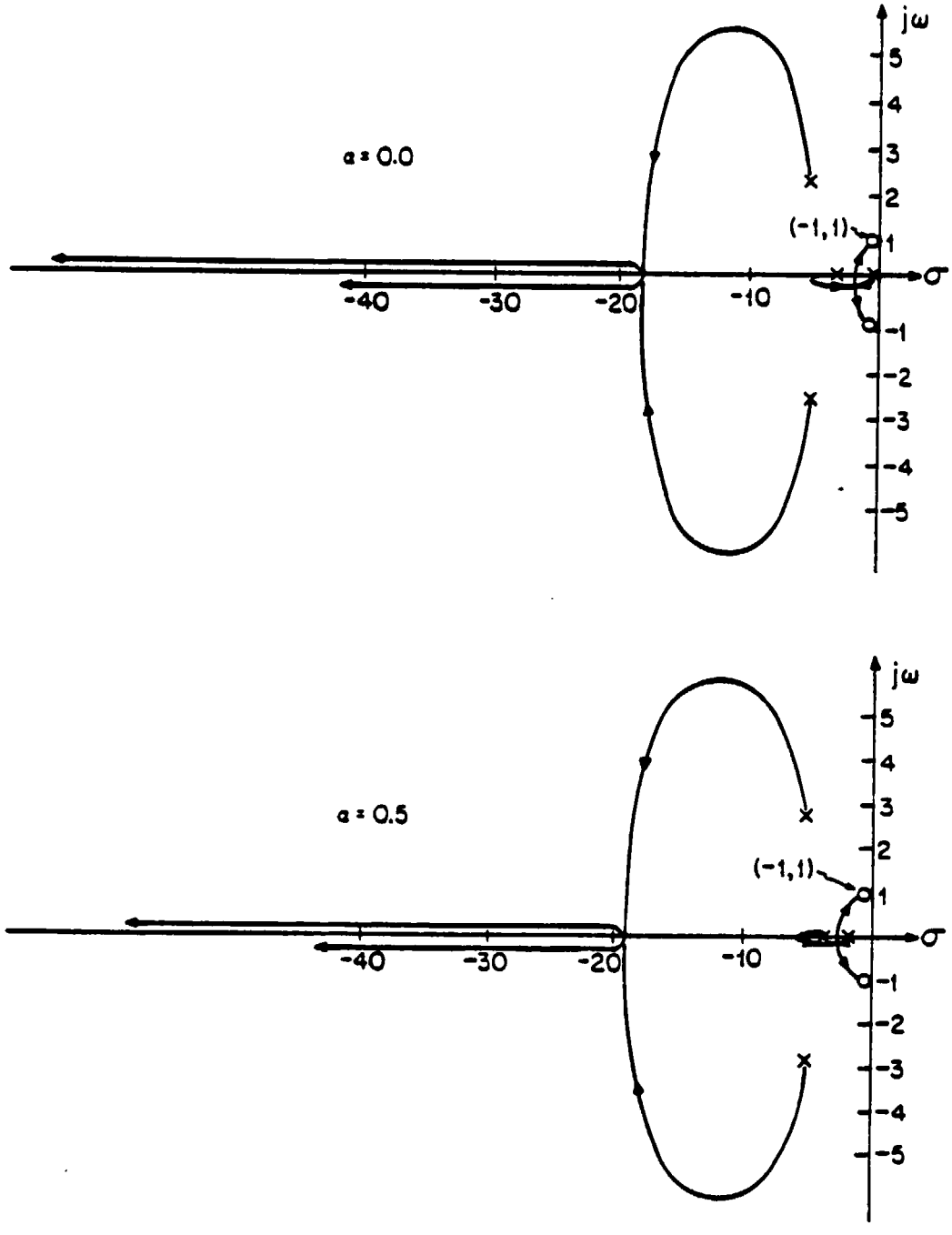

FIG. 3.4 Root-Loci of a Multiple-Input RPDS with Different Values of α

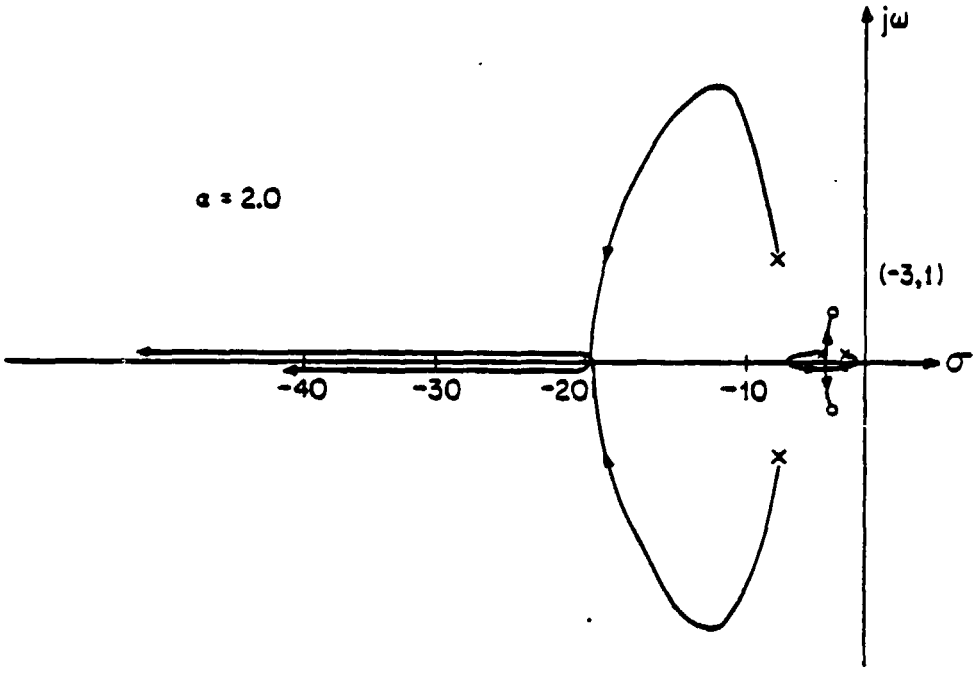

FIG. 3.4 Root-Loci of a Multiple-Input RPDS with Different Values of α

continuation from pg 59

the system zeroes $-1.0 \pm j\ 1.0$. If α is larger than 1.0, these branches approach instead $-2\alpha + 1 \pm j\ 1.0$.

3.4 Regulators with Prescribed Damping Ratio

A class of LQ regulators are those with prescribed damping ratio (RPDR). A LQ regulator is said to have a damping ratio $\cos\theta$ if it is stable and each of its closed-loop poles $\sigma_i \pm j\omega$ satisfies $\left|\frac{\sigma_i}{\omega_i}\right| \leq \tan\theta$ for some given θ. Diagramatically (Figure 1.2), all the closed-loop poles are found in a cone centered at the origin of the complex plane with edges extending along an angle of size 2θ which is symmetric about the negative real axis. For stability, the value of θ has to lie between 0 and $\frac{\pi}{2}$. The procedure described in the following theorem solves the RPDR problem as a special case of the RPDS problem.

Theorem 3.3 Consider the following LQ regulator problem

$$\min_{u(t)} J = \lim_{t_1 \to \infty} \int_0^{t_1} e^{2\alpha t} [\underline{x}^T(t) \quad \underline{Q}\,\underline{x}(t) + \underline{u}^T(t)\, \rho \underline{R}\, \underline{u}(t)]dt \quad ; \ \rho > 0 \tag{3.57}$$

subject to the dynamic constraint

$$\dot{\underline{x}}(t) = \underline{A}\,\underline{x}(t) + \underline{B}\,\underline{u}(t) \tag{3.58}$$

Suppose that all the requirements on $\underline{A}$, $\underline{B}$, $\underline{Q}$ and $\underline{R}$ that guarantee the existence of a stable minimizing control law are satisfied and that the scalar ρ is an arbitrary positive constant. The factor α is selected in the following manner. For each open-loop pole $\sigma_i + j\omega_i$ of $\underline{A}$, we associate a positive scalar α_i which is defined by

$$\alpha_i = \begin{cases} 0 & \text{if } \dfrac{|\sigma_i|}{|\omega_i|} < \tan\theta \\ |\sigma_i - (\tan\theta)^{-1}|\omega_i|| \Big/ 2.0 & \text{otherwise.} \end{cases} \tag{3.59}$$

α is then chosen to be the largest of the α_i's and used in (3.57).

Let $\underline{u}(t) = -\underline{R}^{-1}\,\underline{B}^T\,\underline{K}_\alpha\,\underline{x}(t)$ be the feedback control law obtained from the above minimization problem as ρ approaches ∞, where $\underline{K}_\alpha = \lim_{\rho\to\infty} \underline{K}_\alpha(\rho)$ and $\underline{K}_\alpha(\rho)$ is the unique positive definite solution of the algebraic Riccati equation

$$\underline{K}_\alpha(\rho)\,(\underline{A} + \alpha\,\underline{I}) + (\underline{A} + \alpha\,\underline{I})^T\,\underline{K}_\alpha(\rho) - \underline{K}_\alpha(\rho)\,\underline{B}\,\frac{1}{\rho}\,\underline{R}^{-1}\,\underline{B}^T\,\underline{K}_\alpha(\rho) + \underline{Q} = \underline{0} \tag{3.60}$$

The LQ regulator resulting from the application of $\underline{u}(t) = -\underline{R}^{-1}\,\underline{B}^T\,\underline{K}_\alpha\,\underline{x}(t)$ to (3.58) has a damping ratio equal to $\cos\theta$.

Proof: Let $\tilde{\sigma}_i + j\,\tilde{\omega}_i$'s be the poles of the closed-loop system described by $\dot{\underline{x}}(t) = (\underline{A} - \underline{B}\,\underline{R}^{-1}\,\underline{B}^T\,\underline{K}_\alpha)\,\underline{x}(t)$. Applying the results of the property (c) of Theorem 3.2 to the previous minimization problem, we obtain

$$\tilde{\sigma}_i + j\tilde{\omega}_i = \begin{cases} \sigma_i + j\,\omega_i & \text{if } \sigma_i < -\alpha \\ -\sigma_i - j\,\omega_i - 2\alpha & \text{if } \sigma_i \geq -\alpha \end{cases} \tag{3.61}$$

We need to show that for each i, the inequality $\left|\dfrac{\tilde{\omega}_i}{\sigma_i}\right| \leq \tan\theta$ is satisfied. There are two different situations that need to be considered individually.

Case (I) $\left|\dfrac{\omega_i}{\sigma_i}\right| \leq \tan\theta$

It follows from (3.61) that $\tilde{\sigma}_i < -|\sigma_i|$ for all values of σ_i. This

in turn implies that

$$\left|\frac{\omega_i}{\tilde{\sigma}_i}\right| < \left|\frac{\omega_i}{\sigma_i}\right| \leq \tan\theta \tag{3.62}$$

Case(II)

$$\left|\frac{\omega_i}{\sigma_i}\right| > \tan\theta$$

By definition of α, and $|\omega_i| > |\sigma_i| \tan\theta$, we have

$$\begin{aligned} \alpha &> \frac{\left|\sigma_i - \frac{|\omega_i|}{\tan\theta}\right|}{2} \\ &= \frac{\frac{|\omega_i|}{\tan\theta} - \sigma_i}{2} \\ &\geq -\sigma_i \end{aligned} \tag{3.63}$$

Hence $\sigma_i \geq -\alpha$ and $\tilde{\sigma}_i = -\sigma_i - 2\alpha$.

Applying the definition of α and α_i, we obtain

$$\begin{aligned} \tilde{\sigma}_i &= -\sigma_i - 2\alpha \\ &\leq -\sigma_i - 2\alpha_i \\ &= -\sigma_i - 2\left(\frac{|\omega_i|}{\tan\theta} - \sigma_i\right)\Big/ 2 \\ &= \frac{-|\omega_i|}{\tan\theta} \end{aligned} \tag{3.64}$$

It follows from (3.64) and $\omega_i = \tilde{\omega}_i$ (Property (c) of Theorem 3.2) that

$$\left|\frac{\tilde{\omega}_i}{\tilde{\sigma}_i}\right| = \left|\frac{\omega_i}{\sigma_i}\right| \leq \tan\theta \tag{3.65}$$

3.6 Concluding Remarks

We have developed in this chapter several techniques for analyzing the eigenstructure properties of RPDS.

Two methods for computing the sensitivity of the closed-loop RPDS poles with respect to the stability factor α are introduced. The one based on the Hamiltonian system is computationally useful for updating the closed-loop poles given small variation of α.

We also present a two-step procedure for plotting the root-loci for single-input RPDS. This procedure also provides the necessary framework for derivation of asymptotic root-loci properties for multiple-input RPDS. Using the property of the RPDS root-loci as the state weightings become vanishingly small, we obtain a novel one-step solution to the Regulator with Prescribed Damping Ratio problem.

CHAPTER IV

ROBUSTNESS PROPERTIES OF REGULATORS WITH A PRESCRIBED DEGREE OF STABILITY

4.1 Introduction

A critical property of feedback systems is their robustness, i.e. their ability to maintain system performance in the face of uncertainties. In particular, it is important that a closed-loop feedback system remains stable despite the difference between the model used for design and the actual plant in the absence of feedback gain recomputation. Such differences commonly arise as a result of unknown and/or unmodelled dynamics of a plant.

So far in this thesis, we have been looking at RPDS design from a transient response point of view (i.e. the ability of the feedback system to attenuate the initial state perturbation at a prescribed rate). The robustness specifications, commonly quantified in terms of stability margins and noise attenuation requirements, have been absent from the RPDS problem formulation. The purpose of this chapter will be to discuss the robustness properties, particularly those related to stability of RPDS and its dual, the Kalman Bucy filter with a prescribed degree of stability (FPDS).

Many of the results (e.g. Theorems 4.8 and Corollaries 4.2, 4.3 and 4.4) presented in this chapter and their robustness interpretations

have been treated by Anderson and Moore for the single-input RPDS problem. The objective of this chapter is to generalize these results for the single-input case to the multiple-input systems.

Required background for robustness analysis of linear time-invariant MIMO feedback systems is briefly reviewed in Section 4.2. The use of minimum singular values of the return difference and inverse return difference matrices as measures of MIMO feedback system's ability to tolerate modelling uncertainties is emphasized.

In Section 4.3, an appropriate framework for robustness analysis of RPDS is introduced. It is shown that the RPDS state feedback loop can be redrawn as a unity negative feedback system, which is the cannonical feedback structure assumed in the current works on robustness theory. Based on such a framework, the properties of the return difference matrices and the inverse return difference matrices of RPDS and their corresponding robustness implications are studied in Sections 4.4 and 4.5 respectively. RPDS is shown to possess excellent stability margins with respect to the stability and degree of stability properties. However, the ability of RPDS to tolerate modelling uncertainties only improves with increasing value of α under very specific context. Section 4.6 discusses the issue of roll-off requirement at high frequencies. This problem is of importance from the robustness point of view because the quality of a nominal design model inevitably deteriorates at high frequencies as a result of unmodelled and/or unknown dynamics. An explicit relation between the cross-over frequency and the choice of α is derived. The robustness results obtained in Sections 4.4, 4.5 and

4.6 are briefly summarized in Section 4.7.

This chapter closes with a discussion on the dual robustness results of FPDS in Section 4.8.

4.2 Robustness Analysis of Linear Time-Invariant MIMO Systems

The robustness analysis of feedback systems requires the determination of regions about the nominal model for which a particular system property is preserved. We shall focus only on the robustness with respect to the closed-loop stability property.

The importance of obtaining robustly stable feedback control systems has long been recognized ([Bo 1], [Ho 1]). In classical frequency domain techniques for single-input single-output (SISO) control system design, the robustness issue is naturally handled. The various graphical means (e.g. Bode plots, Nyquist diagrams and Nichols charts) for displaying the system model in terms of its frequency response allow the control system designers to determine by inspection the minimum change in the frequency response of the model dynamics that leads to instability. These changes are commonly quantified in terms of the gain and phase margins.[1]

Extension of these SISO robustness measures to the MIMO case is by no means straight forward. A satisfactory notion of stability margins for a multi-loop feedback system must be able to characterize the ability of a system to tolerate gain and phase variations in all of its loops simultaneously. It is not until recently that an appropriate framework for this purpose has become available. The basic work in this

---

[1] Readers are referred to section 3.2 of [Le 1] for a comprehensive discussion of these measures.

area is due to Safonov [Sa 2]. His work was formulated in the time domain and used some basic concepts of functional analysis, as in modern input-output formulation of stability theory. The approach adopted here for analyzing robustness properties of time-invariant RPDS is based on the frequency domain formulation developed by Doyle [Do 4] and Lehtomaki [Le 1].

A review of MIMO system robustness results that are relevant to the subsequent development of this chapter are presented in subsections 4.2.1 to 4.2.4.

4.2.1 Characterization of Model Error

We shall base our discussion for the remainder of this chapter on the unity negative feedback system depicted in Fig. 4.1. $\underline{T}(s)$ is assumed to be a strictly proper rational transfer matrix (i.e. the state space realization has no feedthrough term) which represents the plant and any compensation that is used. The perturbed version of $\underline{T}(s)$ is denoted by $\tilde{\underline{T}}(s)$ where $\tilde{\underline{T}}(s)$ is again a proper rational transfer matrix. Before introducing the various robustness tests for MIMO feedback systems, we need to define some appropriate measures of deviation between $\tilde{\underline{T}}(s)$ and $\underline{T}(s)$. There are many ways that one can represent the model uncertainties. It is important to point out that different types of model error representation will emphasize different aspects of the differences between $\underline{T}(s)$ and $\tilde{\underline{T}}(s)$ and will thus give essentially different assessment of the robustness properties under certain circumstances.[1]

---

[1] For a concrete illustration of this point, readers are referred to section 4.5 of this chapter.

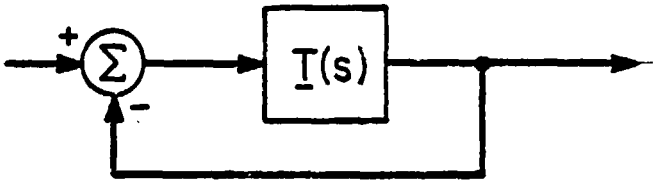

FIG. 4.1 Unity Negative Feedback System with Loop Transfer Matrix Given by $\underline{T}(s)$

Following the notation of [Le 1], we let the matrix $\underline{E}_i(s)$ denote the particular modelling error under consideration where the index i is used to distinguish between different types of error models. The two most intuitive characterizations of model error are given by

$$\underline{E}_1(s) = \tilde{\underline{T}}(s) - \underline{T}(s) \tag{4.1}$$

which is the absolute error in $\underline{T}(s)$ and

$$\underline{E}_2(s) = \underline{T}^{-1}(s)\ (\tilde{\underline{T}}(s) - \underline{T}(s)) \tag{4.2}$$

which is the relative error in $\underline{T}(s)$. It is convenient for the subsequent development to define the multiplicative perturbation matrix $\underline{L}(s)$ by

$$\tilde{\underline{T}}(s) = \underline{T}(s)\ \underline{L}(s) \tag{4.3}$$

Note that $\underline{L}(s)$ has a nominal value of $\underline{I}$. Based on the above definition, we can reexpress (4.2) as

$$\underline{E}_2(s) = \underline{L}(s) - \underline{I} \tag{4.4}$$

A feedback representation of the perturbed system using $\underline{T}(s)$ and $\underline{L}(s)$ is depicted in Fig. 4.2. The two error measures introduced above are obvious multivariable generalization of the error measures $\tilde{t}(s) - t(s)$ and $(\tilde{t}(s) - t(s))/t(s)$ which are commonly employed in classical stability analysis using the Nyquist diagrams.

In view of the use of the inverse transfer function $g^{-1}(s)$ in stability results employing the inverse Nyquist diagram [Ro 1], it seems natural to introduce an alternative definition of the absolute and relative error between the nominal and the perturbed system in terms of $\underline{T}^{-1}(s)$ and $\tilde{\underline{T}}^{-1}(s)$. With this type of error representation, the absolute error is given by

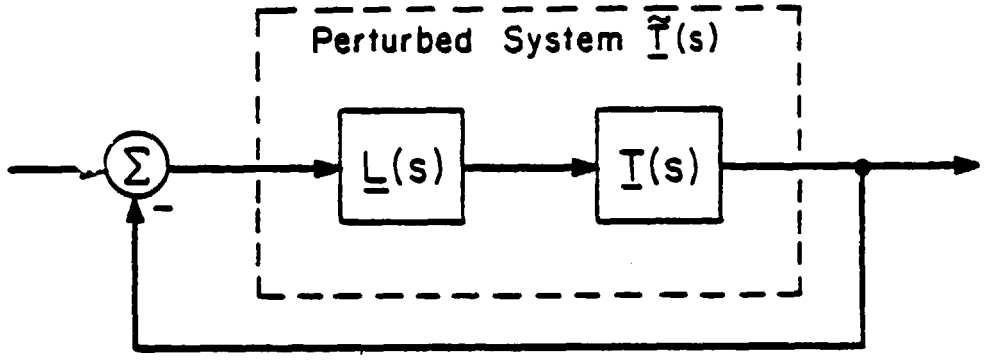

FIG. 4.2 Feedback System with Multiplicative Representation of Uncertainties in $\underline{T}(s)$

$$\underline{E}_3(s) = \tilde{\underline{T}}^{-1}(s) - \underline{T}^{-1}(s) \tag{4.5}$$

and the relative error by

$$\underline{E}_4(s) = (\tilde{\underline{T}}^{-1}(s) - \underline{T}^{-1}(s))\, \underline{T}(s) \tag{4.6}$$

$$= \underline{L}^{-1}(s) - \underline{I} \tag{4.7}$$

Several comments are in order here. First, the absolute type of errors defined above are additive in nature whereas the relative type of errors are multiplicative in nature. While both types of errors can be used to derive robustness theorems, the notions of gain and phase margin are associated only with the relative type of errors. Second, the magnitude of the absolute type of errors is affected by both the modelling uncertainties and the compensator gains. This in turn makes it very difficult to assess the improvement of uncertainty tolerance due to compensator adjustments. Problems of this nature do not occur with relative type of errors, since the scaling effect of the compensator gain is naturally handled by normalization (i.e. by multiplication of $\underline{T}(s)$ and $\underline{T}^{-1}(s)$). In this thesis, we shall only work with robustness theorems that are based on relative type of errors.

4.2.2 Multivariable Nyquist Theorem and its Generalization

All robustness results that we are going to present in the sequel are based on the multivariable Nyquist theorem. This theorem can be stated as follows.

Theorem 4.1 The MIMO system in Fig. 4.1 is closed-loop stable if and only if the image of the Nyquist contour (Fig. 4.3) under the map

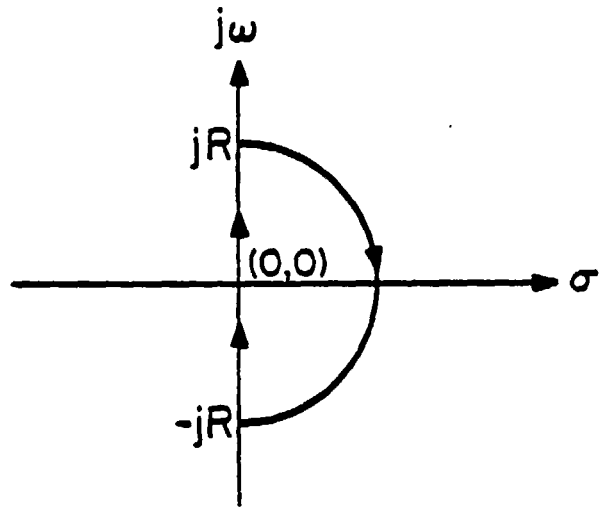

FIG. 4.3 Nyquist Contour Enclosing all the Unstable Open-Loop Poles of $\underline{T}(s)$

det $(\underline{I} + \underline{T}(s))$ encircles the origin P times in the counterclockwise direction where P is the number of unstable poles of $\underline{T}(s)$ that are encircled by the Nyquist contour as the radius R of the half circle becomes sufficiently large.

Remark This theorem is a natural generalization of the familiar Nyquist criterion with $\det(\underline{I} + \underline{T}(s))$ taking the place of $1 + t(s)$. It is derived using the relationship

$$\det(I + \underline{T}(s)) = \frac{\phi_{CL}(s)}{\phi_{OL}(s)} \tag{4.8}$$

where $\phi_{OL}(s)$ and $\phi_{CL}(s)$ are respectively the open-loop and closed-loop characteristic polynomials of the underlying system, and the Principle of Argument of complex variable theory.

Remark The Nyquist diagram of $\det(\underline{I} + \underline{T}(s))$ is commonly called the multivariable Nyquist diagram. Despite the similarity in form between the above theorem and the Nyquist criterion for SISO system, it is not possible to infer robustness properties of a MIMO system by inspection of its multivariable Nyquist diagram. In other words, the distance between the multivariable Nyquist diagram to the origin of the complex plane does not constitute an appropriate measure of stability margin. The reason for this will become clear in the next section.

The multivariable Nyquist theorem provides a procedure for checking the presence of closed-loop poles inside the domain enclosed by the Nyquist contour. Generalization of such procedure to regions enclosed by other contours in the complex plane is straightforward.

This can be accomplished by plotting the image of the contour in question under the map $\det(I + \underline{T}(s))$ and counting the resulting number of encirclements about the origin. If this number turns out to be identical to the number of open-loop poles enclosed by the countour of interest, we can then conclude the absence of closed-loop poles inside the region enclosed by such contour.

Remark A rigorous justification of the above discussion follows directly from the application of the Principle of Argument and (4.8).

A contour of significance for the analysis of feedback systems is the α - Nyquist contour. This contour is obtained from the conventional Nyquist contour by shifting the $j\omega$-axis to the line $\sigma = -\alpha$ (see Fig.4.4) Applying the procedure discussed above to this contour results in a graphical test for checking the degree of stability. A precise description of this result is given in the following theorem.

Theorem 4.2 The MIMO system in Fig. 4.1 has a degree of stability α if and only if the image of the α - Nyquist contour (Fig. 4.4) under the map $\det(I + \underline{T}(s))$ encircles the origin P times in the counterclockwise direction where P is the number of poles of $\underline{T}(s)$ that are enclosed by the α - Nyquist contour as the radius R of the half circle becomes sufficiently large.

Remark The SISO version of the above theorem was employed by Anderson and Moore [An 1] for interpretation of KPDS rebustness properties.

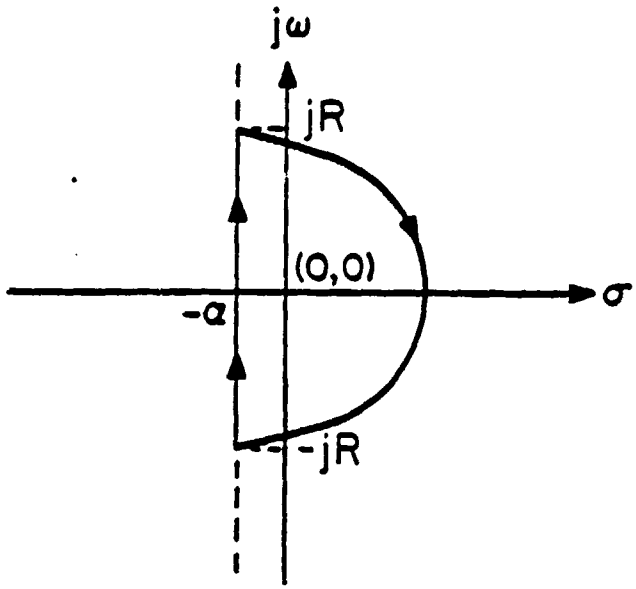

FIG. 4.4 α-Nyquist Contour Enclosing All the Poles of $\underline{T}(s)$ with Real Part Larger than $-\alpha$

4.2.3 Robustness Theorems for MIMO Systems

In this section, we review several theorems that are key to the study of RPDS robustness properties. The derivation of these results from the basic theorems (Theorems 4.1 and 4.2) are sketched in a tutorial fashion. For convenience, we will assume that in all the remaining theorems and corollaries, the Nyquist contour (α-Nyquist contour) is chosen with R sufficiently large so that Theorem 4.1 (Theorem 4.2) may be applied.

Suppose that the nominal closed-loop system in Fig. 4.1 is stable and that $\underline{T}(s)$ and $\tilde{\underline{T}}(s)$ have the same number of unstable poles. Then it follows from Theorem 4.1 that the perturbed system is stable if and only if the image of the Nyquist contour under $\det(I + \underline{T}(s))$ and $\det(I + \tilde{\underline{T}}(s))$ have the same number of encirclements about the origin.

Consider the case where $\tilde{\underline{T}}(s)$ is a continuous deformation of $\underline{T}(s)$. For a sufficiently small deformation, the number of encirclements of the multivariable Nyquist diagram about the origin stays unchanged. Consequently, the perturbed system will remain stable. However, if the deformation makes the multivariable Nyquist diagram crossing the origin, the number of encirclements about the origin will change as a result and the perturbed system becomes unstable. The point where crossing of the origin takes place is characterized mathematically by

$$\det(I + \tilde{\underline{T}}_0(j\omega)) = 0 \tag{4.9}$$

for some value of $\omega \geq 0$ where $\tilde{\underline{T}}_0(s)$ is the deformation of $\underline{T}(s)$ that touches the origin for the first time. This point clearly marks the borderline between stability and instability. It seems natural from

the above discussion to characterize the stability margin of a system at each frequency ω by the nearness of the nominal return difference matrix $(I + \underline{T}(j\omega))$ to singularity.

The determinant $\det(I + \underline{T}(j\omega))$ appears to be an obvious candidate for such measure since the determinant of a matrix is zero if and only if it is singular. Moreover, the size of $\det(I + \underline{T}(s))$ at each frequency ω can be readily obtained by inspection of the multivariable Nyquist diagram. Unfortunately, the determinant of a nonsingular matrix turns out to be an unreliable measure of closeness to singularity. It is well known that a matrix with a reasonably large determinant can be made singular by a small perturbation (compared with the determinant of its elements). The standard measure for closeness to singularity of a matrix is given in terms of the matrix norms. When the 2-norm is used (as is the case of this thesis), the distance from singularity for a given matrix $\underline{A}$ is quantified by the minimum singular value $\sigma\min(\underline{A})$.[1] The precise use of $\sigma\min(\underline{A})$ in detection of closeness to singularity is given in the following theorem.

Theorem 4.3 Given a nonsingular complex matrix $\underline{A}$, a solution to the following minimization problem

$$\min \|\underline{E}\| : \underline{A} + \underline{E} \quad \text{is singular} \tag{4.10}$$

is given by

$$\|\underline{E}\| = \sigma\min(\underline{A}) \tag{4.11}$$

and

$$\underline{E} = \sigma\min(\underline{A})\, \underline{U}\, \underline{V}^H \tag{4.12}$$

[1] Readers unfamiliar with singular value may refer to [Str 1] for an overview of their properties

where $\underline{U}$ and $\underline{V}$ are the right and left singular vectors of $\underline{A}$ corresponding to $\sigma\min(\underline{A})$.

In other words, if $\underline{A} + \underline{E}$ is singular, then

$$||\underline{E}|| = \sigma\max(\underline{E}) \geq \sigma\min(\underline{A}) \tag{4.13}$$

The following corollary to Theorem 4.3 is the key to the derivation of robustness theorems that are based on the multivariable Nyquist theorem.

Corollary 4.1 Let $\underline{A}$ be a nonsingular complex matrix and

$$\sigma\max(\underline{E}) < \sigma\min(\underline{A}) \tag{4.14}$$

then $\underline{A} + \underline{E}$ is nonsingular.

Remark The condition (4.14) is sufficient but not necessary, because only magnitude information of $\underline{A}$ and $\underline{E}$ are employed.

Before applying the previous corollary to derive the robustness theorems for MIMO feedback systems, note that we can rewrite the perturbed return difference matrix

$$\underline{I} + \tilde{\underline{T}}(s) = \underline{I} + \underline{T}(s)\,\underline{L}(s) \tag{4.15}$$

in two different ways

$$\begin{aligned} I + \underline{T}(s)\,\underline{L}(s) &= (\underline{L}^{-1}(s) + \underline{T}(s))\,\underline{L}(s) \\ &= [(\underline{I} + \underline{T}(s)) + (\underline{L}^{-1}(s) - \underline{I})]\,\underline{L}(s) \end{aligned} \tag{4.16}$$

and

$$\begin{aligned} I + \underline{T}(s)\,\underline{L}(s) &= \underline{T}(s)\,(\underline{T}^{-1}(s) + \underline{L}(s)) \\ &= \underline{T}(s)\,[(\underline{I} + \underline{T}^{-1}(s)) + (\underline{L}(s) - \underline{I})] \end{aligned} \tag{4.17}$$

Direct application of Corollary 4.1 to (4.15) results in the following condition that guarantees the nonsingularity of $(\underline{I} + \underline{T}(s)\ \underline{L}(s))$.

$$\sigma\max(\underline{L}^{-1}(s) - \underline{I}) < \sigma\min(I + \underline{T}(s)) \tag{4.18}$$

In view of the discussion at the beginning of this section, it is clear that any perturbation matrix $\underline{L}(s)$ satisfying condition (4.18) for all values of s along the Nyquist contour will not destabilize the closed-loop system. This result is formally stated in the following theorem.

Theorem 4.4 If the MIMO feedback system in Fig. 4.1 is stable, then the perturbed system in Fig. 4.2 is stable if

(i) $\underline{T}(s)$ and $\tilde{\underline{T}}(s) = \underline{T}(s)\ \underline{L}(s)$ have the same number of unstable poles (4.19)

(ii) $\underline{T}(s)$ has no pole along the $j\omega$-axis[1] (4.20)

(iii) $\underline{L}(j\omega)$ has no eigenvalue at 0 or on the negative real axis for $\omega \geq 0$ (4.21)

(iv) $$\sigma\max(\underline{L}^{-1}(j\omega) - I) = \sigma\max(\underline{E}_4(j\omega)) < \sigma\min\ (\underline{I} + \underline{T}(j\omega)) \tag{4.22}$$

where $$\underline{E}_4(s) = (\tilde{\underline{T}}^{-1}(s) - \underline{T}^{-1}(s))\ \underline{T}(s) \tag{4.23}$$

Another useful nonsingularity characterization of $(I + \underline{T}(s)\ \underline{L}(s)))$ is provided by the condition

$$\sigma\max(\underline{L}(s) - I) < \sigma\min(I + \underline{T}^{-1}(s)) \tag{4.24}$$

This is readily obtained by applying Corollary 4.1 to the alternative

---

[1] This condition can be relaxed by indenting the Nyquist contour along the $j\omega$-axis at locations of open-loop imaginary poles

expression of $\underline{I} + \underline{T}(s)\ \underline{L}(s)$ as given in (4.17). The related robustness theorem is stated below.

Theorem 4.5 If the MIMO feedback system in Fig. 4.1 is stable, then the perturbed system in Fig. 4.2 is stable if

(i) $\underline{T}(s)$ and $\tilde{\underline{T}}(s) = \underline{T}(s)\ \underline{L}(s)$ have the same number of unstable poles (4.25)

(ii) $\underline{T}(s)$ has no pole on the $j\omega$-axis (4.26)

(iii) $\sigma\max(\underline{L}(j\omega) - \underline{I}) = \sigma\max(\underline{E}_3(j\omega)) < \sigma\min(\underline{I} + \underline{T}^{-1}(j\omega))$ for all $\omega \geq 0$ (4.27)

where $\underline{E}_3(s) = \underline{T}^{-1}(s)(\tilde{\underline{T}}(s) - \underline{T}(s))$ (4.28)

Remark Strictly speaking, the arguments given above are not enough to prove the robustness theorems in this section. A major part that has been omitted is the embedding argument which ensures that the perturbed multivariable Nyquist diagram associated with $\underline{I} + \tilde{\underline{T}}(j\omega)$ can be reached through a continuous deformation of the original Nyquist diagram which preserves the number of encirclement of the origin. The results presented in Theorems 4.4 and 4.5 are however correct. Readers interested in more technical details should consult [Le 1].

We shall make several brief comments on the relationship between Theorems 4.4 and 4.5. Observe from inequalities (4.22) and (4.27) that as $\sigma\min(\underline{I} + \underline{T}(j\omega))$ and $\sigma\min(\underline{I} + \underline{T}^{-1}(j\omega))$ increases, bounds on the respective kind of model error become less stringent. For purpose of improving the system's ability to tolerate uncertainties, it would

seem desirable to make both the quantities $\sigma\min(I + \underline{T}(j\omega))$ and $\sigma\min(I + \underline{T}^{-1}(j\omega))$ as large as possible. This is however impossible because the return difference matrix $(I + \underline{T}(j\omega))$ and the inverse return difference matrix $(I + \underline{T}^{-1}(j\omega))$ are related by the following matrix identity

$$(\underline{I} + \underline{T}^{-1}(j\omega))^{-1} + (\underline{I} + \underline{T}(j\omega))^{-1} = \underline{I} \tag{4.29}$$

which prevents us from making both $\sigma\min(\underline{I} + \underline{T}(j\omega))$ and $\sigma\min(\underline{I} + \underline{T}^{-1}(j\omega))$ large independently.

In the low frequency regions where $\sigma\min(\underline{T}(j\omega))$ is large (i.e. large loop gain in all feedback loops), the quantity $\sigma\min(\underline{I} + \underline{T}(j\omega))$ is also large. This in turn constraints $\sigma\min(\underline{I} + \underline{T}^{-1}(j\omega))$ to assume values close to unity. Consequently, Theorem 4.4 will tend to give a less conservative test with respect to the multiplicative errors (i.e. errors of the form $\tilde{\underline{T}}(s) = \underline{T}(s)\ \underline{L}(s)$) than will Theorem 4.3 at low frequencies.

Likewise, when $\sigma\max(\underline{T}(j\omega))$ is small (as is the case in the high frequency region), Theorem 4.4 will provide a less conservative test with respect to the multiplicative errors. This is a consequence of $\sigma\min(\underline{I} + \underline{T}^{-1}(j\omega))$ being large and $\sigma\min(\underline{I} + \underline{T}(j\omega))$ being near to unity.

Using $\det(I + \underline{T}(s-\alpha)\ \underline{L}(s-\alpha))$ (i.e. the image of the α-Nyquist contour under $\det(I + \underline{T}(s))$ in place of $\det(I + \underline{T}(s)\ \underline{L}(s))$, and repeating the argument (based on the deformation of the multivariable Nyquist diagram) employed in the derivation of Theorems 4.2 and 4.3 leads directly to the following theorem on robustness with respect to degree of stability.

Theorem 4.6 If the MIMO feedback system in Fig. 4.1 has a degree of stability α, then the perturbed system in Fig. 4.2 possesses the same degree of stability if

(i) $\underline{T}(s-\alpha)$ and $\tilde{\underline{T}}(s-\alpha) = \underline{T}(s-\alpha)\,\underline{L}(s-\alpha)$ have the same number of unstable poles (4.30)

(ii) $\underline{T}(s-\alpha)$ has no pole along the $j\omega$-axis (4.31)

(iii) $\underline{L}(j\omega-\alpha)$ has no eigenvalue at 0 or on the negative real axis for $\omega \geq 0$ (4.32)

(iv) $\sigma\max(\underline{L}^{-1}(j\omega-\alpha) - \underline{I}) = \sigma\max \underline{E}_4(j\omega-\sigma) < \min(\underline{I} + \underline{T}(j\omega-\sigma))$ for all $\omega \geq 0$ (4.33)

where $\underline{E}_4(s) = (\tilde{\underline{T}}^{-1}(s) - \underline{T}^{-1}(s))\,\underline{T}(s)$ (4.34)

Theorem 4.7 If the MIMO feedback system in Fig. 4.1 has a degree of stability α, then the perturbed system in Fig. 4.2 has the same degree of stability if

(i) $\underline{T}(s-\alpha)$ and $\tilde{\underline{T}}(s-\alpha) = \underline{T}(s-\alpha)\,\underline{L}(s-\alpha)$ have the same number of unstable poles (4.35)

(ii) $\underline{T}(s-\alpha)$ has no pole on the $j\omega$-axis (4.36)

(iii) $\sigma\max(\underline{L}(j\omega-\alpha) - \underline{I}) = \sigma\max(\underline{E}_3(j\omega-\alpha)) < \sigma\min(\underline{I} + \underline{T}^{-1}(j\omega-\alpha))$ for all $\omega \geq 0$ (4.37)

where $\underline{E}_3(s) = \underline{T}^{-1}(s)\,(\tilde{\underline{T}}(s) - \underline{T}(s))$ (4.38)

Remark Our remark on the relative effectiveness of the robustness tests prescribed by Theorems 4.4 and 4.5 at different frequency regions also applies to Theorems 4.6 and 4.7.

C-2

4.2.4 Multi-loop Stability Margins

A natural extension of the gain and phase margin measure to MIMO systems can be obtained by using Theorems 4.4 and 4.5. It turns out that these stability margins can be conveniently characterized in terms of the lower bound of $\sigma\min(\underline{I} + \underline{T}(j\omega))$ and $\sigma\min(\underline{I} + \underline{T}^{-1}(j\omega))$ for $\omega \geq 0$. The definition of the multi-loop margins given below are due to Lehtomaki [Le 1]. Diagonal (i.e. noninteracting) perturbation of the multiplicative type is assumed throughout (see Fig. 4.5).

Definition 4.1 The multi-loop gain margin is the pair of real numbers c_1 and c_2 defining the largest interval (c_1,c_2) such that when $\ell_i(s)$, $i = 1,2,\ldots m$ in Fig. 4.5 are all real, and satisfy the inequalities

$$c_1 < \ell_i < c_2 \qquad i = 1,2,\ldots m \tag{4.39}$$

the closed-loop system remains stable.

Definition 4.2 The multi-loop phase margin is the pair of real numbers θ_1 and $-\theta_1$ defining the largest interval $(-\theta_1,\theta_1)$ such that when $\ell_i(j\omega)$, $i = 1,2,\ldots m$ in Fig. 4.5 are of the form $e^{j\phi_i}$ where ϕ_i's are real and satisfy the inequality

$$-\theta_1 < \phi_i < \theta_1 \qquad i = 1,2\ldots m \tag{4.40}$$

the closed-loop system remains stable.

Following the notation in [Le 1], we denote the multi-loop gain margin of (4.39) by

$$GM = (c_1,c_2)$$

and the multi-loop phase margin of (4.40) by

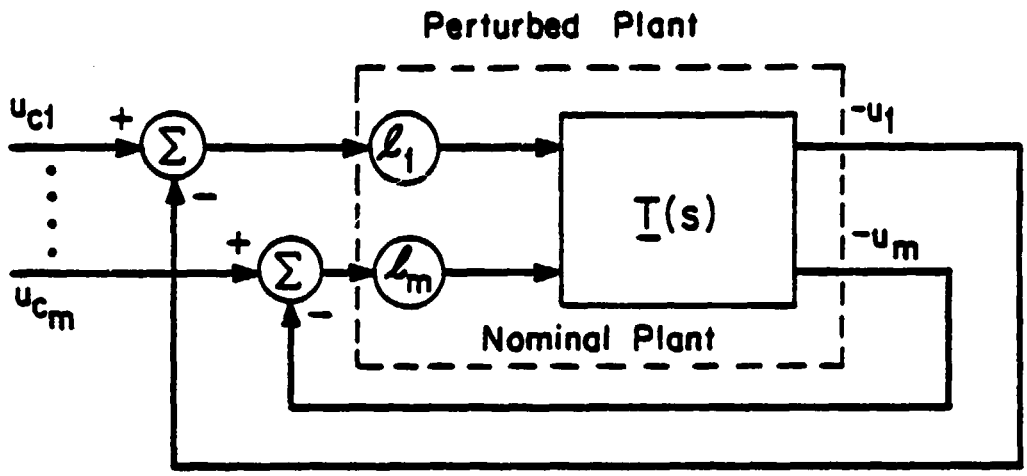

FIG. 4.5 Configuration for Definition of Multi-Loop Margins

$$PM = (-\theta_1, \theta_1)$$

In a similar fashion, we can define multi-loop gain and phase margins that guarantee a prescribed degree of stability for the closed-loop system. These bounds are useful for characterization of a system's ability to maintain a specified speed of response in the face of uncertainties.

Definition 4.3 The multi-loop α - gain margin (denoted by GM_α) is the pair of real numbers c_1 and c_2, defining the largest interval (c_1, c_2) such that when $\ell_i(j\omega)$, $i = 1,2,\ldots m$ in Fig. 4.5 are of the form ℓ_i, where ℓ_i's are real and satisfy the inequality

$$c_1 < \ell_i < c_2 \quad , \qquad i = 1,2,\ldots m \tag{4.41}$$

the closed-loop system retains a degree of stability α .

Definition 4.4 The multi-loop α-phase margin (denoted by PM_α) is the pair of real numbers $-\theta_1$ and θ_1, defining the largest interval $(-\theta_1, \theta_1)$ such that when $\ell_i(j\omega)$, $i = 1,2,\ldots m$ in Fig. 4.5 are of the form $e^{j\phi_i}$ where ϕ_i's are real and satisfy the inequality

$$-\theta_1 < \phi_i < \theta_1 \quad , \qquad i = 1,2,\ldots m \tag{4.42}$$

the closed-loop system retains a degree of stability α .

The interpretation of the two types of gain and phase margins defined above require some explanation. First of all, these margins are valid for perturbations (either pure gain or pure phase changes)

applied simultaneously at each input channel. This does not exclude the possibility of having pure gain changes at some channels and pure phase changes at others. Thus, they differ from those stability margins obtained by breaking one loop at a time. However, the word 'simultaneously' does not suggest that one can change the gains and phases of each input channel simultaneously inside the limit prescribed by (4.39) and (4.40) ((4.41) and (4.42)) without causing instability (the degree of stability to go below α). Secondly, the multi-loop margins only cover a limited class of perturbations. In particular, they are based on the assumption of diagonal $\underline{L}(s)$.

The following corollaries to Theorems 4.4 and 4.5 provide a characterization of multi-loop GM and PM in terms of the lower bound for $\sigma\min(\underline{I} + \underline{T}(j\omega))$ and $\sigma\min(\underline{I} + \underline{T}^{-1}(j\omega))$.

Corollary 4.1 If the nominal closed-loop system in Fig. 4.1 is stable with no open-loop pole on the $j\omega$-axis and

$$\sigma\min(\underline{I} + \underline{T}(j\omega)) > \beta , \quad 0 < \beta \leq 1, \quad \text{for all } \omega \geq 0 \tag{4.43}$$

then the multi-loop gain and phase margins are characterized by

$$GM \supset \left(\frac{1}{1+\beta} , \frac{1}{1-\beta}\right) \tag{4.44}$$

and

$$PM \supset \left(-2 \sin^{-1}\frac{\beta}{2} , 2 \sin^{-1}\frac{\beta}{2}\right) \tag{4.45}$$

respectively.

Remark The case for $\beta < 1$ is not considered because it is inconsistent with the strict properness assumption of $\underline{T}(s)$.

Corollary 4.3 If the nominal closed-loop system in Fig. 4.1 is stable with no open-loop pole on the $j\omega$-axis, and

$$\sigma_{min}(\underline{I} + \underline{T}^{-1}(j\omega)) > \beta \qquad \text{for all } \omega \geq 0 \tag{4.46}$$

then the multi-loop gain and phase margins are characterized by

$$GM \supset (1-\beta, \quad 1+\beta) \tag{4.47}$$

and

$$PM \supset (-2\sin^{-1}\frac{\beta}{2}, \quad 2\sin^{-1}\frac{\beta}{2}) \tag{4.48}$$

respectively.

Likewise, we can characterize the multi-loop margins with respect to degree of stability in terms of the bound for $\sigma_{min}(\underline{I} + \underline{T}(\alpha-j\omega))$ and $\sigma_{min}(\underline{I} + \underline{T}^{-1}(\alpha-j\omega))$ respectively. The result is summarized in the following corollaries to Theorems 4.5 and 4.6.

Corollary 4.4 If the nominal closed-loop system in Fig. 4.1 has a degree of stability α with no open-loop pole on $\sigma = -\alpha$, and

$$\sigma_{min}(\underline{I} + \underline{T}(j\omega-\alpha)) > \beta \ , \ 0 < \beta \leq 1 \quad \text{for all } \omega \geq 0 \tag{4.49}$$

then the multi-loop gain and phase margins with respect to the degree of stability α are characterized by

$$GM_\alpha \supset (\frac{1}{1+\beta} \ , \ \frac{1}{1-\beta}) \tag{4.50}$$

and

$$PM_\alpha \supset (-2\sin^{-1}\frac{\beta}{2} \ , \ 2\sin^{-1}\frac{\beta}{2}) \tag{4.51}$$

respectively.

Corollary 4.5 If the nominal closed-loop system in Fig. 4.1 has a degree of of stability α with no open-loop pole on $\sigma = -\alpha$, and

$$\sigma\min(\underline{I} + \underline{T}^{-1}(j\omega-\alpha)) \geq \beta \qquad \text{for all } \omega \geq 0 \tag{4.52}$$

then the multi-loop gain and phase margins with respect to the degree of stability α is characterized by

$$GM_\alpha \subset (1 - \beta\ ,\ 1 + \beta) \tag{4.53}$$

and

$$PM_\alpha \subset (-2 \sin^{-1} \frac{\beta}{2}\ ,\ 2 \sin^{-1} \frac{\beta}{2}) \tag{4.54}$$

respectively.

It is important to emphasize that the bounds on the multi-loop gain and phase margin characterization provided by the above corollaries are in general very conservative. This is a result of the fact that only magnitude but no structural information on $\underline{I} + \underline{T}(j\omega)$ and $\underline{I} + \underline{T}^{-1}(j\omega)$ are employed in the derivation of these bounds. These stability margins are commonly known as the guaranteed gain and phase margins.

4.3 Formulation of the RPDS Robustness Problem

Consider a LTI system described by the dynamical equations

$$\dot{\underline{x}}(t) = \underline{A}\,\underline{x}(t) + \underline{B}\,\underline{u}(t) \tag{4.55}$$

$$\underline{y}(t) = \underline{C}\,\underline{x}(t) \tag{4.56}$$

Let

$$\underline{u}(t) = -\underline{G}_\alpha\,\underline{x}(t) \tag{4.57}$$

be a state feedback control law for the above system. The resulting state feedback configuration is shown in Fig. 4.6.

Since the stability of a RPDS is characterized by the eigenvalues of the closed-loop matrix $(\underline{A} - \underline{B}\,\underline{G}_\alpha)$, it is strictly a property of the state feedback loop and is independent of the output matrix $\underline{C}$. To

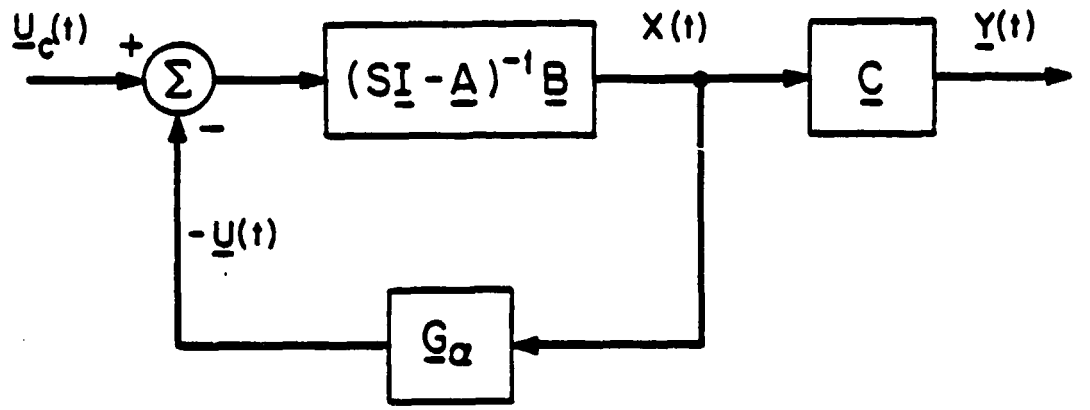

FIG. 4.6 State Feedback Configuration for RPDS

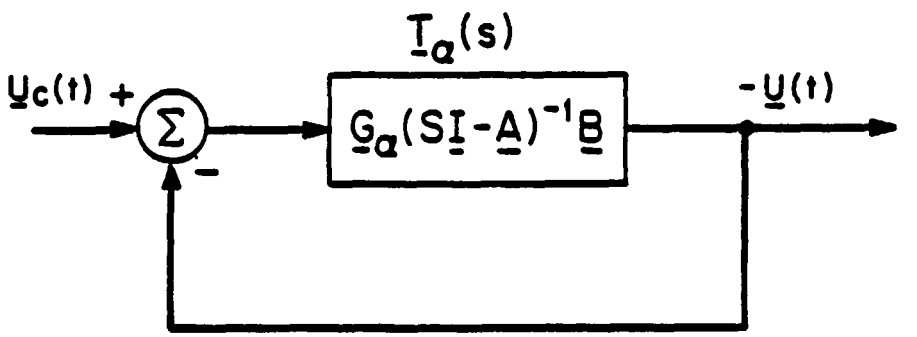

FIG. 4.7 Feedback Configuration for Robustness Analysis of RPDS

perform robustness analysis, we can redraw the RPDS state feedback loop in a unity negative feedback form (see Fig. 4.7) that is compatible with the robustness theorems considered in the last section. The RPDS feedback system is therefore akin to that found in classical situation where unity negative feedback is applied around a system with loop-transfer matrix given by $\underline{G}_\alpha\ (s\underline{I} - \underline{A})^{-1}\ \underline{B}$.

Now, it becomes clear that we can characterize the robustness properties of RPDS in terms of the two quantities $\sigma\min(\underline{I} + \underline{T}_\alpha(j\omega))$ and $\sigma\min(\underline{I} + \underline{T}_\alpha^{-1}(j\omega))$ where we define

$$\underline{T}_\alpha(j\omega) \triangleq \underline{G}_\alpha(j\omega\underline{I} - \underline{A})^{-1}\ \underline{B} \tag{4.58}$$

4.4 Properties of RPDS Return Difference Matrices and Related Robustness Results

Several well known feedback properties of LQ regulators are characterized in terms of its return difference matrices by the Kalman Frequency Domain Equality([Ka 1], [Le 1]). Since RPDS represents a special case of LQ regulator, it seems natural to begin our study of its return difference by introducing two modified versions of Kalman Frequency Domain Equality that are obtained directly from the RPDS Riccati equation. The derivation of these results are given in section 4.4.1. The three subsections that follow discuss three important consequences of these equalities and their respective robustness interpretations.

4.4.1 Two Fundamental Equalities

There are two versions of Kalman Frequency Domain Equality for RPDS. Each of them results from a different arrangement of the RPDS

algebraic Riccati equation. These results can be stated as follows.

Theorem 4.8 Let the matrix $\underline{K}_\alpha$ be the unique positive definite solution to the algebraic Riccati equation

$$(\underline{A} + \alpha \underline{I})^T \underline{K}_\alpha + \underline{K}_\alpha(\underline{A} + \alpha \underline{I}) + \underline{Q} - \underline{K}_\alpha \underline{B} \underline{R}^{-1} \underline{B}^T \underline{K}_\alpha = \underline{0} \tag{4.59}$$

with

$$\text{(i)} \quad \underline{Q} \geq \underline{0} \quad \text{and} \quad \underline{R} > \underline{0} \tag{4.60}$$

$$\text{(ii)} \quad (\underline{A}, \underline{B}) \text{ controllable} \tag{4.61}$$

$$\text{(iii)} \quad (\underline{Q}^{1/2}, \underline{A}) \text{ observable} \tag{4.62}$$

then

$$(\underline{I} + \underline{T}_\alpha(-\alpha-s))^T \underline{R} (I + \underline{T}_\alpha(-\alpha+s)) = \underline{R} + \underline{H}(-s,s) \tag{4.63}$$

and

$$(\underline{I} + \underline{T}_\alpha(-s))^T \underline{R}(\underline{I} + \underline{T}_\alpha(s)) = \underline{R} + \underline{H}_\alpha(-s,s) \tag{4.64}$$

where $\underline{H}(\zeta,s) = \underline{B}^T(\zeta \underline{I} - \alpha I - \underline{A}^T)^{-1} \underline{Q}(s\underline{I} - \alpha \underline{I} - \underline{A})^{-1} \underline{B}$ (4.65)

and

$$\underline{H}_\alpha(\zeta,s) = \underline{B}^T(\zeta \underline{I} - \underline{A}^T)^{-1} (2\alpha \underline{K}_\alpha + \underline{Q}) (s\underline{I} - \underline{A})^{-1} \underline{B} \tag{4.66}$$

Proof: Direct manipulation of (4.59) yields

$$(-s\underline{I} - \underline{A} - \alpha I)^T \underline{K}_\alpha + \underline{K}_\alpha(s\underline{I} - \underline{A} - \alpha \underline{I}) + \underline{K}_\alpha \underline{B} \underline{R}^{-1} \underline{B} \underline{K}_\alpha = \underline{Q} \tag{4.67}$$

upon premultiplying and postmultiplying (4.67) by $[(-s\underline{I} - \alpha \underline{I} - \underline{A})^{-1} \underline{B}]^T$ and $[(s\underline{I} - \alpha \underline{I} - \underline{A})^{-1} \underline{B}]$ respectively, we obtain

$$\underline{R}\, \underline{T}_\alpha(s-\alpha) + \underline{T}_\alpha^T(s-\alpha)\, \underline{R} + \underline{T}_\alpha^T(-s-\alpha) \underline{R} \underline{T}_\alpha (s-\alpha) = \underline{H}(-s,s) \tag{4.68}$$

adding $\underline{R}$ to both sides of (4.68) gives (4.63).

To derive (4.64), note that we can rewrite (4.59) as follows

$$\underline{A}^T \underline{K}_\alpha + \underline{K}_\alpha \underline{A} + (\underline{Q} + 2\alpha \underline{K}_\alpha) - \underline{K}_\alpha \underline{B} \underline{R}^{-1} \underline{B}^T \underline{K}_\alpha = \underline{0} \tag{4.69}$$

by regrouping the two terms involving $\alpha \underline{K}_\alpha$. Repeating the same algebraic manipulations as before with (4.69) we obtain (4.64) and this completes the proof.

Remark As expected, both equalities (4.63) and (4.64) reduce to the familiar Kalman Frequency Equality for LQ regulators when $\alpha = 0$.

Furthermore, if

$$\det(j\omega \underline{I} - \underline{A}) \neq 0 \qquad \text{for all } \omega \geq 0 \tag{4.70}$$

we can rewrite equality (4.64) as

$$(\underline{I} + \underline{T}_\omega(j\omega))^H \underline{R} (\underline{I} + \underline{T}_\alpha(j\omega)) = \underline{R} + \underline{H}_\alpha(-j\omega, j\omega) \tag{4.71}$$

for values of s on the $j\omega$-axis.

Similarly, if

$$\det(j\omega \underline{I} - \underline{A} - \alpha \underline{I}) \neq 0 \quad \text{for all } \omega \geq 0 \tag{4.72}$$

we can rewrite equality (4.63) as

$$(\underline{I} + \underline{T}_\alpha(-\alpha + j\omega))^H \underline{R} (\underline{I} + \underline{T}_\alpha(-\alpha + j\omega)) = \underline{R} + \underline{H}(-j\omega, j\omega) \tag{4.73}$$

for values of s on the $j\omega$-axis.

4.4.2 Common properties with LQ Regulators

It was pointed out in our remark to Corollary 2.5 that RPDS is a special case of LQ regulators. As a result, it possesses all the robustness properties of the latter. A formal verification of this fact is provided in this section. The following corollary to Theorem 4.8 is key to the derivation of all the subsequent results on LQ-related

properties of RPDS.

Corollary 4.6 Let the matrix $\underline{K}_\alpha$ be the unique positive definite solution of the algebraic Riccati equation (4.59) (with all conditions on $\underline{A}$, $\underline{B}$, $\underline{Q}$ and $\underline{R}$ satisfied), and $\det(j\omega\underline{I} - \underline{A}) \neq 0$ for all $\omega \geq 0$.
Then

$$(\underline{I} + \underline{T}_\alpha(j\omega))^H \underline{R}(\underline{I} + \underline{T}_\alpha(j\omega)) > \underline{R} \qquad \text{for all } \omega \geq 0 \qquad (4.74)$$

Proof: The inequality (4.74) holds if and only if $\underline{H}_\alpha(-j\omega,j\omega) > 0$ for $\omega \geq 0$. The positive definiteness of $\underline{H}_\alpha(-j\omega,j\omega)$ in turn follows from that of $\underline{K}_\alpha$ and this completes the proof.

Remark The result described in this corollary is the well known Kalman Inequality for LQ regulators. In the single-input case (4.74) reduced to the following scalar inequality [Ka 1]

$$|1 + t_\alpha(j\omega)| > 1 \qquad \text{for } \omega \geq 0 \qquad (4.75)$$

By inspection of the Nyquist diagram corresponding to (4.75) (see Fig.4.8) it is straightforward to observe that a single-input RPDS state feedback regulator has a guaranteed GM of $(\frac{1}{2}, \infty)$ and a guaranteed PM of $(-60^\circ, 60^\circ)$.

In the multiple-input case, the inequality (4.74) does not provide a bound on the quantity $\sigma\min(\underline{I} + \underline{T}_\alpha(j\omega))$ for arbitrary choices of $\underline{R}$. In cases where $\underline{R}$ is chosen to be a scaled identity (i.e. $\underline{R} = c\underline{I}$ for some $c > 0$), then (4.74) reduces to

$$(\underline{I} + \underline{T}_\alpha(j\omega))^H (\underline{I} + \underline{T}_\alpha(j\omega)) > I \qquad \text{for all } \omega \geq 0 \qquad (4.76)$$

which in turn provides a lower bound

$$\sigma\min(\underline{I} + \underline{T}_\alpha(j\omega)) > 1 \qquad \text{for all } \omega \geq 0 \qquad (4.77)$$

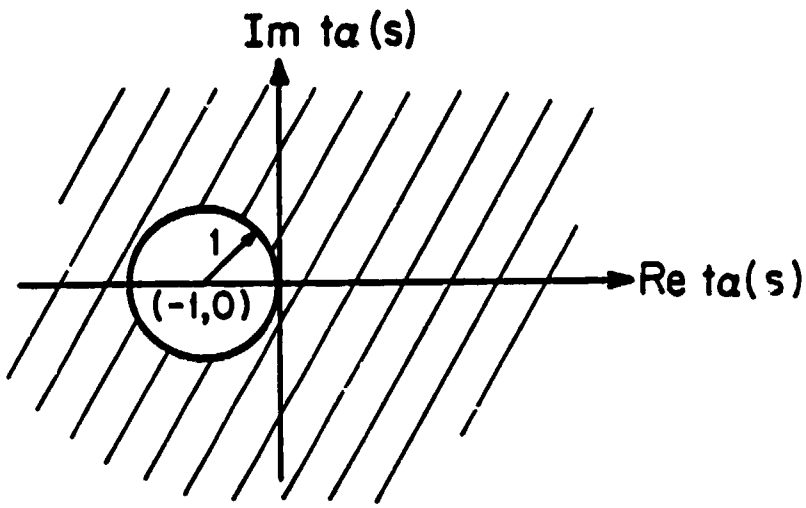

FIG. 4.8 Set of Allowable Values (shaded) of $t_\alpha(s)$ when $|1 + t_\alpha(s)| > 1$

for the minimum singular value of $\underline{I} + \underline{T}_\alpha(j\omega)$. It follows immediately from Corollaries 4.2 and 4.3 and (4.74) that RPDS designs with $\underline{R}$ chosen to be a scaled identity matrix have a guaranteed multi-loop gain margin given by $(0.5,\infty)$ and a guaranteed phase margin given by $(-60^\circ,60^\circ)$.

It turns out that these guaranteed stability margins also apply to RPDS designs with $\underline{R}$ chosen to be diagonal. The derivation of this more general results is due to Lehtomaki (see [Le 1], [Le 2]) and is included here for completeness. The proof is motivated by the observation that (4.74) can be rewritten as

$$(\underline{I} + \hat{\underline{T}}_\alpha(j\omega))^H \; (\underline{I} + \hat{\underline{T}}_\alpha(j\omega)) > \underline{I} \qquad \text{for all} \quad \omega \geq 0 \qquad (4.78)$$

where we define

$$\hat{\underline{T}}_\alpha(j\omega) = \underline{R}^{1/2} \; \underline{T}_\alpha(j\omega) \; \underline{R}^{-1/2} \qquad (4.79)$$

Inequality (4.78) then provides a bound

$$\sigma\min(\underline{I} + \hat{\underline{T}}_\alpha(j\omega)) > 1 \qquad \text{for all} \quad \omega \geq 0 \qquad (4.80)$$

on the minimum singular value of $\underline{I} + \hat{\underline{T}}_\alpha(j\omega)$. If $\hat{\underline{T}}_\alpha(j\omega)$ is used instead of $\underline{T}_\alpha(j\omega)$ in the stability test based on Theorem 4.4, it is necessary to manipulate Fig. 4.7 into the equivalent form depicted in Fig. 4.9[1]

Using Theorem 4.4 and (4.80) leads directly to the following result

Theorem 4.9 Given a RPDS system with loop-transfer matrix $\underline{T}_\alpha(s)$, the perturbed regulator with loop-transfer matrix $\tilde{\underline{T}}_\alpha(s) = \underline{T}_\alpha(s) \; \underline{L}(s)$ is closed-loop stable if

---

[1] This ensures the equivalence (from stability point of view) of the feedback loops in Fig. 4.7 and Fig. 4.9.

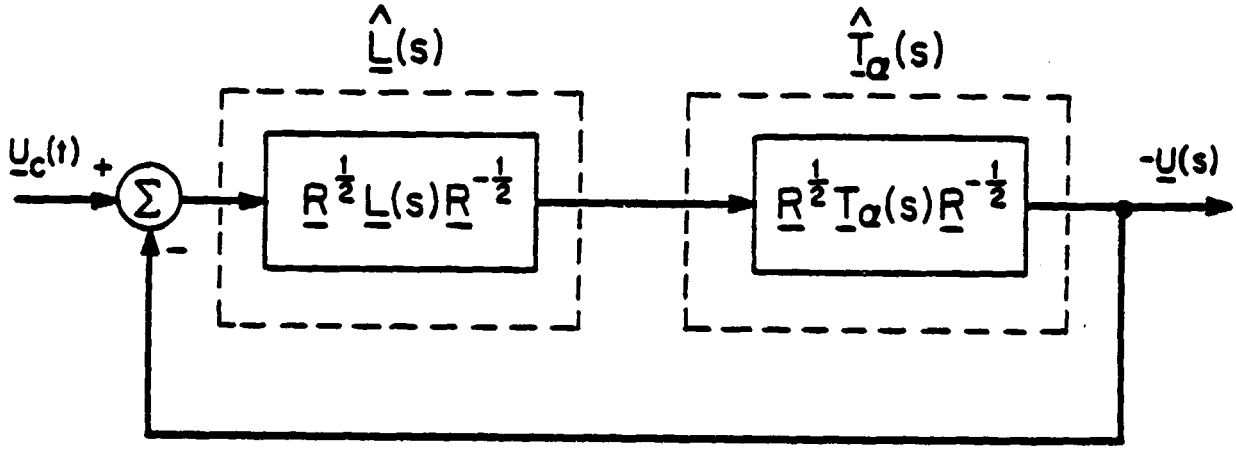

FIG. 4.9 Feedback System for Stability Margin Derivation

(i) $\underline{T}_\alpha(s)$ and $\underline{\tilde{T}}_\alpha(s)$ have the same number of unstable poles (4.81)

(ii) $\underline{T}_\alpha(s)$ has no pole on the $j\omega$-axis (4.82)

(iii) $\sigma\max(\underline{R}^{1/2}\ \underline{L}^{-1}(j\omega)\ \underline{R}^{-1/2} - \underline{I}) \leq 1$ for all $\omega \geq 0$ (4.83)

Observe that the condition $\sigma\max(\underline{R}^{-1/2}\ \underline{L}^{-1}(j\omega)\ \underline{R}^{-1/2} - \underline{I}) \leq 1$ in (4.83) can be written as (see [Sa 3])

$$\underline{R}\ \underline{L}(j\omega) + \underline{L}^{H}(j\omega)\ \underline{R} - \underline{R} \geq 0 \qquad \text{for all } \omega \geq 0 \tag{4.84}$$

If $\underline{R}$ and $\underline{L}(j\omega)$ are diagonal, (4.84) simplifies to the following conditions

$$\mathrm{Re}(\ell_i(j\omega)) \geq \frac{1}{2} \qquad \text{for all } \omega \geq 0 \text{ and } i = 1,2,\ldots m \tag{4.85}$$

The corresponding guaranteed gain and phase margins properties can be readily obtained from (4.85) by assuming $\ell_i(j\omega)$ to be a real scalar and $\ell_i(j\omega) = e^{j\phi_i}$, respectively, for $i = 1,2,\ldots m$.

4.4.3 The Effect of the Stability Factor α on RPDS Return Difference Matrices

The effect of the stability factor α on the matrix $(\underline{I} + \underline{T}_\alpha(-s))^T\ \underline{R}(\underline{I} + \underline{T}_\alpha(s))$ is provided by the following corollary to Theorem 4.4.

Corollary 4.7 Let the matrices $\underline{K}_{\alpha_1}$ and $\underline{K}_{\alpha_2}$ be the unique positive definite solutions of the RPDS algebraic Riccati equations

$$(\underline{A} + \alpha_1\underline{I})^T\ \underline{K}_{\alpha_1} + \underline{K}_{\alpha_1}\ (\underline{A} + \alpha_1\underline{I}) + \underline{Q} - \underline{K}_{\alpha_1}\ \underline{B}\ \underline{R}^{-1}\ \underline{B}^T\ \underline{K}_{\alpha_1} = \underline{0} \tag{4.86}$$

---

[1] It can be trivially shown that condition (iii) in (4.79) automatically guarantees condition (iii) of Theorem 4.4.

and

$$(\underline{A} + \alpha_2 \underline{I})^T \underline{K}_{\alpha_2} + \underline{K}_{\alpha_2} (\underline{A} + \alpha_2 \underline{I}) + \underline{Q} - \underline{K}_{\alpha_2} \underline{B} \underline{R}^{-1} \underline{B}^T \underline{K}_{\alpha_2} \tag{4.87}$$

respectively with

(i) $\underline{Q} \geq 0, \quad \underline{R} > 0$ (4.88)

(ii) $(\underline{A}, \underline{B})$ controllable (4.89)

(iii) $(\underline{Q}^{1/2}, \underline{A})$ observable (4.90)

and (iv) $\det(j\omega \underline{I} - \underline{A}) \neq 0 \qquad$ for all $\omega \geq 0$ (4.91)

then

$$(\underline{I} + \underline{T}_{\alpha_1}(j\omega))^H \underline{R} (\underline{I} + \underline{T}_{\alpha_1}(j\omega))$$

$$> (\underline{I} + \underline{T}_{\alpha_2}(j\omega))^H \underline{R} (\underline{I} + \underline{T}_{\alpha_2}(j\omega)) \qquad \text{for all } \omega \geq 0 \tag{4.92}$$

$$\text{if } \alpha_1 > \alpha_2 \geq 0$$

Proof: Direct application of Theorem 4.4 to the algebraic Riccati equations (4.86) and (4.87) yields

$$(\underline{I} + \underline{T}_{\alpha_1}(j\omega))^H \underline{R} (\underline{I} + \underline{T}_{\alpha_1}(j\omega)) = \underline{H}_{\alpha_1}(-j\omega, j\omega) + \underline{R} \tag{4.93}$$

and

$$((\underline{I} + \underline{T}_{\alpha_2}(j\omega))^H \underline{R} (\underline{I} + \underline{T}_{\alpha_2}(j\omega)) = \underline{H}_{\alpha_2}(-j\omega, j\omega) + \underline{R} \tag{4.94}$$

respectively. It follows from Lemma 3.1 and condition (iv) in the theorem statement that

$$\underline{H}_{\alpha_1}(-j\omega, j\omega) > \underline{H}_{\alpha_2}(-j\omega, j\omega) \qquad \text{for all } \omega \geq 0 \tag{4.95}$$

Adding $\underline{R}$ to both sides of (4.95) yields

$$\underline{R} + \underline{H}_{\alpha_1}(-j\omega, j\omega) > \underline{R} + \underline{H}_{\alpha_2}(-j\omega, j\omega) \qquad \text{for all } \omega \geq 0 \tag{4.96}$$

and the theorem is proved.

For single-input RPDS (4.92) reduces to the following scalar inequality

$$|1 + t_{\alpha_1}(j\omega)| > |1 + t_{\alpha_2}(j\omega)| \qquad \text{for all } \omega \geq 0 \qquad (4.97)$$

Geometrically, (4.97) means that for each value of frequency ω, the point $t_{\alpha_1}(j\omega)$ in the complex plane is always farther away from the critical point (-1,0) than the point $t_{\alpha_2}(j\omega)$ (see Fig. 4.10)).

In the multiple-input case, the inequality (4.92) does not in general imply $(\underline{I} + \underline{T}_{\alpha_1}(j\omega))^H (\underline{I} + \underline{T}_{\alpha_1}(j\omega)) > (\underline{I} + \underline{T}_{\alpha_2}(j\omega))^H (\underline{I} + \underline{T}_{\alpha_2}(j\omega))$ for $\alpha_1 > \alpha_2$. However, if $\underline{R}$ is chosen to be a scaled identity matrix, (4.92) then simplifies to

$$(\underline{I} + \underline{T}_{\alpha_1}(j\omega))^H (\underline{I} + \underline{T}_{\alpha_1}(j\omega)) > (\underline{I} + \underline{T}_{\alpha_2}(j\omega))^H (\underline{I} + \underline{T}_{\alpha_2}(j\omega)) \qquad (4.98)$$

$$\text{for all } \omega \geq 0$$

The following inequality on the minimum singular value of RPDS return difference can be readily derived from (4.98) by using the properties of singular values

$$\sigma\min(\underline{I} + \underline{T}_{\alpha_1}(j\omega)) > \sigma\min(\underline{I} + \underline{T}_{\alpha_2}(j\omega)), \qquad \text{for all } \omega \geq 0 \qquad (4.99)$$

Inequalities (4.98) and (4.99) allow us to assess the effect of α on the robustness properties of RPDS design with $\underline{R}$ chosen to be a scaled identity matrix. It follows directly from condition (4.21) in Theorem 4.4 that the tolerance of modelling error of the form $\underline{E}_4(s) = (\underline{\tilde{T}}^{-1}_{\alpha}(s) - \underline{T}^{-1}_{\alpha}(s))\ \underline{T}_{\alpha}(s)$ improves with increasing values the stability factor α. Unfortunately, the use of the matrix function $\underline{T}^{-1}_{\alpha}(s)$ is not common, thus making the above conclusion somewhat difficult to interprete. We shall explore further

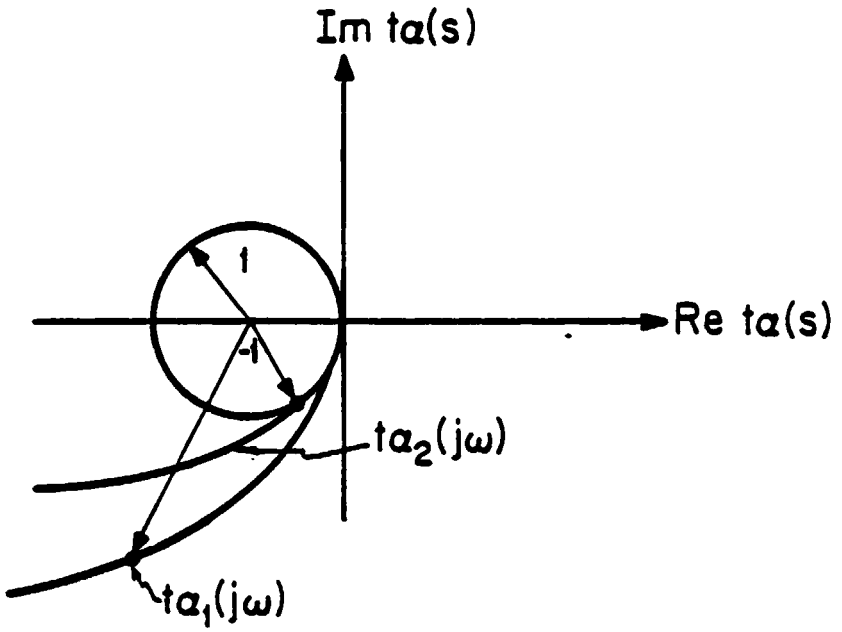

FIG. 4.10 Nyquist Diagrams for RPDS Loop Transfer Functions $t_{\alpha_1}(s)$ and $t_{\alpha_2}(s)$ with $\alpha_1 > \alpha_2$

consequences of this result by restricting ourselves to perturbation matrices $\underline{L}(s)$ that are diagonal. Then condition (4.22) in Theorem 4.4 simplifies to

$$|\ell_i^{-1}(j\omega) - 1| < \beta(j\omega) \triangleq \sigma\min(\underline{I} + \underline{T}_\alpha(j\omega)) \quad \text{for all } \omega \geq 0, \; i = 1,2,\ldots,m \tag{4.100}$$

The allowable values for $\ell_i(j\omega)$ as defined by (4.100) are depicted in Fig. 4.11. It is clear from the diagram that the area of allowable (shaded) region for $\ell_i(j\omega)$ increases with $\beta(j\omega)$ which is itself and increasing function of α. This represents a very special type of robustness improvement for RPDS made possible by increasing the value of α. Attempts the find a characterization of robustness variations with α for error models defined in terms of $\underline{T}_\alpha(s)$ have not been successful. This is so because robustness theorems relating $\sigma\min(\underline{I} + \underline{T}_\alpha(j\omega))$ and error models defined in terms of $\underline{T}_\alpha(s)$ are only available for the absolute type of error representation. We have already pointed out in section 4.2 the difficulty in accounting for the effect of compensator with this type of error model. Indeed, an increase in the value of α will increase both the error and the quantity $\sigma\min(\underline{I}+\underline{T}_\alpha(j\omega))$, thus making it impossible to ascertain the effect of α on robustness.

We shall conclude this section by discussing the effect of α on the guaranteed and actual stability margins of RPDS. Since $\underline{T}_\alpha(s)$ is a strictly proper, rational matrix function, it follows that

$$\lim_{\omega \to \infty} \sigma\min(\underline{I} + \underline{T}_\alpha(j\omega)) = 1 \qquad \text{for all values of } \alpha > 0 \tag{4.101}$$

This in turn implies that we cannot find a lower bound larger than 1 for

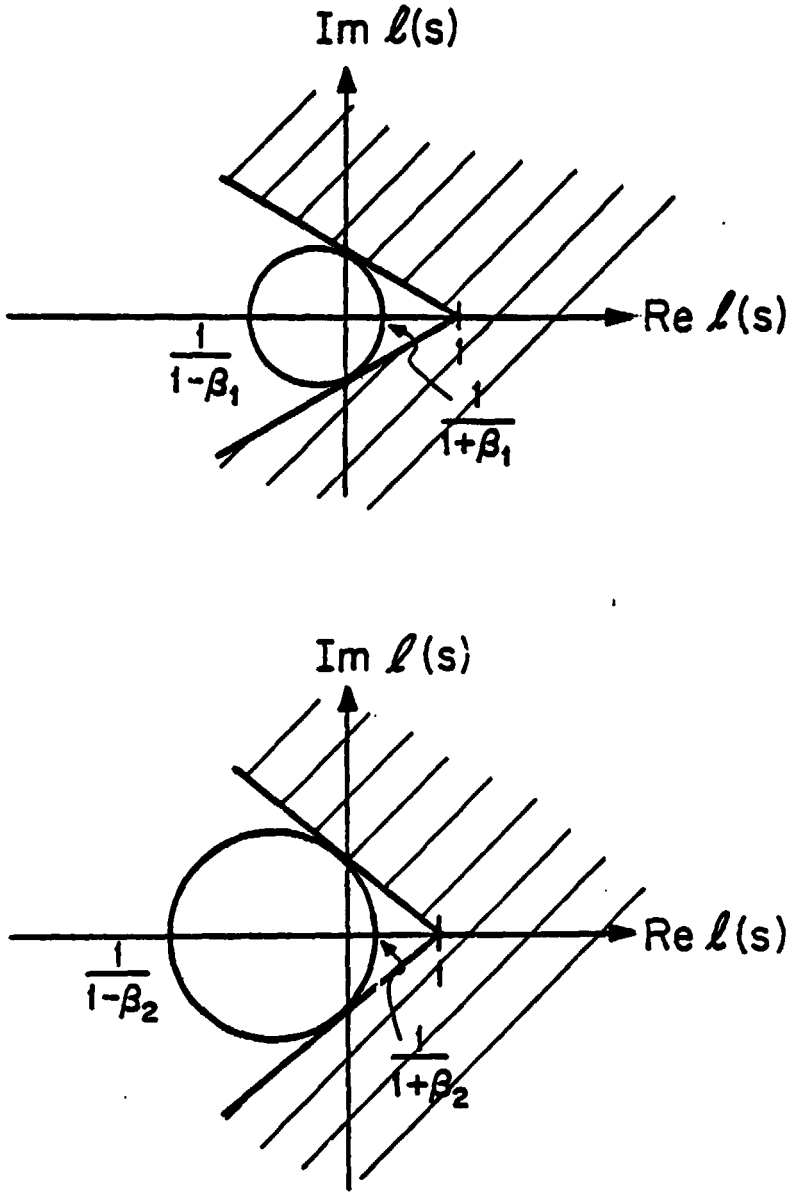

FIG. 4.11 Set of Allowable Values (shaded) for $\ell_1(s)$ Corresponding to $\sigma\min(\underline{I} + \underline{T}_{\alpha_1}(j\omega)) = \beta_1$ (4.12a) and $\sigma\min(\underline{I} + \underline{T}_{\alpha_2}(j\omega)) = \beta_2$ (4.12b) $\alpha_1 > \alpha_2$

$\sigma\min(\underline{I} + \underline{T}_\alpha(j\omega))$ that holds for all values of ω. As a result, the guaranteed gain and phase margins for RPDS with $\underline{R}$ chosen to be a scaled identity matrix is unaffected by the choice of α. It can be shown that this result also holds for RPDS design when $\underline{R}$ is chosen to be diagonal.

The effect of α on the actual stability margins of RPDS turns out to be highly system dependent. As expected, the upward gain margin is always ∞ (since actual gain margin can be no worse than guaranteed gain margin). The downward gain margin and phase margin may however either improve or deteriorate with increasing α. The following simple example illustrates this point.

Example 4.1 Consider the following RPDS problem

$$\min_{u(t)} \lim_{t\to\infty} \int_0^{t_1} e^{2\alpha t} (x^2(t) + u^2(t))dt \tag{4.102}$$

$$\dot{x}(t) = ax(t) + u(t) \tag{4.103}$$

If $a = -1$, the RPDS feedback gain is given by

$$g_\alpha = (\alpha - 1) + [(\alpha - 1)^2 + 1]^{1/2} \tag{4.104}$$

and the corresponding gain and phase margin are given by

$$GM = (-g_\alpha^{-1}, \infty) \tag{4.105}$$

and

$$PM = (-\pi + \tan^{-1}(g_\alpha^2 - 1)^{1/2}, \quad \pi - \tan^{-1}(g_\alpha^2 - 1)^{1/2}) \tag{4.106}$$

respectively. It follows from the fact that g_α is an increasing function of α that both the downward gain margin $-g_\alpha^{-1}$ and the phase margin given

by (4.106) deteriorate with increasing α (see Fig. 4.12a). If we have $a = 1$ instead, (i.e. the open-loop system is unstable) then the gain and phase margin of the resulting design become

$$GM = (g_\alpha^{-1}, \infty) \tag{4.107}$$

and

$$PM = (-\tan^{-1}(g_\alpha^2 - 1)^{1/2}, \quad \tan^{-1}(g_\alpha^2 - 1)^{1/2}) \tag{4.108}$$

respectively, where g_α is now given by

$$g_\alpha = (\alpha + 1) + [(\alpha + 1)^2 + 1]^{1/2} \tag{4.109}$$

Note that in this case, both the downward gain margin and the phase margin increase monotonically with α (see Fig. 4.12b).

4.4.4 Properties of the RPDS Return Difference Matrices on the α-Nyquist Contour

Thus far, we have not been using the version of the RPDS Frequency Domain Equality given by (4.64). A useful matrix inequality similar to (4.74) can be derived from this equation.

Corollary 4.8 Let the matrix $\underline{K}_\alpha$ be the unique positive definite solution of the algebraic Riccati equation (4.59) with the respective conditions on $\underline{A}$, $\underline{B}$, $\underline{Q}$ and $\underline{R}$ satisfied and $\det(j\omega \underline{I} - \underline{A} - \alpha\underline{I}) \neq 0$ for all $\omega > 0$, then

$$(I + \underline{T}_\alpha(-\alpha + j\omega))^H \underline{R}(I + \underline{T}_\alpha(-\alpha + j\omega)) \geq \underline{R} \qquad \text{for all} \quad \omega > 0 \tag{4.110}$$

Proof: The inequality (4.110) holds if and only if $\underline{H}(-j\omega, j\omega) \geq 0$, for all $\omega \geq 0$. The positive semi-definiteness of $\underline{H}(-j\omega, j\omega)$ in turn follows from

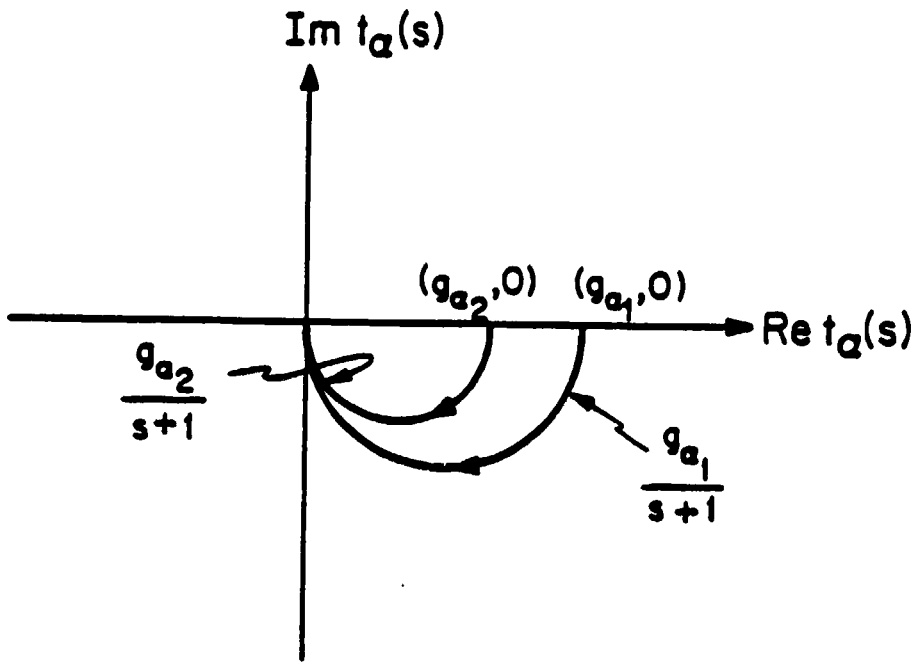

FIG. 4.12(a) Nyquist Diagrams for $\frac{g\alpha_1}{s+1}$ and $\frac{g\alpha_2}{s+1}$; $\alpha_1 > \alpha_2$

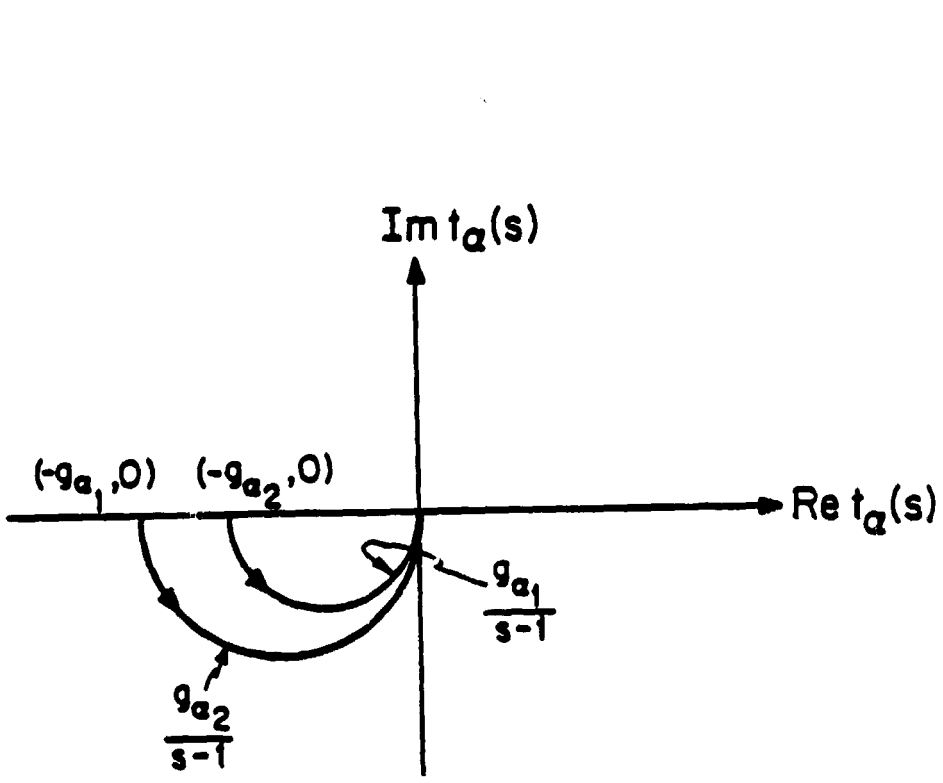

FIG. 4.12(b) Nyquist Diagrams for $\frac{g\alpha_1}{s-1}$ and $\frac{g\alpha_2}{s-1}$; $\alpha_1 > \alpha_2$

$\underline{Q} \geq 0$, $(\underline{Q}^{1/2}, \underline{A})$ observable and $\det(j\omega \underline{I} - \underline{A} - \alpha \underline{I}) \neq 0$ for all $\omega \geq 0$, and this completes the proof.

Note that inequalities (4.74) and (4.110) become identical when $\alpha = 0$. For the case $\alpha \neq 0$, we can regard (4.110) as arising from (4.74) by replacing $\pm j\omega$ by $\pm j\,\omega-\alpha$. Indeed the values of the matrix function for $\omega \geq 0$ on the left hand side of (4.110) can be obtained by evaluating the RPDS return difference matrix along the α-Nyquist contour shown in Fig. (4.4). For the single-input case, (4.110) simplifies to the following scalar inequality

$$|1 + t_\alpha(-\alpha + j\omega)| > 1 \qquad \text{for all } \omega \geq 0 \tag{4.111}$$

which admits the same geometrical interpretation as (4.75) in that every point on the Nyquist diagram of $t_\alpha(s)$ evaluated along the α-Nyquist contour is away from the critical point by a distance of at least unity (see Fig. (4.8)).

Recognizing the similarities between inequalities (4.74) and (4.110) it seems natural to use the closed-loop system depicted in Fig. 4.9 in order to interprete robustness implications of (4.110). The following result can be readily obtained using inequality (4.110) and Theorem 4.6.

Theorem 4.10 Given a RPDS with loop transfer matrix $\underline{T}_\alpha(s)$ and a prescribed degree of stability α , the perturbed regulator with loop transfer matrix $\underline{\tilde{T}}_\alpha(s) = \underline{T}_\alpha(s)\,\underline{L}(s)$ will retain a degree of stability if

(i) $\underline{T}_\alpha(s-\alpha)$ and $\underline{\tilde{T}}_\alpha(s-\alpha)$ have the same number of unstable poles (4.112)

(ii) $\underline{T}_\alpha(s-\alpha)$ has no pole on the $j\omega$-axis (4.113)

$$\text{(iii)} \quad \sigma_{max}(\underline{R}^{1/2}\,\underline{L}^{-1}\,(j\omega - \alpha)\,\underline{R}^{-1/2} - \underline{I}) < 1 \qquad \text{for all} \quad \omega \geq 0 \tag{4.114}$$

Note that condition $\sigma_{max}(\underline{R}^{1/2}\,\underline{L}^{-1}(j\omega - \alpha)\,\underline{R}^{-1/2} - \underline{I}) < 1$ in (4.114) can be rewritten as

$$\underline{R}\,\underline{L}(j\omega - \alpha) + \underline{L}^{H}(j\omega - \alpha)\,\underline{R} > \underline{R} \qquad \text{for all } \omega \geq 0 \tag{4.115}$$

If both $\underline{R}$ and $\underline{L}(s)$ are chosen to be diagonal, then (4.115) above simplifies to the following set of inequalities

$$\text{Re}(\ell_i(j\omega - \alpha)) > \frac{1}{2} \qquad \text{for all } \omega \geq 0 \text{ and } i = 1,2,\ldots,m \tag{4.116}$$

For case of ℓ_i representing a pure gain change, it is clear from (4.116) that the perturbed regulator will retain a degree of stability α if each ℓ_i satisfies $\ell_i > \frac{1}{2}$. Similarly, for $\ell_i = e^{j\phi_i}$, we can conclude from (4.116) that the perturbed regulator will retain a degree of stability α for $|\phi_i| < 60^{\circ}$, $i = 1,2,\ldots,m$. It is interesting to note that these guaranteed margins with respect to degree of stability are identical to the guaranteed stability margins derived in Section 4.4.2.

4.5 Properties of the RPDS Inverse Return Difference Matrices and Related Robustness Results

We have noted in section 4.2 that useful robustness characterizations (including the guaranteed gain and phase margins) for MIMO systems can be stated in terms of the minimum singular value of the inverse return difference matrix. It was also mentioned briefly in section 4.2 that this quantity is a useful complement to the minimum singular value of the return difference matrix. The purpose of this section is to examine

several important properties of RPDS inverse return difference matrix and the related robustness interpretations. Results in this section are presented in a fashion which closely parallels that of section 4.4.

4.5.1 Properties in Common with LQ Regulators

Unlike the case of the return difference matrices, no useful frequency domain characterization of inverse return difference matrices is known for LQ regulators. However, when the control weighting matrix is chosen to be a scaled identity matrix, then a lower bound for the minimum singular value of the LQ inverse return difference matrix can be obtained in terms of the lower bound for the minimum singular value of the LQ return difference matrix derived in the last section. A precise statement of this result is given by the following theorem.

Theorem 4.11 Let the matrix $\underline{K}_\alpha$ be the unique positive definite solution of the algebraic Riccati equation (4.59) with conditions on $\underline{A}$, $\underline{B}$, $\underline{Q}$ and $\underline{R}$ satisfied. Also assume that

$$\det(j\omega \underline{I} - \underline{A}) \neq 0 \qquad \text{for all } \omega \geq 0 \tag{4.117}$$

and that

$$\underline{T}_\alpha(j\omega) \text{ is invertible at all } \omega \geq 0 \tag{4.118}$$

Then

$$\sigma\min\left(\underline{I} + \underline{T}_\alpha^{-1}(j\omega)\right) \geq \frac{\sigma\min(\underline{I} + \underline{T}_\alpha(j\omega))}{1 + \sigma\min(\underline{I} + \underline{T}_\alpha(j\omega))} \tag{4.119}$$

$$\geq \frac{1}{2} \qquad \text{for all } \omega \geq 0 \tag{4.120}$$

Proof: The relation (4.119) follows from direct application of an inequality due to Nuzman and Sandell [Nu 1]. To derive (4.120) from

(4.119), we make use of the Kalman's Inequality (4.80) derived in the last section and this completes the proof.

It follows from Corollary 4.1 and the above theorem that RPDS design with $\underline{R}$ chosen to be a scaled identity matrix has a guaranteed gain margin given by $(\frac{1}{2}, \frac{3}{2})$ and a guaranteed phase margin given by $(-30^{\circ}, 30^{\circ})$. Both of these margins turn out to be more conservative than those derived using the RPDS return difference matrix.

It is also possible to obtain these guaranteed stability margins for RPDS designs with $\underline{R}$ chosen to be a diagonal matrix. The derivation is analogous to that of Theorem 4.5 and requires the use of the equivalent system depicted in Fig. 4.9. Based on the equivalent system, we can rewrite (4.119) and (4.120) in Theorem (4.11) as

$$\sigma\min(\underline{I} + \hat{\underline{T}}_{\alpha}^{-1}(j\omega)) \geq \frac{\sigma\min(\underline{I} + \hat{\underline{T}}_{\alpha}(j\omega))}{1 + \sigma\min(\underline{I} + \underline{T}_{\alpha}(j\omega))} \tag{4.121}$$

$$\geq \frac{1}{2} \tag{4.122}$$

Using inequality (4.122) together with Theorem 4.5 leads directly to the following result . Invertibility of $\underline{T}_{\alpha}(j\omega)$ for $\omega \geq 0$ is assumed.

Theorem 4.12 Given a RPDS with loop-transfer matrix $\underline{T}_{\alpha}(s)$, the loop-transfer matrix $\tilde{\underline{T}}_{\alpha}(s) = \underline{T}_{\alpha}(s)\ \underline{L}(s)$ is stable if

(i) $\underline{T}_{\alpha}(s)$ and $\tilde{\underline{T}}_{\alpha}(s)$ have the same number of unstable poles (4.123)

(ii) $\underline{T}_{\alpha}(s)$ has no pole on the $j\omega$-axis (4.124)

(iii) $\sigma\max\ (\underline{R}^{1/2}\ \underline{L}(j\omega)\ \underline{R}^{-1/2} - \underline{I}) < \frac{1}{2}$ for all $\omega \geq 0$ (4.125)

When $\underline{R}$ and $\underline{L}(s)$ are chosen to be diagonal, condition (4.125) in the above theorem reduces to

$$|\ell_i(j\omega) - 1| < \frac{1}{2} \qquad \text{for all} \quad \omega \geq 0 \quad \text{and } i = 1,2,\ldots,m \tag{4.126}$$

We can now employ (4.126) to establish the guaranteed gain and phase margins by assuming $\ell_i(s)$ to be real and $\ell_i(s) = e^{j\phi_i}$, respectively, for $i = 1,2,\ldots,m$.

It is important to emphasize that the guaranteed stability margins derived above and those in section 4.2 are margins that apply to all RPDS designs with diagonal $\underline{R}$. The remarkable generality of these results in turn account for their conservative nature. Less conservative margins can be obtained if the actual values of the design parameters $\underline{A}$, $\underline{B}$, $\underline{R}$ and $\underline{Q}$ are taken into account in the robustness test. For a given RPDS design, the quantity β_o defined by

$$\beta_o = \min_{\omega \geq 0} \sigma\min(\underline{I} + \hat{\underline{T}}_\alpha(j\omega)) \tag{4.127}$$

is in fact often greater than $\frac{1}{2}$. In cases when this is true, we can replace condition (4.125) in Theorem 4.12 with a less stringent bound

$$\sigma\max(\underline{R}^{1/2}\ \underline{L}(j\omega)\ \underline{R}^{-1/2} - I) < \beta_o \qquad \text{for all} \quad \omega \geq 0 \tag{4.128}$$

If $\underline{R}$ and $\underline{L}(s)$ are both chosen to be diagonal, then the inequality (4.125) implies an improved guaranteed gain margin of $(1 - \beta_o,\ 1 + \beta_o)$ and a guaranteed phase margin of $(-2 \sin^{-1} \frac{\beta_o}{2},\ 2 \sin^{-1} \frac{\beta_o}{2})$.

It is also noteworthy that guaranteed stability margins obtained from robustness tests based on $\sigma\min(\underline{I} + \underline{T}_\alpha(j\omega))$ cannot be further tightened by taking into considerations the specific values of the design parameters. The quantity $\sigma\min(\underline{I} + \underline{T}_\alpha(j\omega))$ is always lower bounded by unity as a result of $\underline{T}_\alpha(s)$ being strictly proper.

Combining the guaranteed stability margins obtained in this section and the last, we arrive at the following improved guaranteed margins that are valid for RPDS designs with $\underline{R}$ chosen to be diagonal.

$$GM \subset (1 - \beta_o, \infty) \tag{4.129}$$

$$PM \subset (\min(-2 \sin^{-1} \frac{\beta_o}{2}, 60^\circ), \tag{4.130}$$

$$(\max(2\sin^{-1} \frac{\beta_o}{2}, 60^\circ) \tag{4.130}$$

(4.129) and (4.130) above represent the tightest guaranteed margins one can obtain using Theorems 4.4 and 4.5. This is an example where appropriate combination of robustness tests can lead to a reduction in conservatism.

4.5.2 The Effect of the Stability Factor α on the RPDS Inverse Return Difference Matrices

If

$$\det(j\omega\underline{I} - \underline{A}) \neq 0 \qquad \text{for } \omega \geq 0 \tag{4.131}$$

and

$$\det(\underline{T}_\alpha(j\omega)) \neq 0 \qquad \text{for } \omega \geq 0, \tag{4.132}$$

we can rewrite the RPDS frequency domain equality (4.63) in the following form

$$(\underline{I} + \underline{T}_\alpha^{-1}(j\omega))^H \ \underline{R}(I + \underline{T}_\alpha^{-1}(j\omega))$$

$$= \underline{T}_\alpha^{-H}(j\omega) \ [\underline{R} + \underline{H}_\alpha(-j\omega, j\omega)] \ \underline{T}_\alpha^{-1}(j\omega) \qquad \text{for } \omega \geq 0 \tag{4.133}$$

Recall from the derivation of Corollary 4.2 that the effect of α on $(\underline{I} + \underline{T}_\alpha(j\omega))^H \ \underline{R}(\underline{I} + \underline{T}_\alpha(j\omega))$ is readily obtained by considering the effect of α on $\underline{H}_\alpha(-j\omega, j\omega)$. To obtain a similar characterization for $(\underline{I} + \underline{T}_\alpha^{-1}(-j\omega)) \ \underline{R}(\underline{I} + \underline{T}_\alpha^{-1}(j\omega))$, we need to consider the effect of α on

$$\underline{H}_o(-s,s) \overset{\Delta}{=} \underline{T}_\alpha^{-T}(-s)(\underline{R} + \underline{H}_\alpha(s))\ \underline{T}_\alpha^{-1}(s) \tag{4.134}$$

$$= [\underline{R}^{-1}\ \underline{B}^T\ \underline{K}_\alpha(-sI - \underline{A})^{-1}\ \underline{B}]^{-T}\ [\underline{R} + \underline{B}^T(-s\underline{I} - \underline{A})^{-1}\ (\underline{Q} + 2\alpha\underline{K}_\alpha)(s\underline{I} - \underline{A})^{-1}\ \underline{B})]$$

$$[\underline{R}^{-1}\ \underline{B}^T\ \underline{K}_\alpha(s\underline{I} - \underline{A})^{-1}\ \underline{B}] \tag{4.135}$$

where $\underline{K}_\alpha$ is the positive definite solution of the RPDS algebraic Riccati equation (4.59). The coefficients of both rational matrices $\underline{T}_\alpha(s)$ and $\underline{H}_\alpha(-s,s)$ are dependent on the stability factor α through the matrix $\underline{K}_\alpha$, which is known to be an increasing function of α (Lemma 3.1). Unfortunately, $\underline{K}_\alpha$ enters the matrix $\underline{H}_o(-s,s)$ in a highly nontrivial fashion and thus makes it difficult to precisely characterize the effect of α on $\underline{H}_o(s)$.

When $\underline{R}$ is chosen to be a scaled identity matrix $\beta\underline{I}$ we can approximate the RPDS inverse return difference with matrix with

$$\underline{I} + \underline{T}_\alpha^{-1}(j\omega))^H\ (\underline{I} + \underline{T}_\alpha^{-1}(j\omega)) \tilde{=} \left(\underline{I} + \left(\frac{\underline{B}^T\underline{K}_\alpha\ \underline{B}}{-j\omega\beta}\right)^{-1}\right)\left(\underline{I} + \left(\frac{\underline{B}^T\ \underline{K}_\alpha\ \underline{B}}{j\omega\beta}\right)^{-1}\right)$$

$$= \underline{I} + \omega^2\ (\underline{B}^T\ \underline{K}_\alpha\ \underline{B})^{-2}\ \beta^2 \tag{4.136}$$

at values of ω where $j\omega\underline{I}$ dominates the matrix $(j\omega\underline{I} - \underline{A})$. Using the incremental property of $\underline{K}_\alpha$ (Lemma 3.1), we can readily show that $\underline{I} + \beta^2\omega^2(\underline{B}^T\underline{K}_\alpha\ \underline{B})^{-2}$ is a monotonically decreasing function of α (i.e. $\underline{I} + \beta^2\omega^2(\underline{B}^T\underline{K}_{\alpha_1}\underline{B})^{-2} < I + \beta^2\omega^2(\underline{B}^T\ \underline{K}_{\alpha_2}\ \underline{B})^{-2}$ for $\alpha_1 > \alpha_2$ and for all $\omega \geq 0$). It follows from this observation that $(\underline{I} + \underline{T}_\alpha^{-1}(j\omega))$ (and thus $\sigma\min(\underline{I} + \underline{T}_\alpha^{-1}(j\omega))$) is a decreasing function of α in the high frequency region. Attempts to characterize $(\underline{I} + \underline{T}_\alpha^{-1}(j\omega))^H\ (\underline{I} + \underline{T}_\alpha^{-1}(j\omega))$ at frequencies where the approximation (4.136) fails to hold has not been successful. However, it is our conjecture that $(\underline{I} + \underline{T}_\alpha^{-1}(j\omega))^H\ (\underline{I} + \underline{T}_\alpha(j\omega))$ will

generally behave as a decreasing function of α at all $\omega > 0$ for $\underline{R}$ chosen to be a scaled identity matrix. If this is indeed the case, then two important design implications follow. First, the quantity β_o defined in (4.127) also becomes a decreasing function of α.[1] As a result, the guaranteed downward gain margin given by $1 - \beta_o$ will deteriorate with increasing α.[2] Second, the maximum RPDS system bandwidth ωmax defined as the highest value of ω (see [Ch 1] section 7.7) at which

$$\sigma\min(\underline{I} + \underline{T}_\alpha^{-1}(j\omega)) = 1 \qquad (4.137)$$

will increase monotonically with α. This can be readily verified by inspection of the $\sigma\min(\underline{I} + \underline{T}_\alpha^{-1}(j\omega))$ plots of a RPDS design (Fig. 4.13) with the minimum singular value of the inverse return difference matrix being a decreasing function of α.

4.5.3 Properties of the RPDS Inverse Return Difference Matrices on the α-Nyquist Contour

The results presented in this section are stronger versions of those considered in section 4.5.1. All the margins derived here apply to the stability as well as the degree of stability property of the underlying RPDS. To begin with, we shall consider RPDS designs where $\underline{R}$ is chosen to be a scaled identity matrix and obtain a lower bound

---

[1] See section 5.4 for an example where $\sigma\min(\underline{I} + \underline{T}_\alpha^{-1}(j\omega))$ is a decreasing function of α for all $\omega \geq 0$.

[2] Recall from Example 4.1 that the same result may not hold for the actual stability margins.

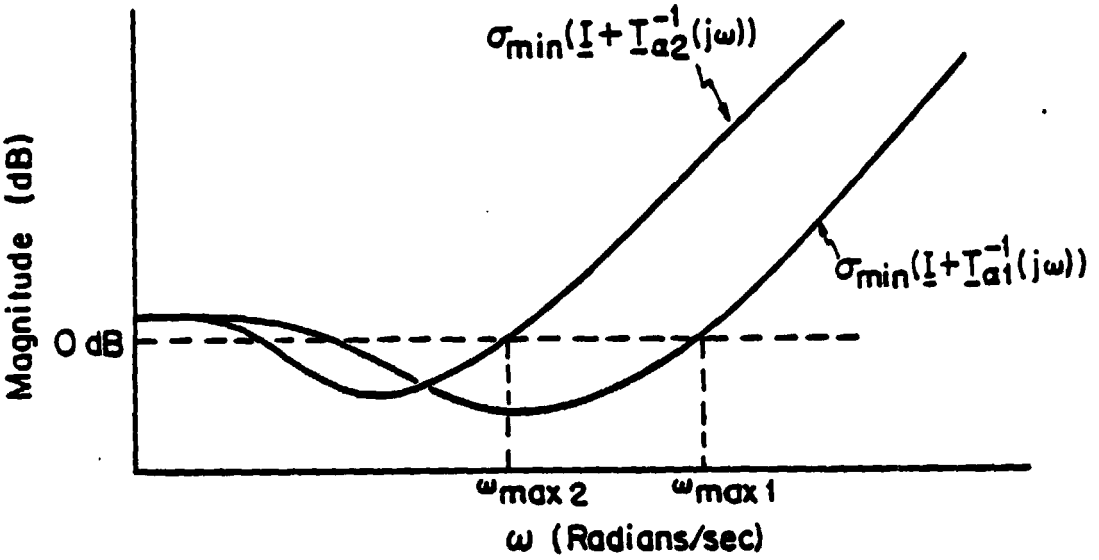

FIG. 4.13 Singular Value Plots for RPDS Design;

$\alpha_1 > \alpha_2$

for the quantity $\sigma\min(\underline{I} + \underline{T}_\alpha^{-1}(j\omega-\alpha))$ that is valid for all $\omega > 0$. A precise statement of the result is given by the following theorem.

Theorem 4.13 Let the matrix $\underline{K}_\alpha$ be the unique positive definite solution of the algebraic Riccati equation (4.59) with conditions on $\underline{A}$, $\underline{B}$, $\underline{Q}$ and $\underline{R}$ satisfied. Also assume that

$$\det((j\omega - \alpha)\underline{I} - \underline{A}) \neq 0 \qquad \text{for all } \omega \geq 0 \tag{4.138}$$

and that

$$\underline{T}_\alpha(-\alpha + j\omega) \text{ is invertible at all } \omega \geq 0 \tag{4.139}$$

Then

$$\sigma\min(\underline{I} + \underline{T}_\alpha^{-1}(-\alpha + j\omega))$$

$$\geq \frac{\sigma\min(\underline{I} + \underline{T}_\alpha(-\alpha + j\omega))}{1 + \sigma\min(\underline{I} + \underline{T}_\alpha(-\alpha + j\omega))} \qquad \text{for all } \omega \geq 0 \tag{4.140}$$

Proof: We shall prove this result from a standpoint different from that adopted in Section 4.4.4. Recall from the proof of Theorem 2.5 that we introduced a time-invariant LQ problem on our way to obtain a solution for the RPDS problem. It was also shown that the desired RPDS feedback gain is identical to that obtained from the related LQ problem where the objective is to minimize

$$J = \lim_{t_1 \to \infty} \int_{t_o}^{t_1} [\underline{x}^T \underline{Q}\, \underline{x}(t) + \underline{u}^T(t)\, \underline{R}\, \underline{u}(t)]dt \tag{4.141}$$

subject to the dynamic constraint

$$\dot{\underline{x}}(t) = (\underline{A} + \alpha \underline{I})\, \underline{x}(t) + \underline{B}\, \underline{u}(t) \tag{4.142}$$

The controllability and the cost observability of this LQ problem follows from those of the original RPDS problem and the RPDS state feedback gain is given by $\underline{G}_\alpha = \underline{R}^{-1} \underline{B}^T \underline{K}_\alpha$ where $\underline{K}_\alpha$ is the positive definite solution of the RPDS Riccati equation (4.59). Applying the result of Theorem 4.10 (which also holds for LQ regulator problems with $\underline{R}$ chosen to be a scaled identity matrix) to the solution of the above LQ problem leads directly to (4.140) and this completes the proof.

Based on the equivalent system given in Fig. 4.9, the following inequality that holds for arbitrary $\underline{R}$ (i.e. $\underline{R}$ not necessarily be diagonal) can be readily obtained

$$\sigma\min(\underline{I} + \underline{R}^{1/2} \underline{T}_\alpha^{-1}(j\omega - \alpha) \underline{R}^{-1/2}) \geq \frac{1}{2} \quad \text{for all } \omega \geq 0 \tag{4.143}$$

The proof of (4.143) is similar to that given in Theorem 4.13 with $\underline{T}_\alpha(s)$ replaced by $\underline{R}^{1/2}\underline{T}_\alpha(s-\alpha)\underline{R}^{-1/2}$. The result below is a direct consequence of (4.143) and Theorem 4.13. Invertibility of $\underline{T}_\alpha(j\omega-\alpha)$ for $\omega \geq 0$ is assumed.

Theorem 4.14 Given a rational transfer matrix $\underline{T}_\alpha(s)$ of a RPDS system with a prescribed degree of stability α, the perturbed system with loop transfer matrix given by $\tilde{\underline{T}}_\alpha(s) = \underline{T}_\alpha(s)\,\underline{L}(s)$ has a degree of stability α if

(i) $\underline{T}_\alpha(s-\alpha)$ and $\tilde{\underline{T}}(s-\alpha)$ have the same number of unstable poles (4.144)

(ii) $\underline{T}_\alpha(s-\alpha)$ has no pole on the $j\omega$-axis (4.145)

(iii) $\sigma\max(\underline{R}^{1/2} \underline{L}(j\omega - \alpha) \underline{R}^{-1/2} - \underline{I}) < \frac{1}{2}$ for all $\omega \geq 0$ (4.146)

If both $\underline{R}$ and $\underline{L}$ are diagonal, then (4.146) reduces to the following set of scalar inequalities

$$|\ell_i(j\omega - \alpha) - 1| < \frac{1}{2} \quad \text{for all } \omega \geq 0 \text{ and } i = 1,2,\ldots m \tag{4.147}$$

For case of ℓ_i representing a pure gain change, it is clear from condition (4.147) that the perturbed system will retain a degree of stability α for ℓ_i satisfying $\frac{1}{2} < \ell_i < \frac{3}{2}$. Similarly, for $\ell_i = e^{j\phi_i}$ the condition (4.147) implies that the perturbed system will not lose the degree of stability for $|\phi_i| < 30^\circ$. A RPDS design with $\underline{R}$ chosen to be diagonal therefore possesses a guaranteed GM_α of $(\frac{1}{2}, \frac{3}{2})$ and a guaranteed PM_α of $(-30^\circ, 30^\circ)$. These margins are found to be more conservative than those derived from (4.116).

To characterize the margin for a given RPDS design, we place condition $\sigma max(\underline{R}^{1/2}\ \underline{L}(j\omega - \alpha)\ \underline{R}^{-1/2} - \underline{I}) < \frac{1}{2}$ in (4.142) by

$$\sigma max(\underline{R}^{1/2}\ L(j\omega - \alpha)\ \underline{R}^{-1/2} - \underline{I}) < \beta\alpha \tag{4.148}$$

where $\beta\alpha$ is defined to be

$$\beta\alpha = \min_{\omega>0}\ \sigma min(\underline{I} + \underline{T}_\alpha^{-1}(j\omega - \alpha)) \tag{4.149}$$

This quantity $\beta\alpha$ turns out to be greater than $\frac{1}{2}$ for most RPDS designs, and thus enables us to obtain an improved guaranteed GM_α of $(1 - \beta\alpha, 1 + \beta\alpha)$ and an improved guaranteed PM_α of $(-2\sin^{-1}\frac{\beta_o}{2}, 2\sin^{-1}\frac{\beta_o}{2})$. Combining the guaranteed GM_α and PM_α obtained here with those derived in section 4.4.5, we arrive at the following guaranteed GM_α and PM_α that hold for a given RPDS design with diagonal $\underline{R}$

$$GM_\alpha \supset (1 - \beta\alpha, \infty) \tag{4.150}$$

$$PM_\alpha \supset (\min(-60^\circ, -2\sin^{-1}\tfrac{\beta\alpha}{2}), \max(60^\circ, 2\sin^{-1}\tfrac{\beta\alpha}{2})) \tag{4.151}$$

These are the best margins that one may derive using Theorems 4.10 and 4.14.

4.6 Roll-Off Requirements at High Frequencies

In our discussion of RPDS robustness properties thus far, we have neglected the important design consideration of having the nominal loop gain sufficiently attenuated over the frequency range where the magnitude of the multiplicative perturbation $\underline{L}(j\omega)$ becomes large compared to unity. It is a physical fact that the quality of a nominal design model inevitably deteriorates at high frequencies as a result of unmodelled and/or unknown dynamics of various types. In the multiplicative form of perturbation $\underline{L}(s)$, this means that $\sigma\max(\underline{L}(j\omega))$ will assume value close to 1.0 at low frequencies but will increase to 2 and beyond at high frequencies. In the face of such uncertainties, the seemingly excellent guaranteed RPDS stability margin is clearly inadequate. In the high frequency region, the $\pm 60^{\circ}$ phase margin is of no value since a neglected time delay will ultimately produce phase error in excess of 180°. Moreover, the return difference inequality (4.74) from which the guaranteed RPDS stability margins are derived does not hold at high frequencies since the frequency response of any physically realizable system must have a roll-off at a rate greater than or equal to s^{-2}. The roll-off requirement of RPDS (and for LQ regulator in general) in the face of uncertainties can be derived from the basic inequality (4.27) in Theorem 4.5.

At frequencies where all the feedback loops of $\underline{T}_{\alpha}(j\omega)$ are rolled off, the quantity $\sigma\max(\underline{T}_{\alpha}(j\omega)) = \sigma\min^{-1}(\underline{T}_{\alpha}^{-1}(j\omega))$ becomes small. As a

result, we can approximate the minimum singular value of $\underline{I} + \underline{T}_\alpha^{-1}(j\omega)$ as

$$\sigma \min(\underline{I} + \underline{T}_\alpha^{-1}(j\omega)) \tilde{=} \sigma\min(\underline{T}_\alpha^{-1}(j\omega))$$

$$= \sigma\max^{-1}(\underline{T}_\alpha(j\omega)) \qquad (4.152)$$

Substituting this approximation into (4.27) gives

$$\sigma\max(\underline{L}(j\omega) - \underline{I})\ \sigma\max(\underline{T}_\alpha(j\omega)) < 1 \qquad (4.153)$$

It is now clear from (4.153) that the loop transfer matrix $\underline{T}_\alpha(j\omega)$ has to attenuate faster than $\sigma\max^{-1}(\underline{L}(j\omega) - \underline{I})$ in order to satisfy the stability requirements at frequencies where the physical process is ill-represented by the model. But the roll-off rate of $\underline{T}_\alpha(j\omega)$ is limited to ω^{-1} as evidenced by the following approximation

$$\underline{T}_\alpha(j\omega) \tilde{=} \frac{\underline{B}^T \underline{K}_\alpha \underline{B}}{j\omega} \qquad (4.154)$$

which holds for values of ω sufficiently large. Substituting (4.154) into (4.153) we obtain

$$\sigma\max(\underline{L}(j\omega) - \underline{I})\ \sigma\max(\underline{B}^T \underline{K}_\alpha \underline{B})|\omega|^{-1} < 1 \qquad (4.155)$$

It follows from (4.155) that the cross-over frequency of $\underline{T}_\alpha(j\omega)$ has to be located well below the frequency where $\sigma\max(\underline{L}(j\omega) - \underline{I})$ starts growing large.

Equation (4. 155) also makes explicit the relationship between the roll-off frequency of $\underline{T}_\alpha(j\omega)$ and the stability factor α . If we define the maximum cross-over frequency $\omega\ \sigma\max$ of $\underline{T}_\alpha(j\omega)$ to be the frequency when

$$\sigma\max(\underline{T}_\alpha(j\omega)) = 1 \qquad (4.156)$$

it can then be readily shown that the quantity $\sigma\max(\underline{B}^T \underline{K}_\alpha \underline{B})$ provides

an upperbound for $\omega\sigma_{max}$. Moreover, we can deduce from Lemma 3.1 that $\sigma_{max}(B^T \underline{K}_\alpha B)$ is an increasing function of α. The implication of the roll-off requirement (4.155) on the choice of stability factor α now becomes clear. While a large value of α will improve the system's speed of response, it may also extend the bandwidth into regions where $\underline{L}(j\omega)$ is large. In picking a value for the stability factor α, the designer needs to find a compromise between the requirements for stability in face of uncertainties and speed of performance.

4.7 Summary of RPDS Robustness Properties

We shall summarize in this section the various robustness properties of RPDS discussed in the two previous sections.

(i) Guaranteed gain and phase margins for stability

If the matrix $\underline{R}$ is chosen to be diagonal, then a RPDS design possesses the following guaranteed stability margins

$$GM \supset (\beta_o, \infty) \tag{4.157}$$

$$PM \supset (\min(-60^\circ, -2\sin^{-1}\frac{\beta_o}{2}), \max(60^\circ, 2\sin^{-1}\frac{\beta_o}{2})) \tag{4.158}$$

where β_o is given by (4.127)

(ii) Guaranteed gain and phase margins for the prescribed degree of stability.

If the matrix $\underline{R}$ is chosen to be diagonal, then a RPDS design possesses the following margins with respect to the prescribed degree of stability

$$GM_\alpha \supset (\beta\alpha , \infty) \tag{4.159}$$

$$PM_\alpha \supset (\min(-2\sin^{-1}\frac{\beta_\alpha}{2} , -60^o) \quad \max(2\sin^{-1}\frac{\beta_\alpha}{2} , 60^o)) \tag{4.160}$$

(iii) Effect of the stability factor α on the robustness properties of RPDS

The RPDS's ability to tolerate modelling error (quantified in terms of the magnitude of the modelling error in question) improves with increasing value of the stability factor α only for some special choices of error representation. Among the four types of modelling error presented in this thesis, we only obtain an improved tolerance for $\underline{E}_4(s) = (\underline{\tilde{T}}^{-1}(s) - \underline{T}^{-1}(s))\,\underline{T}(s)$ with increasing α . The guaranteed RPDS margins summarized in (i) and (ii) above may deteriorate with increasing α if β_o and β_α turn out to be a monotonically decreasing functions of α (see section 5.4 for an example of β_o being a decreasing function of α).

It was shown in section 4.4.4 that the behavior of the actual RPDS gain and phase margins with changing value of α is highly system dependent.

(iv) High frequency roll-off requirement

The bound $\sigma\max(\underline{B}^T\,\underline{K}_\alpha\,\underline{B})$ for the maximum cross-over frequency of RPDS is an increasing function of α(see section 4.6). This in turn imposes an upper limit on the value of α that we may employ in RPDS design. It is well known to control system designers that too large a cross-over frequency may result in excitation of the unmodelled and/or unknown dynamics at high frequencies which is undesirable from a stability robustness point of view.

It is important to emphasize that the conclusions summarized in this section are only valid with respect to the types of model error under investigation. The relative error in $\underline{T}_\alpha^{-1}(s)$ is particularly useful for our purpose, because its associated robustness theorems (Theorems 4.4 and 4.6) allow simple derivation of RPDS multi-loop margins with respect to stability and degree of stability. Further study on the ability of RPDS to tolerate model errors other than those considered here (see [Le 1] Section 3.9 is needed for a more complete understanding of its robustness properties.

4.8 Robustness Properties of Kalman Bucy Filter with a Prescribed Degree of Stability (FPDS)

As we have noted in Chapter II, KBF with a prescribed degree of stability (FPDS) is the mathematical dual of RPDS. Dual robustness results are therefore obtainable for such designs. These robustness properties ensure the nondivergence of the filter under variation in the nominal model of the plant which is to be estimated. In section 4.8.1 we set up the framework for robustness analysis of FPDS. The robustness properties for this class of filter are discussed in sections 4.8.2. to 4.8.4.

4.8.1 Formulation of the Robustness Problem for Kalman Bucy Filters with a Prescribed Degree of Stability

The basic FPDS problem considered here is identical to that discussed in Theorem 2.5. The underlying linear system is given by

$$\dot{\underline{x}}(t) = \underline{A}\,\underline{x}(t) + \underline{\zeta}(t) \tag{4.161}$$

$$\underline{y}(t) = \underline{C}\,\underline{x}(t) + \underline{\theta}(t) \tag{4.162}$$

where $\underline{\zeta}(t)$ and $\underline{\theta}(t)$ are zero mean white noise processes with spectral intensity matrices $\underline{\Xi}$ and $\underline{\Theta}$ respectively. We also assume the observability of $(\underline{C}, \underline{A})$ and controllability of $(\underline{A}, \underline{\Xi}^{1/2})$. The state estimate $\hat{\underline{x}}(t)$ is then specified by

$$\dot{\hat{\underline{x}}}(t) = \underline{A}\,\hat{\underline{x}}(t) + \underline{H}_\alpha\,\underline{\nu}(t) \tag{4.}$$

$$\underline{\nu}(t) = \underline{y}(t) - \underline{C}\,\hat{\underline{x}}(t) \tag{4.164}$$

where

$$\underline{H}_\alpha = \underline{\Sigma}_\alpha\,\underline{C}^T\,\underline{\Theta}^{-1} \tag{4.165}$$

and $\underline{\Sigma}_\alpha$ is the unique positive definite solution of the Riccati equation

$$(\underline{A} + \alpha\underline{I})\underline{\Sigma}_\alpha + \underline{\Sigma}_\alpha(\underline{A} + \alpha I)^T + \underline{\Xi} - \underline{\Sigma}_\alpha\underline{C}^T\,\Theta^{-1}\,\underline{C}\,\underline{\Sigma}_\alpha = \underline{0} \tag{4.166}$$

A useful method for describing the state estimate dynamics of FPDS (in fact for KBF in general) is given by the following set of feedback equations

$$\dot{\underline{e}}(t) = \underline{A}\,\underline{e}(t) + \underline{w}(t) \tag{4.167}$$

$$\underline{s}(t) = \underline{C}\,\underline{e}(t) - \underline{\theta}(t) \tag{4.168}$$

$$\underline{w}(t) = -\underline{H}_\alpha\,\underline{s}(t) - \underline{\zeta}(t) \tag{4.169}$$

where $s(t) = \hat{\underline{y}}(t) - \underline{y}(t)$ (4.170)

and

$$\underline{e}(t) = \hat{\underline{x}}(t) - \underline{x}(t) \tag{4.171}$$

A block diagram representation of these equations is given in Fig. 4.14. By ignoring the noise sources, this can be rearranged into a unity feedback of the type considered in Section 4.2. It is now readily

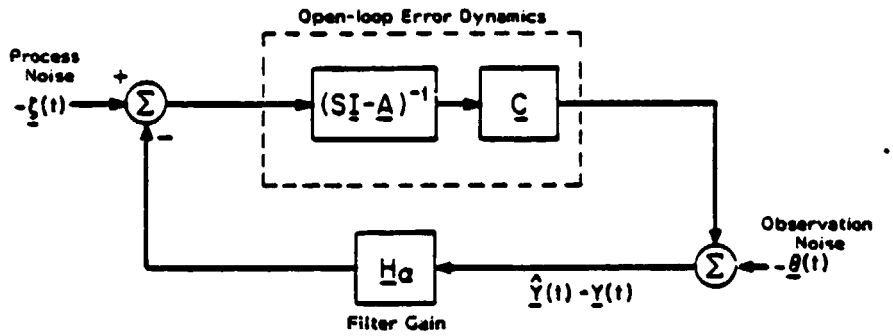

FIG. 4.14 Feedback Representation of the Error Dynamics of FPDS

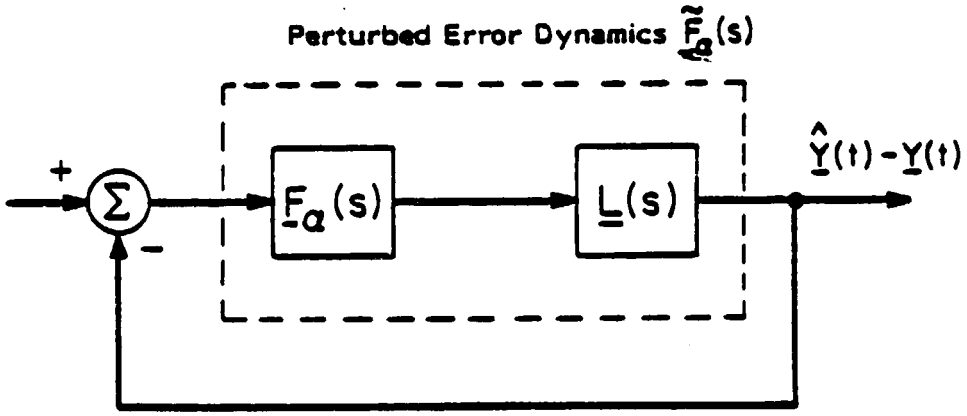

FIG. 4.15 Feedback Configuration for Robustness Analysis of FPDS Error Dynamics

apparent that

$$\underline{F}_\alpha(s) \triangleq \underline{C}(s\underline{I} - \underline{A})^{-1} \underline{H}_\alpha \tag{4.172}$$

the loop transfer matrix of the error dynamics loop of KBF with prescribed degree of stability is the dual of $\underline{T}_\alpha(s)$ for RPDS. The discrepancy between the linear model employed in the design of the filter gain and the actual system dynamics are modelled as multiplicative perturbations $\underline{L}(s)$ inserted in the closed-loop after $\underline{C}$ (see Fig. 4.15).

4.8.2 Common Robustness Properties with KBF

Based on the feedback representation of the FPDS error-dynamics, we are ready to characterize the stability margins of KBF with a prescribed degree of stability. The nominal error-dynamics model corresponds to the ideal situation in which the linear design model represented by (4.161) and (4.162) are exact. Since all the results developed in this section are mathematically dual to the RPDS results obtained in sections 4.4 and 4.5, the respective derivations will be omitted. The main emphasis will be on the interpretation of robustness results in the estimation context. All the FPDS robustness properties presented in this section are known properties of KBF, and are included here for completeness.

To begin with, we state two frequency domain equalities for FPDS. These are the exact dual of (4.63) and (4.64) in Theorem 4.8 and are basic to the derivations of the robustness results given in this section.

Theorem 4.15 Let the matrix Σ_α be the unique positive definite solution of the algebraic Riccati equation

$$\underline{\Sigma}_\alpha(\underline{A} + \alpha \underline{I})^T + (\underline{A} + \alpha \underline{I})\underline{\Sigma}_\alpha + \underline{\Xi} - \underline{\Sigma}_\alpha \underline{C}^T \underline{\Theta}^{-1} \underline{C} \underline{\Sigma}_\alpha = \underline{0} \tag{4.173}$$

with

$$\text{(i)} \quad \underline{\Xi} \geq 0 \text{ and } \underline{\Theta} > 0 \tag{4.174}$$

$$\text{(ii)} \quad (\underline{A}, \underline{\Xi}^{1/2}) \text{ controllable} \tag{4.175}$$

$$\text{(iii)} \quad (\underline{C}, \underline{A}) \text{ observable} \tag{4.176}$$

then

$$(\underline{I} + \underline{F}_\alpha(-\alpha + s))\ \underline{\Theta}(\underline{I} + \underline{F}_\alpha\ (-\alpha - s))^T = \underline{\Theta} + \underline{M}\ (s,-s) \tag{4.177}$$

and

$$(\underline{I} + \underline{F}_\alpha(s))\ \underline{\Theta}(\underline{I} + \underline{F}_\alpha(-s))^T = \underline{\Theta} + M_\alpha(s,-s) \tag{4.178}$$

where we define

$$\underline{M}(\zeta,s) = \underline{C}(\zeta \underline{I} - \alpha \underline{I} - \underline{A})^{-1} \underline{\Xi}(s\underline{I} - \alpha \underline{I} - \underline{A})^{-T} \underline{C}^T \tag{4.179}$$

and

$$\underline{M}_\alpha(\zeta,s) = \underline{C}(\zeta \underline{I} - \underline{A})^{-1} (2\alpha \underline{\Sigma}_\alpha + \underline{\Xi})\ (s\underline{I} - \underline{A})^{-T} \underline{C}^T \tag{4.180}$$

Remark The equalities (4.179) and (4.180) are derived from the FPDS algebraic Riccati equations using manipulations similar to those employed in the proof of Theorem 4.8.

Remark The two frequency domain equalities stated in Theorem 4.14 correspond to the two interpretations of FPDS given in section 2.4.

Using the positive definitness of $\underline{\Sigma}_\alpha$ and equation (4.180) we can readily obtain the following corollary to Theorem 4.15.

Corollary 4.9 If $\underline{\Sigma}_\alpha$ is the unique positive definite solution of the FPDS algebraic Riccati equation (4.173), with the respective requirements on $\underline{A}$, $\underline{C}$, $\underline{\Xi}$, and $\underline{\Theta}$ being satisfied and if $\det(j\omega I - \underline{A}) \neq 0$ for

all $\omega \geq 0$, we have

$$(\underline{I} + \underline{F}_\alpha(j\omega))\ \underline{\Theta}(\underline{I} + \underline{F}_\alpha(j\omega))^H > \underline{\Theta} \quad \text{for all } \omega \geq 0 \tag{4.181}$$

Combining inequality (4.181) with Theorem 4.4 readily leads to the following robustness theorem which holds for KBF in general.

Theorem 4.16 Given a FPDS with loop transfer matrix of error dynamics given by $\underline{F}_\alpha(s)$, the mismatched error dynamics with loop transfer matrix $\tilde{\underline{F}}_\alpha(s) = \underline{L}(s)\ \underline{F}_\alpha(s)$ [1] is closed-loop stable if

(i) $\underline{F}_\alpha(s)$ and $\tilde{\underline{F}}_\alpha(s)$ have the same number of unstable poles (4.182)

(ii) $\underline{F}_\alpha(s)$ has no pole on the $j\omega$-axis (4.183)

(iii) $\sigma\max\ (\underline{\Theta}^{-1/2}\ \underline{L}^{-H}(j\omega)\ \underline{\Theta}^{1/2} - \underline{I}) \leq 1 \quad \text{for all } \omega \geq 0$ (4.184)

The condition (4.184) describes the inherent robustness properties of the FPDS design procedure. It says that every FPDS design can tolerate at least multiplicative perturbation $\underline{L}(s)$ satisfying the bound (4.184) If the observation noise at each output channel are uncorrelated (i.e. $\underline{\Theta}$ is diagonal) and if the model mismatch can be represented by a diagonal multiplicative perturbation of the error dynamics, condition (4.184) can then be interpreted in terms of the gain and phase margins of each output channel in the feedback representation of error dynamics (Fig 4.15).

The derivation follows from recognizing the equivalence between

$$\sigma\max(\underline{\Theta}^{-1/2}\ \underline{L}^{-H}(j\omega)\ \underline{\Theta}^{1/2} - \underline{I}) \leq 1 \quad \text{for all } \omega \geq 0 \tag{4.185}$$

---

[1] It can be readily shown that Theorems 4.4 to 4.7 also apply to model error described by $\underline{T}(s) = \underline{L}(s)\ \underline{T}(s)$

and

$$\Theta \underline{L}^{H}(j\omega) + \underline{L}(j\omega)\,\underline{\Theta} - \underline{\Theta} \geq 0 \qquad \text{for all } \omega \geq 0 \tag{4.186}$$

When $\underline{\Theta}$ and $\underline{L}(s)$ are both diagonal, (4.182) further simplifies to

$$2\mathrm{Re}(\ell_i(j\omega)) \geq 1 \qquad \text{for all } \omega \geq 0,\ i = 1,2,\ldots,m \tag{4.187}$$

If $\ell_i(j\omega)$ is real, then (4.187) becomes

$$\ell_i \geq \frac{1}{2} \tag{4.188}$$

Alternately, if $\ell_i(j\omega) = e^{j\phi_i}$, then condition (4.187) becomes

$$|\phi_i| \leq 60^{\circ} \tag{4.189}$$

The conditions (4.188) and (4.189) can be interpreted as implying that FPDS design employing uncorrelated observation noise leads to a guaranteed gain margin of $(\frac{1}{2}, \infty)$ and guaranteed phase margin of $(-60^{\circ}, 60^{\circ})$ in each output channel of the error dynamics feedback system (Fig. 4.14). These margins are relative to the ideal situation that (4.161) and (4.162) are exact.

It is important to stress that the guaranteed margins thus derived holds for <u>every</u> FPDS design using diagonal $\underline{\Theta}$. The generality of this result in turn accounts for its conservatism. Less conservative margins can be obtained for a <u>given</u> FPDS design if we combine the bounds derived above with those derived using Theorem 4.5 and Corollary 4.3. The resulting guaranteed gain and phase margins obtained from the latter are given by $(1 - \gamma_o,\ 1 + \gamma_o)$ and $(-2\sin^{-1}\frac{\gamma_o}{2},\ 2\sin^{-1}\frac{\gamma_o}{2})$ respectively where γ_o is defined to be

$$\gamma_o = \min_{\omega \geq 0} \sigma\min(\underline{I} + \underline{\Theta}^{-1/2}\,\underline{F}_{\alpha}^{-H}(j\omega)\,\underline{\Theta}^{1/2}) \tag{4.190}$$

and $\underline{\Theta}$ is diagonal.

Since the value of γ_o usually lies between $\frac{1}{2}$ and 1, the downward gain margin $1 - \beta_o$ results from application of Corollary 4.3 is therefore always less than or equal to $\frac{1}{2}$. However, the related guaranteed phase margin $(-2\sin^{-1}\frac{\gamma_o}{2}, 2\sin^{-1}\frac{\gamma_o}{2})$ will extend beyond the interval $(-60^o, 60^o)$ only when $\gamma_o > 1$.

It is clear from the above discussion that the following guaranteed GM and PM hold for error dynamics of a given FPDS design with Θ chosen to be diagonal

$$GM \supset (1 - \gamma_o, \infty) \tag{4.191}$$

$$PM \supset (\min(-60^o, 2\sin^{-1}\frac{\gamma_o}{2}), \max(60^o, 2\sin^{-1}\frac{\gamma_o}{2})) \tag{4.192}$$

(4.191) and (4.192) indeed yield the least conservative guaranteed margins one can obtain using Theorem 4.4 and 4.5.

4.8.3 The Effect of the Stability Factor α on the Robustness Properties of RPDS

Like the case of RPDS, the effect of α on the robustness properties of the FPDS error-dynamics can be characterized in terms of the effect of α on the matrix function $\underline{I} + \underline{F}_\alpha(s)$ and $\underline{I} + \underline{F}_\alpha^{-1}(s)$.

The result described in the following corollary to Theorem 4.14 makes precise the behavior of $\underline{I} + \underline{F}_\alpha(s)$ as α varies. It is the exact dual of Corollary 4.2.

Corollary 4.10 Let the matrix $\underline{\Sigma}_{\alpha_1}$ and $\underline{\Sigma}_{\alpha_2}$ be the unique positive solutions of FPDS algebraic Riccati equations

$$(\underline{A} + \alpha\underline{I})\,\underline{\Sigma}_{\alpha_1} + \underline{\Sigma}_{\alpha_1}(\underline{A} + \alpha\underline{I})^T + \underline{\Xi} - \underline{\Sigma}_{\alpha_1}\,\underline{C}^T\,\underline{\Theta}^{-1}\,\underline{C}\,\underline{\Sigma}_{\alpha_1} = \underline{0} \qquad (4.193)$$

and

$$(\underline{A} + \alpha\underline{I})\underline{\Sigma}_{\alpha_1} + \underline{\Sigma}_{\alpha_2}\,(\underline{A} + \alpha\underline{I})^T + \underline{\Xi} - \underline{\Sigma}_{\alpha_2}\,\underline{C}^T\,\underline{\Theta}^{-1}\,\underline{C}\,\underline{\Sigma}_{\alpha_2} = \underline{0} \qquad (4.194)$$

where

$$\text{(i)} \quad \underline{\Xi} \geq 0, \quad \underline{\Theta} > 0 \qquad (4.195)$$

$$\text{(ii)} \quad (\underline{C}, \underline{A}) \text{ observable} \qquad (4.196)$$

$$\text{(iii)} \quad (\underline{\Xi}^{1/2}, \underline{A}) \text{ observable} \qquad (4.197)$$

and $$\text{(iv)} \quad \det(j\omega\underline{I} - \underline{A}) \neq 0 \quad \text{for} \quad \omega \geq 0 \qquad (4.198)$$

Then one has $(\underline{I} + \underline{F}_{\alpha_1}(j\omega))\underline{\Theta}\ (\underline{I} + \underline{F}_{\alpha_1}(j\omega))^H$

$$> (\underline{I} + \underline{F}_{\alpha_2}(j\omega))\underline{\Theta}\ (\underline{I} + \underline{F}_{\alpha_2}(j\omega))^H \quad \text{for all} \quad \omega \geq 0$$

$$\text{if } \alpha_1 > \alpha_2 \geq 0 \qquad (4.199)$$

When $\underline{\Theta}$ is a scaled identity matrix (i.e. the noises at each output channel have the same intensity and are uncorrelated), the following inequality on the minimum singular value of FPDS can be readily derived from (4.199) by using the properties of singular values.

$$\sigma\min(\underline{I} + \underline{F}_{\alpha_1}^H(j\omega)) > \sigma\min(\underline{I} + \underline{F}_{\alpha_2}^H(j\omega)) \quad \text{for all } \omega \geq 0 \qquad (4.200)$$

This inequality provides us with a useful way of assessing the effect of α on the robustness properties of the FPDS designs. Using condition (4.22) of Theorem 4.4 together with condition (4.198) leads directly to the conclusion that FPDS tolerance of model mismatch represented by[1]

$$\underline{E}_4(s) = (\tilde{\underline{F}}_\alpha^{-T}(-s) - \underline{F}_\alpha^{-T}(-s))\,\underline{F}_\alpha^T(-s) \qquad (4.201)$$

---

[1] The singular values of $\underline{E}_4(s)$ given in (4.201) will be different from those of $\underline{E}_4$ defined by $\underline{E}_4(s) = (\tilde{\underline{F}}_\alpha^{-1}(s) - \underline{F}_\alpha^{-1}(s))\,\underline{F}_\alpha(s)$

improves with α . As we have noted before, error measure of this type is unintuitive and difficult to interprete.

Like the case of RPDS, a precise characterization of $\underline{I} + \underline{F}_\alpha^{-H}(j\omega)$ with respect to change of α is not available. However, when $\underline{\Theta}$ is an identity matrix, it can again be shown that $\sigma\min(\underline{I} + \underline{F}_\alpha^{-H}(j\omega))$ is a decreasing function of α for sufficiently large value of ω.

4.8.4 Robustness Properties with Respect to the Degree of Stability α

We shall first examine the robustness interpretations of equality (4.179) for FPDS. The following corollary to Theorem 4.15 that characterizes the behavior of the FPDS return difference matrix on the α-Nyquist contour is the exact dual of Corollary 4.8

Corollary 4.11 Let $\underline{\Sigma}_\alpha$ be the unique positive definite solution of the algebraic Riccati equation (4.163), with the respective requirements on $\underline{A}$, $\underline{C}$, $\underline{\Xi}$ and $\underline{\Theta}$ being satisfied and $\det(j\omega\underline{I} - \alpha\underline{I}) \neq 0$ for all $\omega \geq 0$. Then

$$(\underline{I} + \underline{F}_\alpha(-\alpha + j\omega))\underline{\Theta} \quad (\underline{I} + \underline{F}_\alpha(-\alpha + j\omega))^H \geq \underline{\Theta} \tag{4.202}$$

Working with the equivalent feedback representation of the FPDS error dynamics given by (4.167) to (4.171), the theorem given below is a direct consequence of (4.202) and Theorem 4.5.

Theorem 4.17 Given a FPDS with a prescribed degree of stability α and a loop transfer matrix $\underline{F}_\alpha(s)$. The mismatched error-dynamics with loop transfer matrix $\tilde{\underline{F}}_\alpha(s) = \underline{L}(s)\,\underline{F}_\alpha(s)$ has a degree of stability α if

(i) $\underset{\sim}{F}(s - \alpha)$ and $\underset{\sim}{\tilde{F}}(s - \alpha)$ have the same number of unstable poles (4.203)

(ii) $\underset{\sim}{F}_\alpha(s - \alpha)$ has no pole on the $j\omega$-axis (4.204)

(iii) $\sigma\max(\underline{\Theta}^{-1/2}\ \underline{L}^{-H}(j\omega - \alpha)\ \underline{\Theta}^{1/2} - \underline{I}) < 1$ for all $\omega \geq 0$ (4.205)

If the margin with respect to the degree of stability α derived from (4.205) is combined with those derived using Theorem 4.5 and Corollary 4.3, we obtain the following improved guaranteed margins that apply to a given FPDS design employing uncorrelated observation noise.

GM_α at each output channel $\subset (1 - \gamma_\alpha, \infty)$ (4.206)

PM_α at each output channel $\subset (\min(-60^\circ, -2\sin^{-1}\frac{\gamma_\alpha}{2}),\ \max(60^\circ, 2\sin^{-1}\frac{\gamma_\alpha}{2}))$ (4.207)

where γ_α is defined by

$$\gamma_\alpha = \min_{\omega \geq 0}\ \sigma\min(\underline{I} + \underline{T}_\alpha^{-H}(-\alpha + j\omega)) \tag{4.208}$$

4.8.5 Concluding Remarks

As we have commented before (see section 2.4), exponential weighting of data is a technique well known to filter designers for curing the filter divergence problems. The general thinking is that this will prevent the old data from saturating the filter. In section 4.8.2 to 4.8.4, intuition of this type is subject to rigorous examination using the recently developed results in robustness analysis for MIMO systems. The results obtained here however apply only to those cases where mismatch between the actual

and the design model can be represented as a multiplicative perturbation at the output matrix $\underline{C}$ in the feedback representation of the filter error dynamics (Fig. 4.15).

It is clear from the discussion of the three previous subsections and the summary remark in section 4.7 for the dual results of RPDS, that improvement of FPDS's ability to tolerate model mismatch of the type depicted in Fig. 4.15 only occur for very special choices of model error representation. The exponential weighting technique is therefore not a universal cure for every possible type of divergence problem. The insights obtained from this section help to identify situations where such technique can be effective.

In many applications of interest, the above conclusion may be excessively conservative. This follows from the fact that we have only used some magnitude information on the model mismatch in our robustness analysis. In the case where structural information is available, the results in Chapter 4 of [Le 1] may be applicable.

CHAPTER V

APPLICATION OF THE REGULATOR WITH A PRESCRIBED DEGREE OF STABILITY TECHNIQUE TO STATE FEEDBACK DESIGN FOR MULTI-TERMINAL DC/AC POWER SYSTEM

5.1 Introduction

The purpose of this chapter is to demonstrate the application of the RPDS technique to design of a state feedback control law for a 9-machine, 4-terminal DC/AC power system. Based on this example, the various robustness properties of RPDS designs discussed in the previous chapter will be illustrated.

Two versions of the 9-machine[1] power system model are available around 5 operating points. They differ in their details of machine description. In the simple version of the model, every generator is represented by a second-order classical machine. This gives a total system order of 18. The open-loop poles of the system are plotted in Fig. 5.1. Each of the 16 complex poles corresponds to a mode of inter-machine oscillation. Frequencies of such oscillations range approximately from 0.3 to 1.0 Hz. The two remaining poles are located on the negative real axis. The one located at the origin corresponds to the mode of clock error. The mode located at .375 is the mode of average frequency.

---

[1] The power system models employed here are generated by Sherman Chan using the Possim program of the General Electric Company

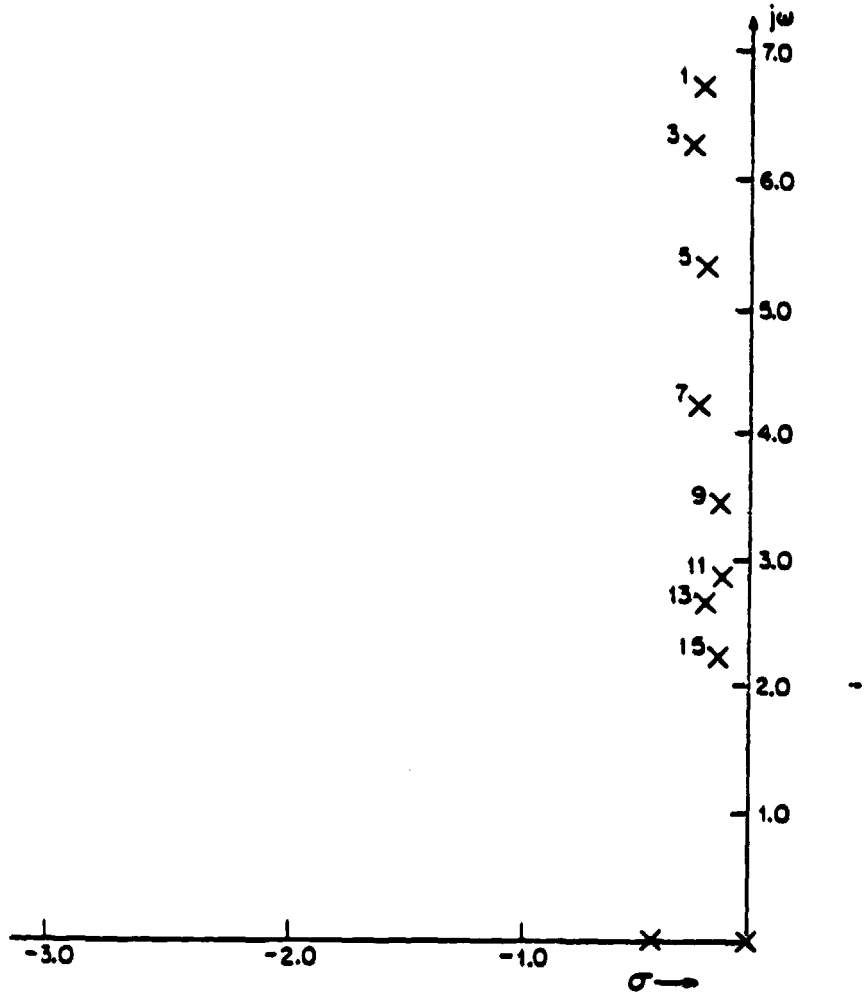

FIG. 5.1 Open-Loop Poles of the Simple Model For the 9-Machine Power System at Operating Point 1

Readers interested in the physical interpretation of these modes may consult Chapter 3 of [Ch 1].

In the detailed version of the model, two of the generators are modelled with four rotor circuits (two in the direct axis and two in the quadrature axis). They are also equipped with IEEE Type 1 exciters and third order power system stabilizers. The total order of this system is 58. The open-loop eigenvalues of this system at operating point 1 are plotted in Fig. 5.2. The complex poles of the system that are associated with machine oscillations are numbered in descending order of their frequency.[1] Comparing the oscillatory modes given by the two models show that they are in good agreement. It is also noteworthy that 6 pairs of the oscillatory modes have no counterpart in the 18-state model, because they are associated with the stabilizing components of the power system.

The basic design objective is to move the open-loop oscillatory poles of the system to an appropriate region in the left-half complex plane. This region is determined approximately by using engineering judgement on how large the closed-loop bandwidth may be without allowing unmodelled high frequency disturbance or dynamics to destabilize the system. For physical considerations, the average frequency mode and the clock error mode are to be kept intact.

In section 5.2, several full state feedback designs are obtained by using the RPDS methodology. A different value of the stability

---

[1] Only one pole of each complex pair is displayed in Fig. 5.2 .

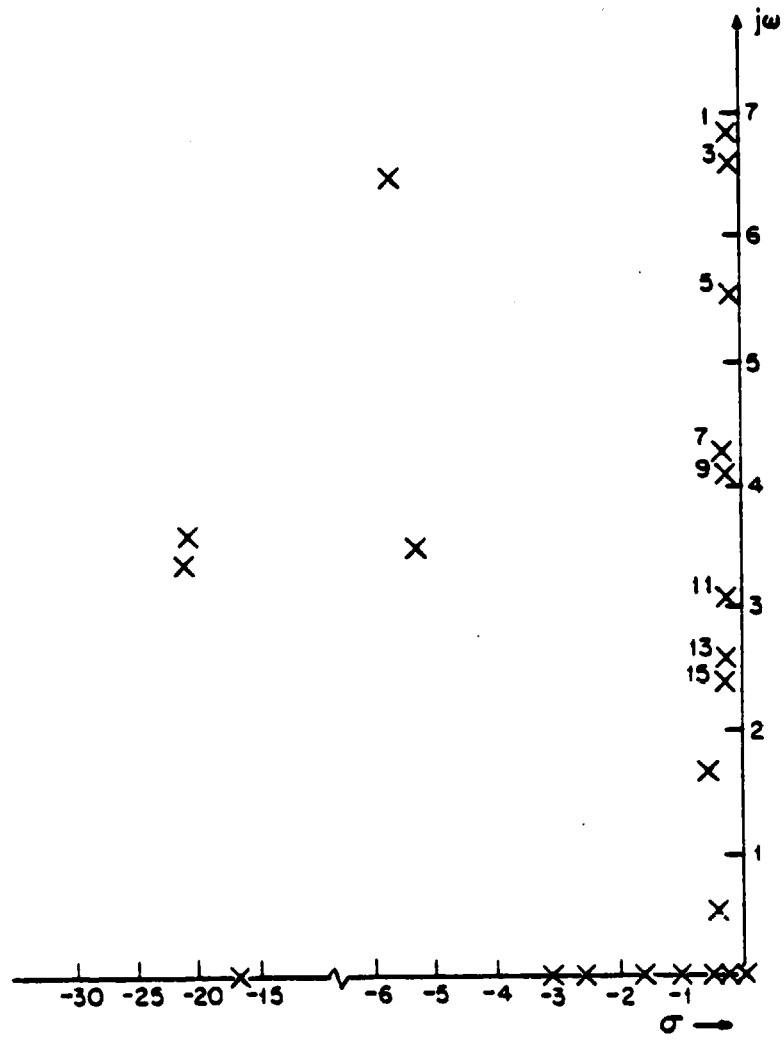

FIG. 5.2 Open-Loop Poles of the Detailed Model for the 9-Machine Power System Model at Operating Point 1

factor α is employed for each design. The resulting closed-loop systems are found to display some desirable properties which are not predicted by the theory developed in the previous chapters.

The robustness properties of the RPDS design are evaluated in two ways. In section 5.3 we apply the control laws obtained for the simple model at operating point 1 to the other four operating points. The resulting movements of the closed-loop poles provide a good indication of the system tolerance to change in operating conditions. The control law obtained for the simple design model are also implemented on the detailed 38 state model at various operating points. This allows us to study the effect of the unmodelled dynamics due to the exciters on RPDS designs - an issue that we feel to be important since in this case the neglected dynamics are no longer separated from the intermachine dynamics.

In section 5.4, we turn to the frequency domain robustness analysis formulated in Theorems 4.4 and 4.5 with emphasis given to the effect of the stability factor α on the quantities $\sigma\max(\underline{I} + \underline{T}_\alpha(j\omega))$ and $\sigma\max(\underline{I} + \underline{T}_\alpha^{-1}(j\omega))$.

5.2 RPDS Designs

The design parameters to be chosen in a RPDS problem are the stability factor α, the state weighting matrix $\underline{Q}$ and the control weighting matrix $\underline{R}$. In the absence of information concerning the relative cost of control for the different DC-terminals, we shall simply pick $\underline{R}$ to be an identity matrix. The state weighting matrix $\underline{Q}$ is chosen to satisfy the following objectives:

(i) Only the oscillatory modes associated with the intermachine oscillation but not the modes associated with the real poles are penalized. This is done to limit the control amplitude and to avoid interaction between the multi-terminal DC controller and existing mechanisms for correcting the generation mismatch and clock errors.

(ii) The damping ratio of the oscillatory modes should be around 0.2. This choice is somewhat arbitrary although it serves to provide a reasonable LQ regulator ($\alpha = 0$) design to start from. This is not the only method of specifying the $\underline{Q}$ matrix in relation to transient response requirements. Indeed, a suitable choice of $\underline{Q}$ has to be considered jointly with the stability factor α.

In cases where $\alpha = 0$ (i.e. the LQ problem), the previous requirements on $\underline{Q}$ can be easily met by application of modal weighting techniques such as Solheim's method [So 1]. When α is nonzero, an additional trick is required to prevent the two real modes from being moved under feedback. To make clear the underlying problem we consider the case where α is picked to be 0.5. This choice of stability factor will result in a matrix $(\underline{A} + \alpha\underline{I})$ with 2 unstable real poles. If the matrix $\underline{Q}$ is chosen to make these poles unobservable, then it follows from the properties of algebraic Riccati equations and the discussion in Chapter 3 concerning the construction of RPDS root-loci that the resulting RPDS feedback law will shift the average frequency mode to -0.625 and the clock error mode to -1.0. A scheme to avoid this problem is outlined below.[1]

[1]This scheme was first suggested to the author by N.A. Lehtomaki

Step 1 Compute a positive semi-definite matrix $\underline{S}$ which is defined as

$$\underline{S} \triangleq -\beta\ (\underline{x}_1\ \underline{y}_1^T + \underline{x}_2\ \underline{y}_2^T) \tag{5.1}$$

where $\underline{x}_1$ $\underline{y}_1$ are the right and left eigenvectors respectively of the average frequency mode, $\underline{x}_2$ $\underline{y}_2$ are the right and left eigenvectors respectively of the clock error mode and β is set to be any positive real number larger than α.

Step 2 Pick a state weighting matrix $\underline{Q}$ that makes the two real poles $(\underline{A} + \underline{S})$ cost-unobservable and the closed-loop oscillatory poles possessing a damping ratio about 0.2.

Step 3 Using $\tilde{\underline{A}} = \underline{A} + S$ in place of $\underline{A}$ in the RPDS design (i.e. solution of the RPDS algebraic Riccati equation). The resulting feedback control law is given by

$$\underline{u}(t) = -\ \underline{B}^T\ \tilde{\underline{K}}_\alpha\ \underline{x}(t) \tag{5.2}$$

where $\tilde{\underline{K}}_\alpha$ is the unique positive semi-definite solution of the equation

$$\tilde{\underline{K}}_\alpha(\underline{A} + \alpha\underline{I}) + \tilde{\underline{A}} + \alpha\underline{I})\ \tilde{\underline{K}}_\alpha - \tilde{\underline{K}}_\alpha\ \underline{B}\ \underline{B}^T\ \tilde{\underline{K}}_\alpha + \underline{Q} = \underline{0} \tag{5.3}$$

It can be readily verified that the procedure described above results in feedback laws that leave the clock error mode and the average frequency mode unchanged. First, note that the matrix $\tilde{\underline{A}}$ has two real poles located at $-\beta$ and $-\beta - 0.375$ with their left and right eigenvectors given by $\underline{y}_1$ $\underline{x}_1$ and $\underline{y}_2$ $\underline{x}_2$ respectively. Moreover, by the choice of β, these two poles will remain in the left-half complex plane upon addition of α to their real parts (as is done in the RPDS design with stability factor given by α). It then follows from the choice of the matrix $\underline{Q}$

and the properties of algebraic Riccati equations that the matrix $(\tilde{\underline{A}} + \alpha\underline{I} - \underline{B}\,\underline{B}^T\,\tilde{\underline{K}}_\alpha)$ which is obtained by applying the state feedback law (5.2) to $\dot{\underline{x}}(t) = (\tilde{\underline{A}} + \alpha\underline{I})\,\underline{x}(t)$ will have two real poles located at $-\beta + \alpha$ and $-0.375 - \beta + \alpha$. Moreover the eigenvectors of these two poles are identical to those of the clock error mode and the average frequency mode respectively. Subtracting $\underline{S} + \alpha\underline{I}$ from $(\tilde{\underline{A}} + \alpha\underline{I} - \underline{B}\,\underline{B}^T\,\tilde{\underline{K}}_\alpha)$ will return these real poles back to their original positions ($-\beta + \alpha - 0.375$ to $-.375$ and $-\beta + \alpha$ to 0) with their corresponding eivenvectors remaining unchanged. It should be emphasized that the matrix $\underline{S}$ is used only for the purpose of computing the feedback law.

The simple model of the 9-machine power system at operating point 1 is chosen to be the nominal model for design. Several values of α ranging from 0.0 to 0.6 are tried in the design. These values of α are compatible with the damping rate observed in the actual power systems. Too large a value of α will result in faster performance at the cost of having inputs with unacceptably large magnitude.

The closed-loop poles of the resulting RPDS design with α equals 0.0, 0.2, 0.4 and 0.6 are plotted in Fig. 5.3. Given the increment of α equals to $\Delta\alpha$, all the oscillatory modes move further out to the left by an amount roughly equal to $-\Delta\alpha$. This is by no means a property common to all RPDS at all values of positive α. Such behavior of RPDS closed-loop poles is probably a result of the fact that all modes to be controlled in the multiterminal DC/AC powe system are of the same nature (i.e. they all represent modes of intermachine oscillations). It is also noteworthy that changes in the imaginary part of the closed-loop poles with respect to α are negligible compared to changes in the real part.

Mode	Open Loop	= 0.0	= 0.2	= 0.4	= 0.6
1,2	-0.18 ±j 6.77	-1.44 ±j 6.77	-1.61 ±j 6.71	-1.82 ±j 6.66	-2.056 ± 6.60
3,4	-0.23 ±j 6.32	-1.34 ±j 6.32	-1.51 ±j 6.31	-1.70 ±j 6.30	1.92 ±j 6.30
5,6	-0.17 ±j 5.32	-1.06 ±j 5.32	-1.20 ±j 5.34	-1.38 ±j 5.41	-1.60 ±j 5.47
7,8	-0.23 ±j 4.18	-0.97 ±j 4.18	-1.11 ±4.20	-1.29 ±j 4.20	-1.518 ±j 4.21
9,10	-0.16 ±j 3.45	-0.68 ±j 3.45	-0.83 ±3.39	-1.01 ±3.32	-1.32 ±j 3.30
11,12	-0.17 ±j 2.80	-0.60 ±j 2.80	-0.72 ±j 2.83	-0.94 ±j 2.87	-1.25 ±j 2.90
13,14	-0.19 ±j 2.60	-0.52 ±j 2.58	-0.65 ±j 2.60	-0.88 ±j 2.60	-1.18 ±j 2.60
15,16	-0.18 ±j 2.20	-0.46 ±j 2.19	-0.56 ±j 2.23	-0.77 ±j 2.25	-1.09 ±j 2.26

TABLE 5.1

Closed-Loop Poles of the Norminal Design

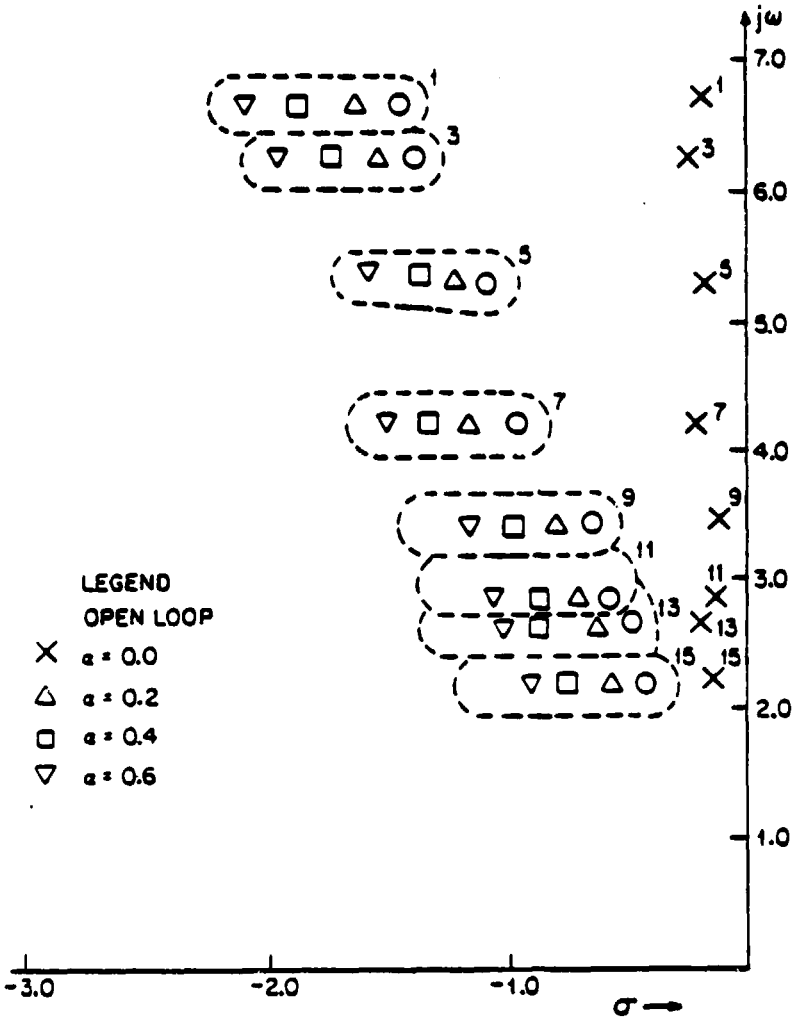

FIG. 5.3 Closed-Loop Poles of the Nominal Design for Various Values of the Stability Factor α

The maximum cross-over frequencies for the various RPDS designs are also computed and listed in Table 5.2. The incremental behavior of this quantity with α agrees with our discussion in section 4.6.

We shall analyze the stability robustness properties of the above designs in the next two sections.

5.3 Behavior of the Closed-Loop Poles in the Face of Perturbations

In this section, we examine the movement of the closed-loop RPDS poles subject to change of operating points and introduction of unmodelled exciter dynamics. In the face of such perturbations, the ability of a state feedback design to hold each closed-loop pole within a small neighborhood of its nominal position is a good indication of its robustness properties. The RPDS designs considered in this section are those obtained in section 5.2 using the simple model of the 9-machine power system at operating point 1. We shall study the robustness properties of such designs in section 5.3.1 and the effect of α on the robustness properties in section 5.3.2.

5.3.1 Robustness Properties with Respect to Change in Operating Points and Unmodelled Exciter Dynamics

In section 5.2 several RPDS control laws were designed for the simple model of the 9-machine power system at operating point 1. We now apply these designs to the other four operating points as well as the detailed 38 state model of the power system, and study the behavior of the resulting closed-loop poles. In Fig. 5.4, the closed-loop poles of the nominal design with choice of stability factor α equals

α	Maximum Crossover Frequencies (Hz)
0.0	0.75
0.2	0.886
0.4	1.078
0.6	1.328

TABLE 5.2

Crossover Frequencies for RPDS Designs

0.4[1] are plotted together with those obtained from application of the same nominal control law to operating points 2 through 5. It can be seen that for each of the oscillatory modes, the closed-loop pole locations at different operating points agree very well with one another. Indeed, with the exception of mode 5,6 and 11,12 locations of the closed-loop poles corresponding to each mode are found to lie within circle of diameter less than 0.5 in the complex plane.

In Fig. 5.5 the oscillatory modes of the detailed model at operating point 1 are plotted alongside those of the simple model for controller design with $\alpha = 0.4$. It is clear from the figure that there is a lack of agreement between the closed-loop poles of the two models. With the exception of modes 5,6 and 9,10 the poles of the detailed model are in general less well damped than those of the simple model. Six oscillatory modes (modes 3,4, 11,12 and 15,16 of the detailed model in fact possess damping ratio of value less than 0.2. Moreover, among these six modes, four of which (modes 11, 12 and 15, 16 have real part of their closed-loop poles less than the stability factor 0.4.

Figure 5.6 displays the closed-loop poles obtained by application of the nominal control law of $\alpha = 0.4$ to the detailed model at all five operating points. Except for the case of modes 5,6,7,8 and 9,10, the closed-loop poles at different operating points for each mode are very close to one another. This indicates the dominance of the unmodelled exciter dynamics over the change of operating points.

---

[1] Throughout this section and section 5.4.2 only those results of the RPDS design with $\alpha = 0.4$ are displayed. The pattern of the closed-loop pole behavior observed for such design is typical of those obtained from the RPDS designs with other values of α.

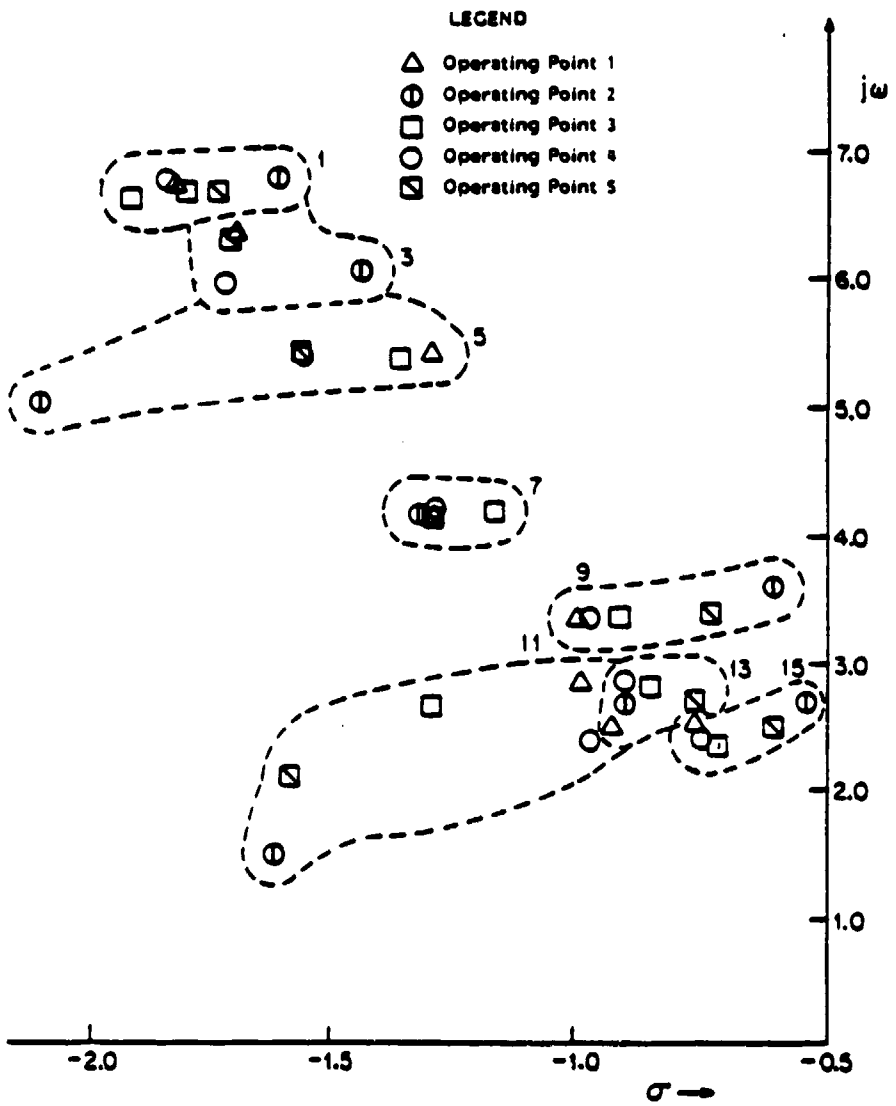

FIG. 5.4 Closed-Loop Poles Result from Application of the Nominal Control Law (Based on the Simple Model at Operating Point 1; $\alpha = 0.4$) to the Simple Power System Model at Various Operating Points

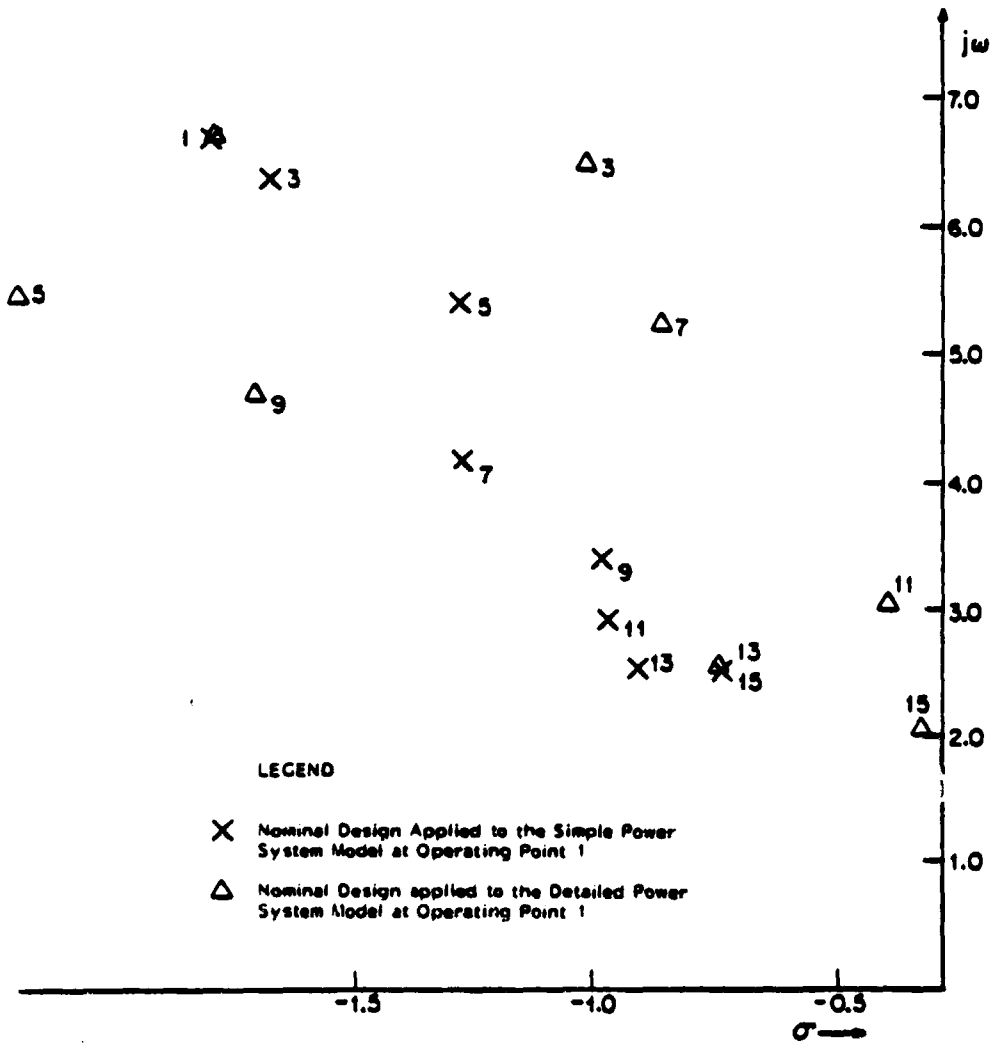

FIG. 5.5 Closed-Loop Poles Related to Machine Oscillation that Results from Application of the Nominal Control Law (Based on the Simple Power System Model at Operating Point 1; α=0.4) to the Simple and the Detailed Power System Models at Operating Point 1

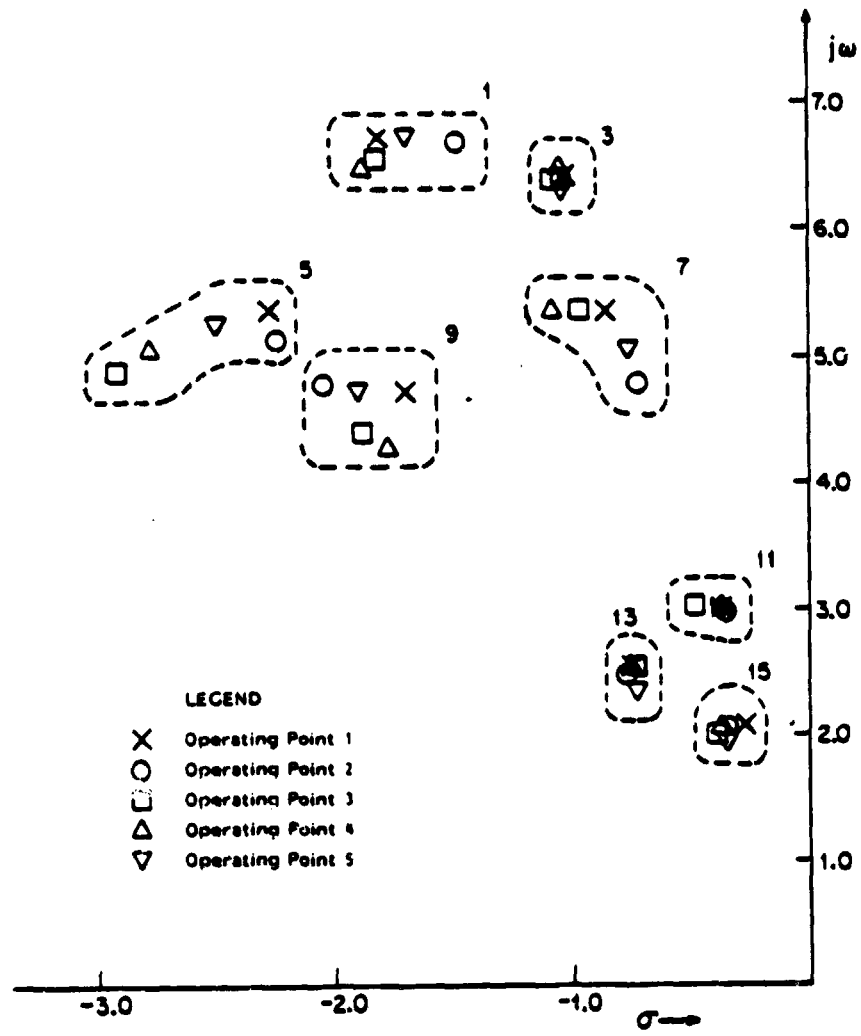

FIG. 5.6 Closed-Loop Poles Related to Machine Oscillations that Result from Application of the Nominal Control Law (Based on the Simple Model at Operating Point 1 with $\alpha = 0.4$) to the Detailed Power System Model at Various Operating Points

It is clear from the above discussion that the RPDS designs obtained in section 5.2 have reasonabley good tolerance of changing operation conditions and unmodelled exciter dynamics. This observation is consistent with the excellent guaranteed stability margins derived for RPDS in Chapter IV.

5.3.2 Effect of the Stability Factor α on Robustness Properties

We next examine the effect of the stability factor α on the behavior of the closed-loop poles subject to perturbation of the system dynamics. This is carried out by applying the RPDS designs with different values of α to operating points 1 through 5. Recall from the last section that the magnitude of the real part of all the closed-loop oscillatory modes display an incremental behavior with α for values of α between 0.0 and 0.6. Moreover, such increment is uniform in the sense that if α is increased by an amount equals to $\Delta\alpha$, then every closed-loop complex pair will be shifted horizontally to the left by a distance roughly equal to $\Delta\alpha$.

Figure 5.7 displays the closed-loop poles that result from applying the RPDS designs of Section 5.2 (which are based on the simple 9-machine model at operating point 1) to operating point 1 for values of α equals to 0.0, 0.2, 0.4 and 0.6. It is observed that as we increase the value of α , all the oscillary modes move further out to the left in the complex plane. However, unlike the case of the nominal design , the amount of pole shifting observed here is no longer proportional to the increment of α. It is also observed that the shift with respect to increment of α tends to be larger for higher values of α.

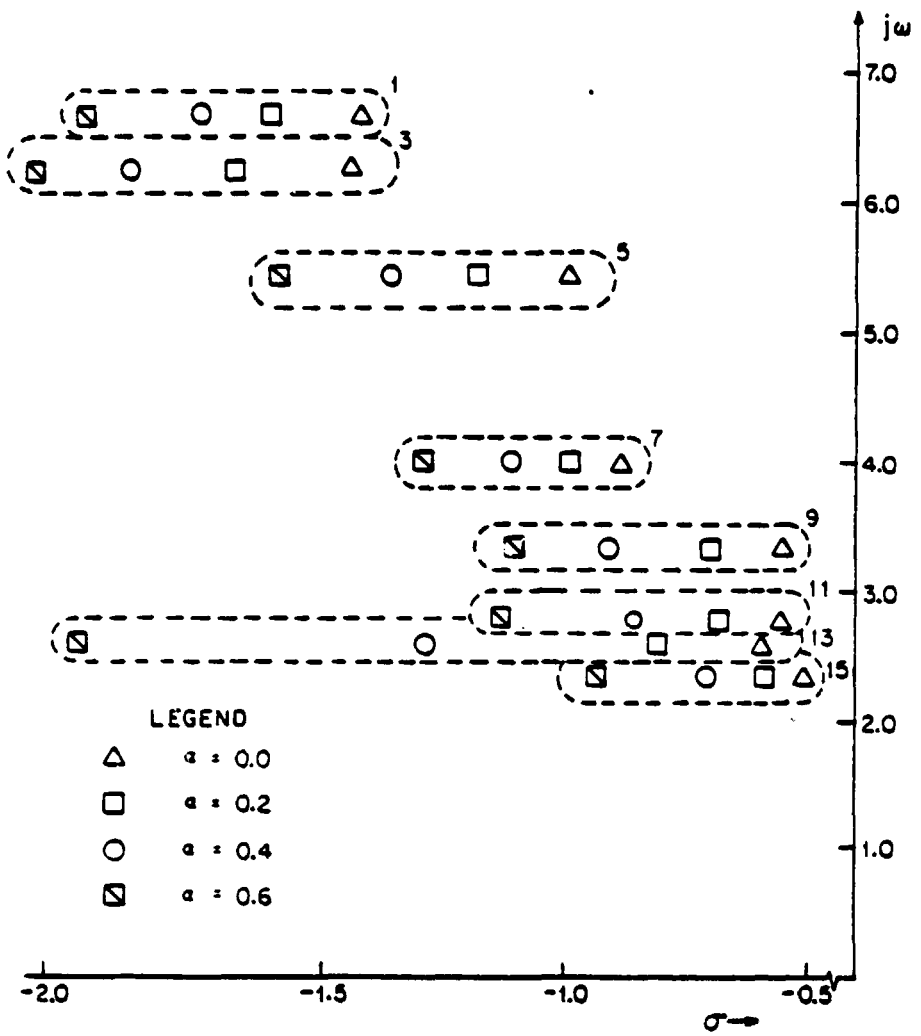

FIG. 5.7 Closed-Loop Poles Result from Application of the Nominal Control Laws (Based on the Simple Model at Operating Point 1; α = 0.0, 0.2, 0.4, 0.6) to the Simple Power System Model at Operating Point 1

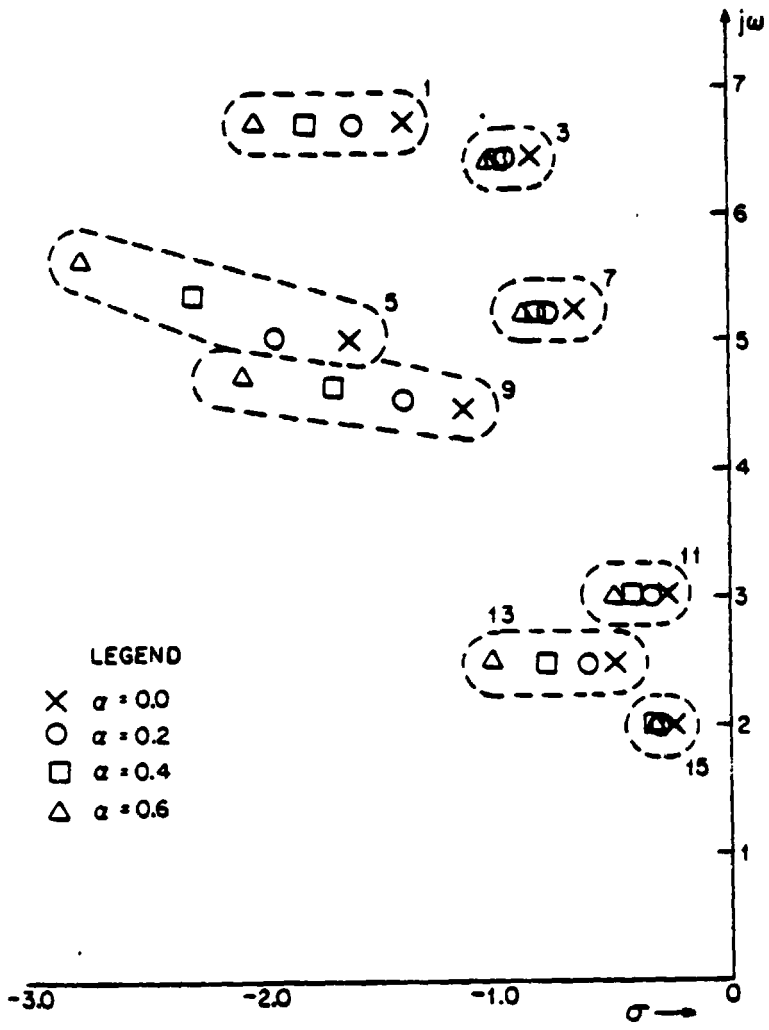

FIG. 5.8 Closed-Loop Poles Related to Machine Oscillations Result from Application of the Nominal Control Laws (Based on the Simple Model at Operating Point 1; α = 0.0, 0.2, 0.4, 0.6) to the Detailed Power System Model at Operating Point 1

The effect of α on the ability of RPDS to tolerate unmodelled exciter dynamics is examined next. The closed-loop poles corresponding to machine oscillations of the detailed model at operating point 1 are plotted in Figure 5.8 for state feedback designs with value of α equals to 0.0, 0.2, 0.4 and 0.6.

It is clear from the figure that the resulting pole pattern again displays an incremental behavior with α, in that the closed-loop poles associated with RPDS design using larger value of α are hold further back from the $j\omega$-axis in the face of unmodelled exciter dynamics.

The above observations suggest improvement of RPDS ability to maintain stability in the face of changing operating points and unmodelled excitor dynamics with increasing value of α . This is a consequence of the fact that large value of α will result in the closed-loop poles being positioned further away from the $j\omega$-axis. It does not however suggest that the ability of RPDS to hold the closed-loop poles near their nominal position under perturbations improves with increasing value of α .

5.4 Frequency Domain Robustness Analysis

Based on the unity negative feedback representation of RPDS in Figure 4.7, frequency domain robustness characterization for the state feedback controllers derived in section 5.2 can be readily obtained. All the RPDS designs studied in this section are again based on the simple model of the 9-machine power system at operating point 1. The behavior of $\sigma\min(\underline{I} + \underline{T}_\alpha(j\omega))$ and $\sigma\min(\underline{I} + \underline{T}_\alpha^{-1}(j\omega))$ with changing α are examined in section 5.4.1. Robustness analysis of the type described in Theorems 4.4

and 4.5 are given in section 5.4.2.

5.4.1 Effect of the Stability Factor α on the Return Difference and Inverse Return Difference Matrices

Minimum singular values of the return difference matrices are plotted in Figure 5.9 for the RPDS designs obtained in Section 5.2. All the singular value plots are found to display a peak in the vicinity of 0.5 Hz, and thereafter roll off in a first order fashion. Moreover, it is clear from the plots that the quantity $\sigma\min(\underline{I} + \underline{T}_\alpha(j\omega))$ increases monotonically with α for all values of ω . This latter observation is consistent with our conclusions in Section 4.4.4 regarding the behavior of RPDS return difference matrices with increasing α[1].

The plots for the complementary quantity $\sigma\min(\underline{I} + \underline{T}_\alpha^{-1}(j\omega))$ of the same RPDS designs are displayed in Figure 5.10. In view of the peak near 0.5 Hz observed in the plots for $\sigma\min(\underline{I} + \underline{T}_\alpha(j\omega))$, it is not at all surprising that the plots for $\sigma\min(\underline{I} + \underline{T}_\alpha^{-1}(j\omega))$ should display a valley at about the same frequency. Beyond this frequency, the plot for $\sigma\min(\underline{I} + \underline{T}_\alpha^{-1}(j\omega))$ began to rise proportionately with ω in a first order fashion. It can also be seen from the plots in Figure 5.10 that $\sigma\min(\underline{I} + \underline{T}_\alpha^{-1}(j\omega))$ is a decreasing function of α for each value of ω. Consequently, the guaranteed margins (as given in (4.12) and (4.13)) for such design will deteriorate with increasing value of α.

---

[1] Due to the presence of the matrix $\underline{S}$ in the algebraic Riccati equation (5.3), one may question the applicability of the conclusions in Chapter IV to the present design example. A closer look at the problem however dismisses such a suspicion. Using the construction of the matrix $\underline{Q}$ and the property of the algebraic Riccati equation, it can be readily demonstrated that $\underline{K}_\alpha \underline{S} = \underline{0}$ where $\underline{K}_\alpha$ is the unique positive definite solution of (5.3). This in turn reduces the Riccati equation (5.3) to one identical to (4.59).

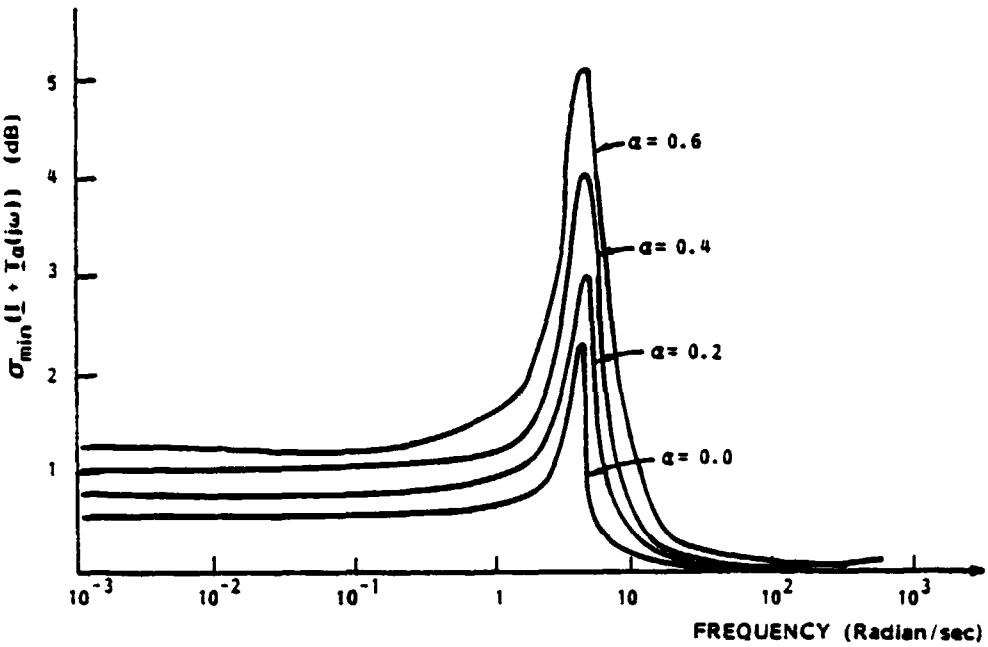

FIG. 5.9 Plots of $\sigma\min(\underline{I} + \underline{T}_\alpha(j\omega))$ for Nominal RPDS Designs Based on the Simple Power System Model at Operating Point 1 with α equals to 0.0, 0.2, 0.4 and 0.6

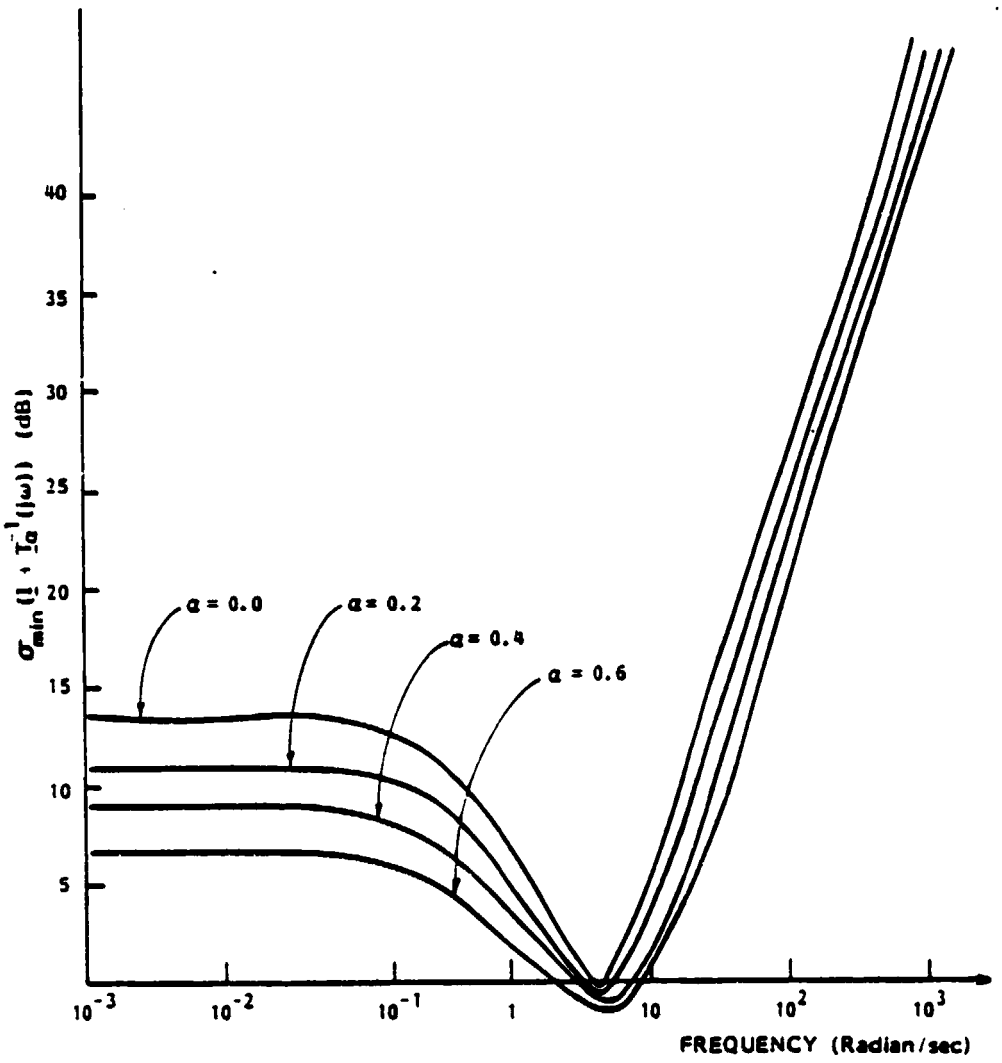

FIG. 5.10 Plots of $\sigma\min(\underline{I} + \underline{T}_\alpha^{-1}(j\omega))$ for Nominal RPDS Designs Based on the Simple Power System Model at Operating Point 1 with α equals to 0.0, 0.2, 0.4 and 0.6

5.4.2 Robustness Tests Based on Singular Values

In order to apply the robustness tests described in Theorems 4.4 and 4.5 to the present example, the multiplicative error matrix $\underline{L}(s)$ with respect to the nominal system model are computed for different perturbed system dynamics. The nominal system model consists of the simple model for the open-loop power system at operating point 1 which is regulated by a state feedback controller with prescribed degree of stability equal to 0.4. This controller is taken directly from the respective RPDS design in Section 5.2.

The various singular values specified by conditions (4.22) and (4.27) are plotted in Figures 5.11 and 5.12 respectively for perturbations corresponding to change of operating points. The singular values plots for $\sigma max(\underline{L}^{-1}(j\omega) - \underline{I})$ and $\sigma max(\underline{L}(j\omega) - \underline{I})$ ar found to display drastically different behavior for different operating points. In particular, the values of $\sigma max(\underline{L}^{-1}(j\omega) - \underline{I})$ and $\sigma max(\underline{L}(j\omega) - \underline{I})$ result from switching from operating point 1 to operating point 2 are noted for their exceptionally large magnitude at low frequencies. This pattern of behavior is in contrast with the insignificant change of the closed-loop pole positions observed in the last section for precisely the same class of perturbations (i.e. change of operating points). It becomes clear from this observation that robustness characcerization based on matrix norms can be very conservative. Conservatism of the norm-based robustness test is further manifested by the fact that conditions (4.22) of Theorem 4.4 and (4.27) of Theorem 4.5 are violated for some nondestabilizing perturbations (such as the change of operating condition from operating point 1 to operating point 2).

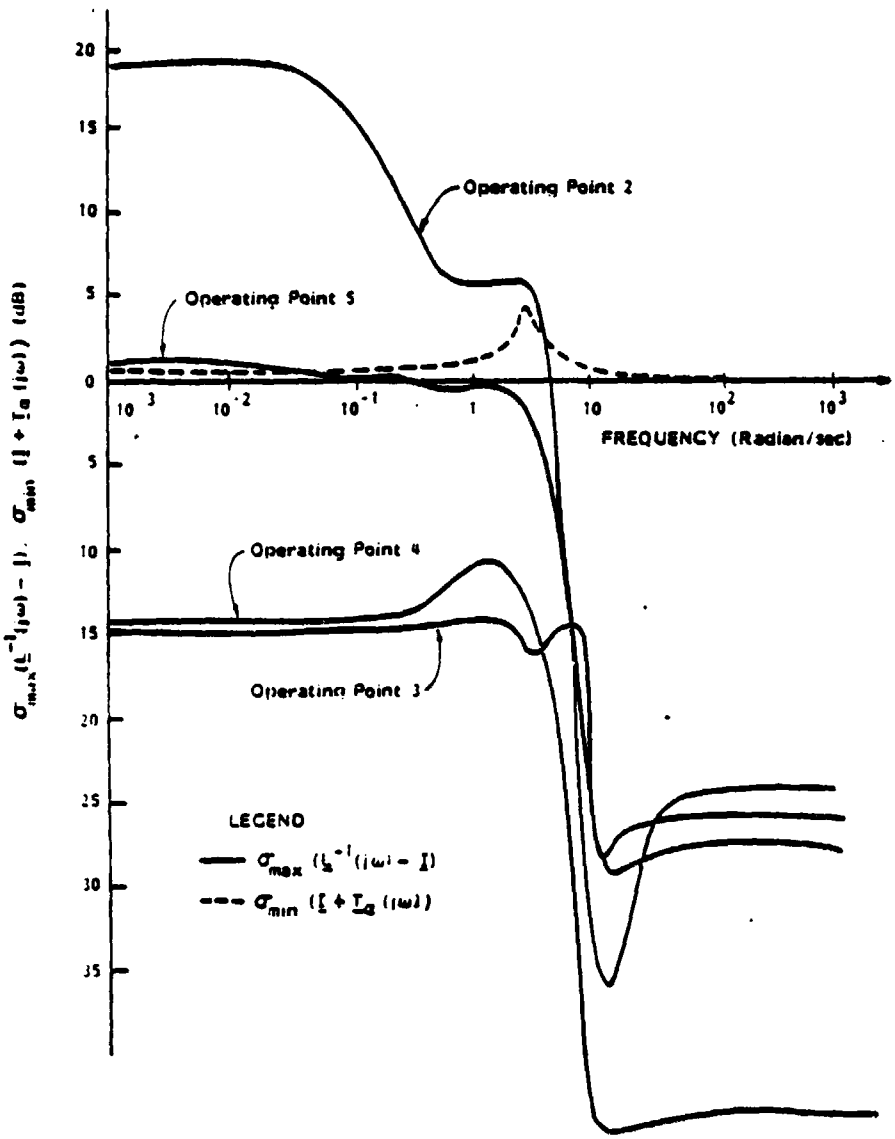

FIG. 5.11 Singular Value Plots for the Robustness Test given in Theorem 4.4. The Nominal System is Obtained by Applying the RPDS Design in Section 5.2 (That are Based on the Simple Power System Model at Operating Point 1; $\alpha = 0.4$) to the Simple Model of the Open-Loop System at Operating Point 1. The Perturbations are due to Change of Operating Points

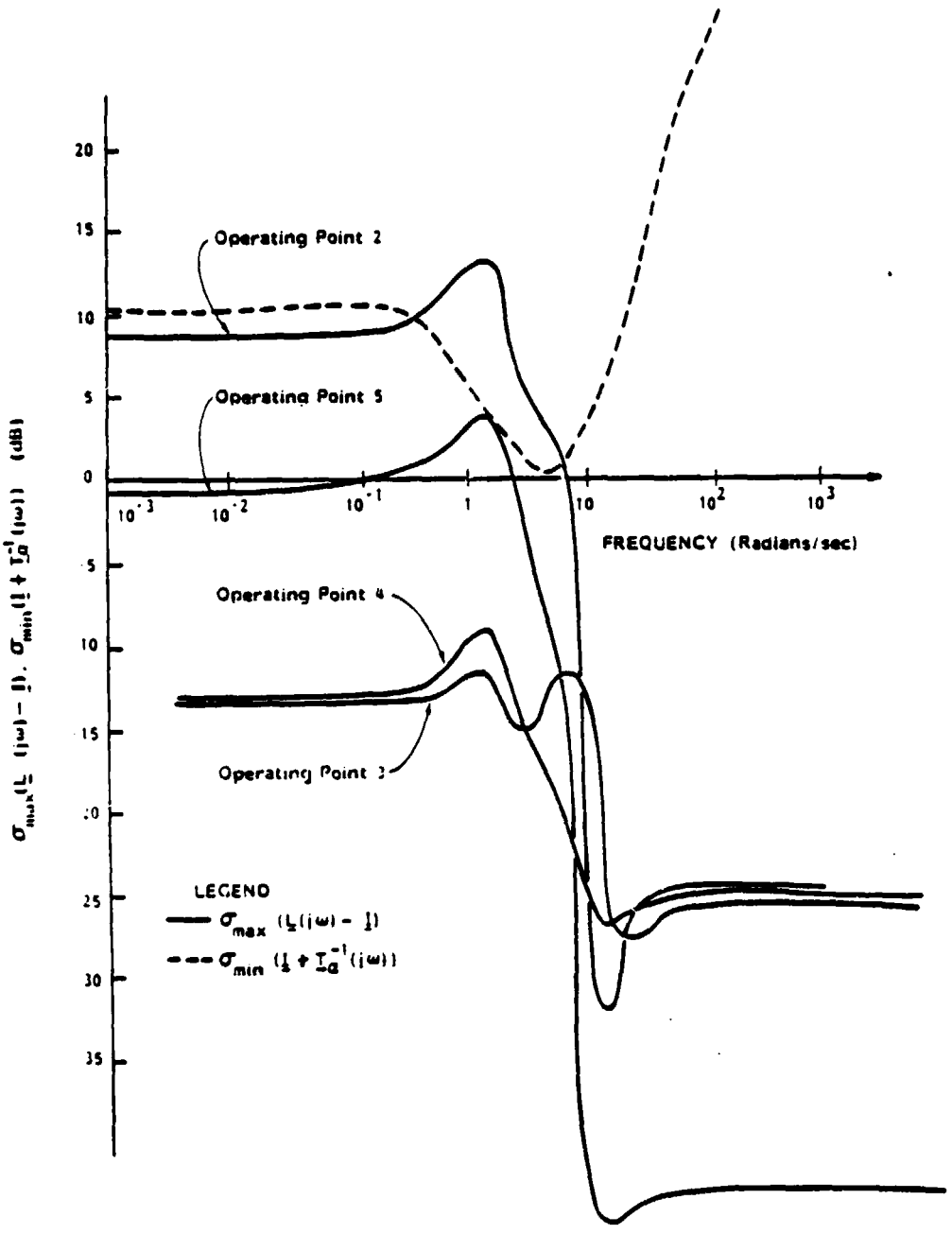

FIG. 5.12 Singular Value Plots for the Robustness Tests Given in Theorem 4.5. Nominal Design is Obtained by Applying the RPDS Design in Section 5.2 (That is Based on the Simple Power System Model at Operating Point 1; $\alpha = 0.4$) to the Simple Model of the Open-Loop System at Operating Point 1. The Perturbations are due to Change of Operating Points

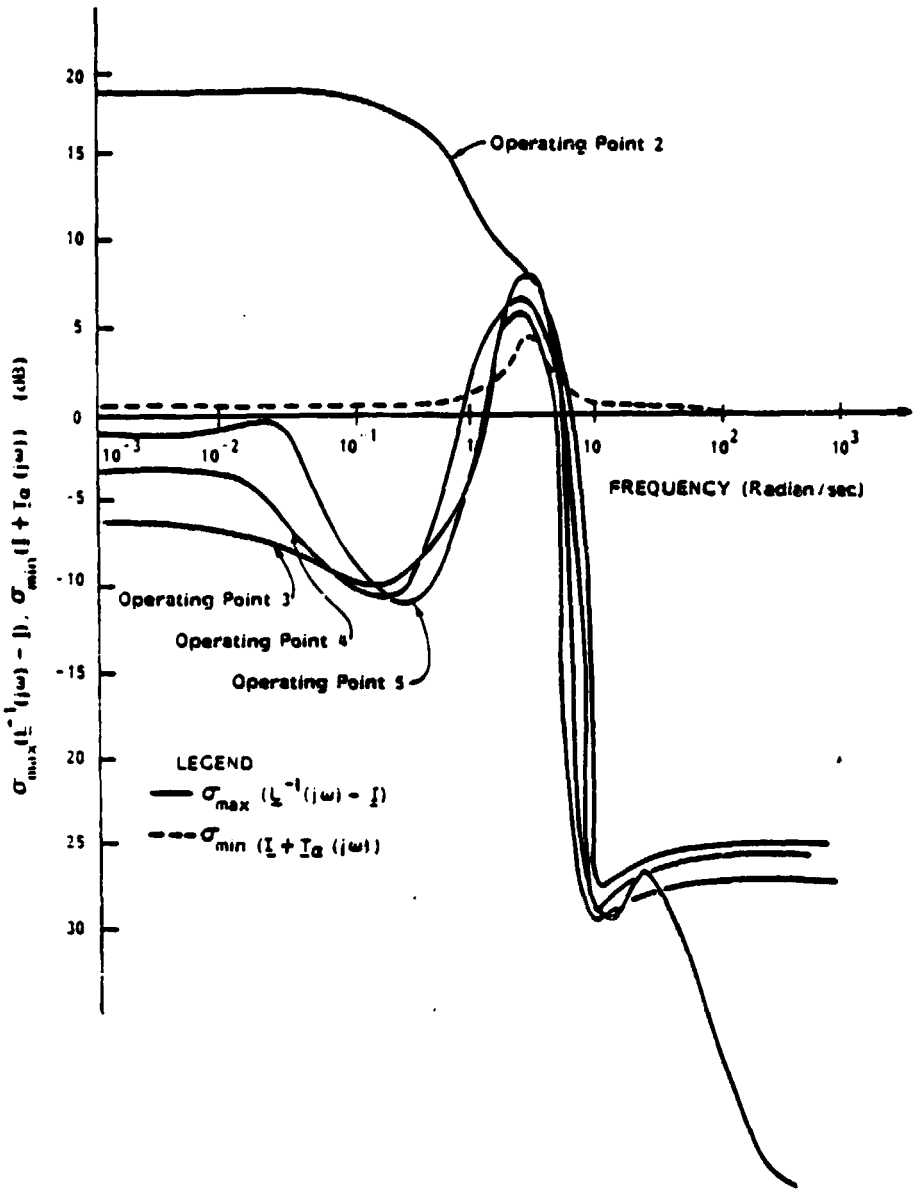

FIG. 5.13 Singular Value Plots for the Robustness Test Given in Theorem 4.4. The Nominal System is Obtained by Applying the RPDS Designs in Section 5.2 (That are Based on the Simple Power System Model at Operating Point 1; $\alpha = 0.4$) to the Simple Model of the Open-Loop System at Operating Point 1. The Perturbations are due to both Change of Operating Points and Unmodelled Exciter Dynamics

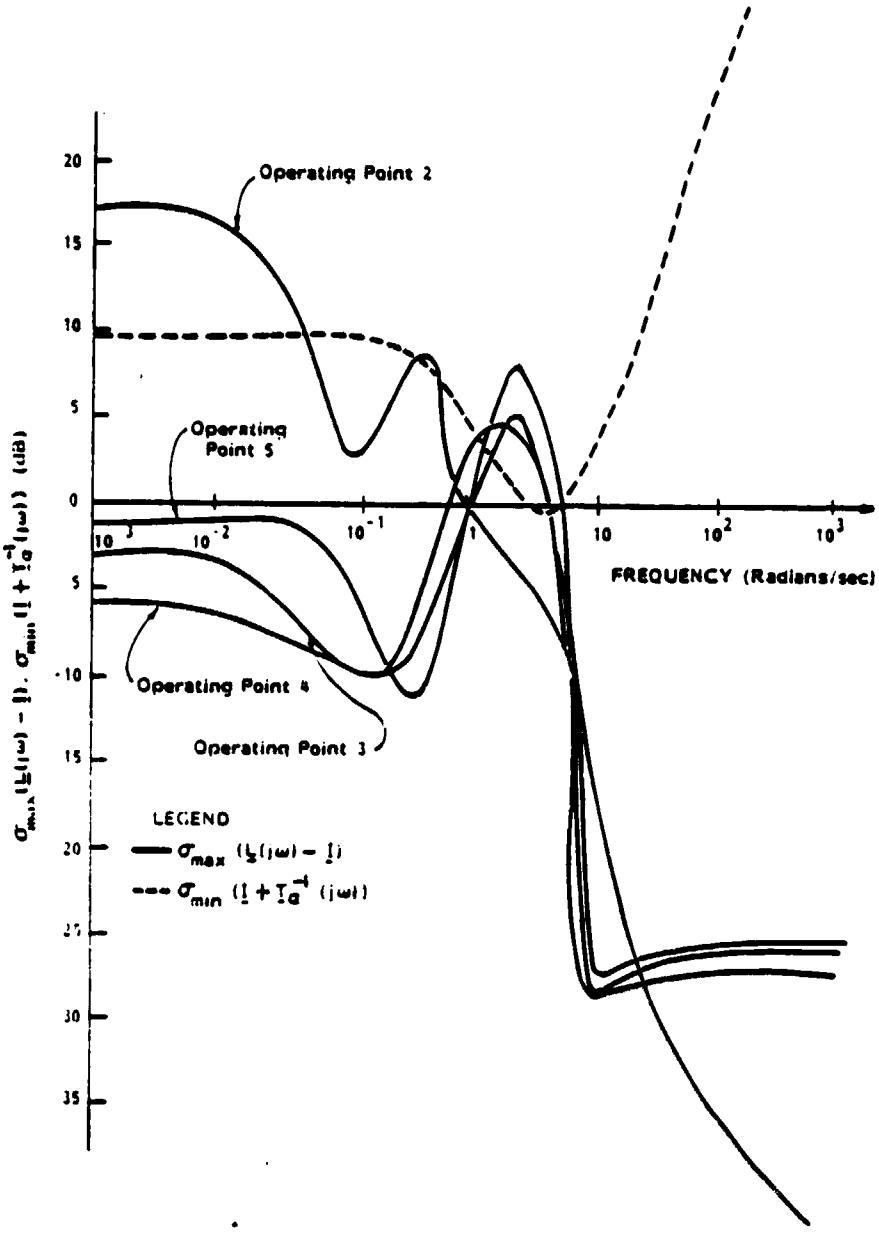

FIG. 5.14 Singular Value Plots for the Robustness Tests Given in Theorem 4.5. Nominal Design is Obtained by Applying the RPDS Design in Section 5.2 (That are Based on the Simple Power System Model at Operating Point 1; $\alpha = 0.4$) to the Simple Model of the Open-Loop System at Operating Point 1. The Perturbations are due to Both Changes of Operating Points and Unmodelled Exciter Dynamics

The above observations also apply to perturbations that result from introduction of unmodelled exciter dynamics in addition to change of operating points (Fig. 5.13 and 5.14). The respective value of $\sigma\max(\underline{L}(j\omega) - \underline{I})$ and $\sigma\max(\underline{L}^{-1}(j\omega) - \underline{I})$ at each value of ω are found to be larger than the corresponding quantities result from changing of operating conditions alone (compare Fig. 5.11 and Fig. 5.12 with Fig. 5.13 and Fig. 5.14 respectively). This again indicates the dominance of the unmodelled dynamics over the change of operating point.

5.5 Concluding Remarks

We have studied in this chapter the application of RPDS technique to design of state feedback control laws for a multi-terminal DC/AC power system. Our major objective is to demonstrate with the aid of a nontrivial multivariable design example the various properties of RPDS discussed in the previous chapter.

With regard to the positioning of closed-loop poles, the RPDS design obtained in section 5.2 are found to possess an interesting property which is not predicted by the results developed in this thesis. For values of α between 0.0 and 0.6, a given increment of α will shift the closed - loop oscillatory modes horizontally to the left by approximately the same amount. This unexpected property of the RPDS design is probably a result of the fact that all the open-loop modes to be stabilized are of the same nature (i.e. they all correspond to modes of intermachine oscillations). It is by no means a result that applies in general.

Robustness properties of the RPDS designs in section 5.2 are evaluated in two complementary ways. In section 5.3, movement of the

closed-loop poles that result from change of operating points and introduction of unmodelled exciter dynamics is examined. In all cases under consideration, the RPDS state feedback controllers are found to maintain a reasonable degree of damping for all the closed-loop oscillatory modes. Moreover, the closed-loop poles associated with RPDS designs that employ a larger value of α are always held further away from the $j\omega$-axis in the face of perturbation. These observations are consistent with the excellent stability margins derived for RPDS systems in Chapter IV. In section 5.4, the frequency domain robustness tests prescribed by Theorem 4.4 and 4.5 are applied to the RPDS designs under consideration. Perturbation of system dynamics that produce closed-loop patterns similar to one another are found to display drastically different behavior in the plots for their respective $\sigma\max(\underline{L}^{-1}(j\omega) - \underline{I})$ and $\sigma\max(\underline{L}(j\omega) - \underline{I})$. This is an indication of the conservatism associated with the norm-based robustness tests. Conservatism of such tests is further reflected by the fact that condition (4.22)of Theorem 4.4 and (4.27) of Theorem 4.5 are both violated in case of nondestabilizing perturbation. We also examine the behavior of the two MIMO frequency domain robustness measures $\sigma\min(\underline{I} + \underline{T}_\alpha(j\omega))$ and $\sigma\min(\underline{I} + \underline{T}_\alpha^{-1}(j\omega))$ with respect to change in α. They are shown to be monotonically increasing and decreasing functions of α respectively for all values of ω . The result obtained for the quantity $\sigma\min(\underline{I} + \underline{T}_\alpha(j\omega))$ agrees with our conclusion in section 4.4.3 while that obtained for $\sigma\min(\underline{I} + \underline{T}_\alpha^{-1}(j\omega))$ confirms a conjecture we made in section 4.5.3 concerning the property of RPDS inverse return difference matrix.

CHAPTER VI

DESIGN OF REGULATOR WITH A PRESCRIBED DEGREE OF STABILITY BASED LQG COMPENSATORS

6.1 Introduction

A basic practical limitation associated with the RPDS design is the assumption of full state feedback. In many practical applications full state feedback can never be exactly realized and often it is either impossible or too expensive to provide enough sensors for achieving even an approximate realization.

The way this problem is handled in modern control theory is through the use of LQG methodology [Ath 1], in which a Kalman-Bucy filter is used to provide the necessary state estimates using noisy output measurements. The class of LQG controllers considered here are the RPDS based LQG controllers. The state feedback gains for such controllers are obtained using the RPDS design methodology discussed in Chapter II.

The standard configuration for a RPDS based LQG control system is depicted in Fig. 6.1 with various points of the loop marked. To determine the robustness properties of the design, we shall insert multiplicative perturbation of the type considered in Section 4.2 at points (2) and (3) and find out the tolerable magnitude of the model error that

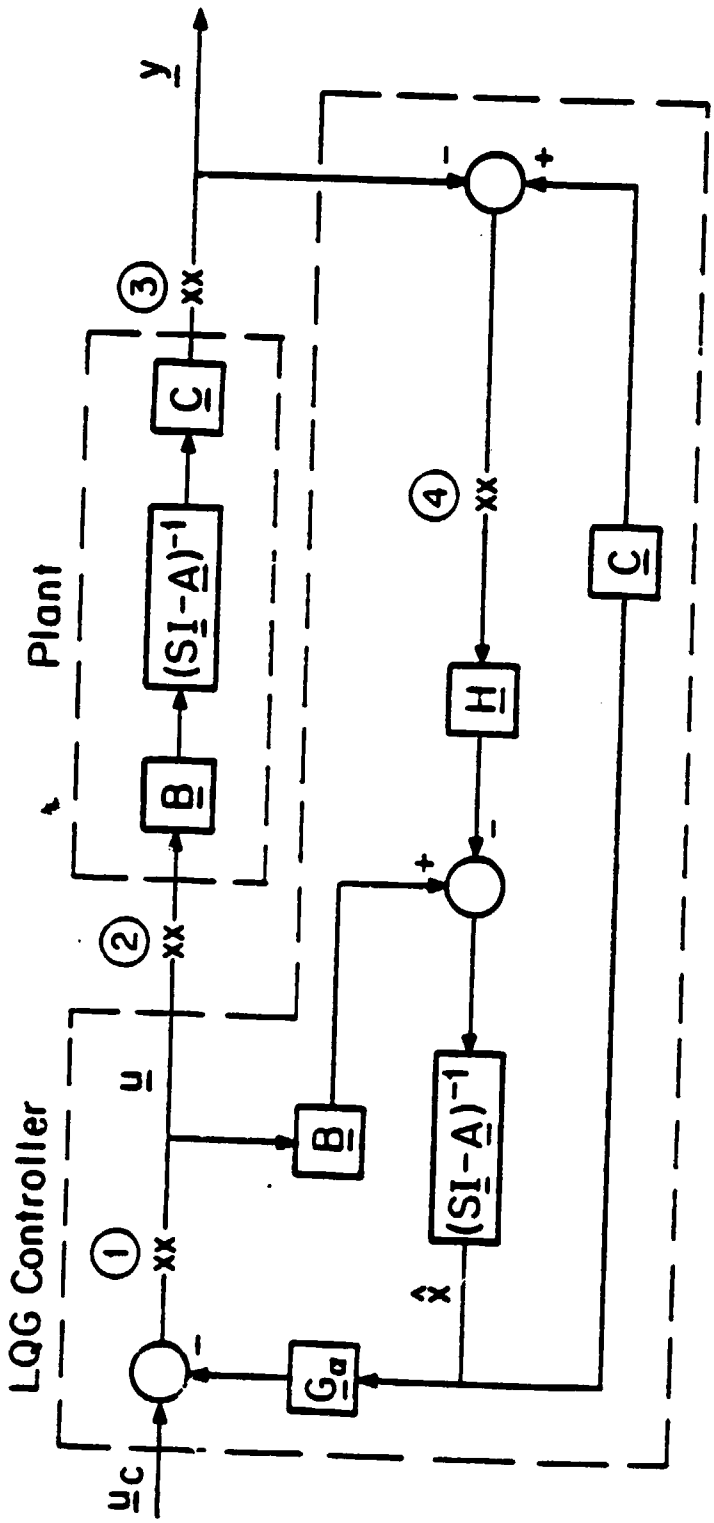

FIG. 6.1 Configuration for RPDS Based LQG Compensator

will not destabilize the system. The other two points (1) and (4) are internal to the LQG compensator and are therefore less significant for robustness analysis. However, they have some desirable loop properties that can be related to the other two points.

Following the notation employed in [Le 1], we shall denote the loop transfer matrix at point (K) by $\underline{T}_K(s)$. Each $\underline{T}_K(s)$ is calculated by breaking the loop at (K) and treating this point as both the input and output. For the four points marked in Fig. 6.1, we have

$$\underline{T}_1(s) = \underline{G}_\alpha \underline{\phi}(s)\, \underline{B} \tag{6.1}$$

$$\underline{T}_2(s) = \underline{G}_\alpha \left(\underline{\phi}^{-1}(s) + \underline{B}\, \underline{G}_\alpha + \underline{H}\, \underline{C}\right)^{-1} \underline{H}\, \underline{C}\, \underline{\phi}(s)\, \underline{B} \tag{6.2}$$

$$\underline{T}_3(s) = \underline{C}\, \underline{\phi}(s)\, \underline{B}\, \underline{G}_\alpha \left(\underline{\phi}^{-1}(s) + \underline{B}\, \underline{G}_\alpha + \underline{H}\, \underline{C}\right)^{-1} \underline{H} \tag{6.3}$$

$$\underline{T}_4(4) = \underline{C}\, \underline{\phi}(s)\, \underline{H} \tag{6.4}$$

where $\underline{\phi}(s) \triangleq (s\underline{I} - \underline{A})^{-1}$ (6.5)

$\underline{G}_\alpha$ is the RPDS state feedback gain and $\underline{H}$ is the KBF gain. Note that points (1) and (4) have loop transfer matrix identical to those of RPDS and KBF respectively. Thus at point (1) the RPDS robustness properties apply. Similarly, the KBF robustness properties are valid at point (4). No guaranteed stability margin is however available at both points (2) and (3), which are the actual interface between the control system and the real world. It was demonstrated by Doyle [Do4] with a simple example that a reasonable looking LQG design may have arbitrarily

[1] It is important to point out that only the state feedback gain of the RPDS based LQG compensators but not the KBF gain is designed with a prescribed degree of stability. Robustness properties of KBF are identical to those of FPDS discussed in section 4.8.2.

small stability margins.

For conventional LQG design (one for which the state feedback gain is obtained by using the LQ instead of the RPDS method),there are two dual robustness recovery procedures that allow us to approximate the transfer matrices $\underline{T}_1(s)$ and $\underline{T}_4(s)$ with $\underline{T}_2(s)$ and $\underline{T}_3(s)$ respectively in a systematic fashion. These procedures use the asymptotic pole properties of LQ regulators and KBF respectively (see [Do 3] for a review of such properties), and can be applied only if the plant is minimum phase.

The robustness recovery procedure due to Doyle and Stein [Do 1] makes $\underline{T}_2(s)$ to approximate $\underline{T}_1(s)$ by using a process noise with spectral intensity of the form $\rho\ \underline{B}\ \underline{B}^T + \underline{\Xi}$ in the KBF Riccati equation and letting ρ go to infinity. As a result, the LQ robustness margins at point (1) can be recovered asymptotically at the input (2). In a dual fashion, the robustness recovery procedure due to Kwakernaak [Kw 3] is used to recover the stability margin for (4) at the output (3). This is accomplished by using a state weighting matrix of the form $\underline{Q} + \rho \underline{C}^T \underline{C}$ and letting ρ go to infinity.

The objective of this chapter is to study the various issues that arise in the application of robustness recovery procedures to design of RPDS based LQG compensators.

6.2 Design of RPDS Based LQG Compensators Using Robustness Recovery Methods

In this section, we illustrate with the aid of numerical examples some considerations that are of importance to design of RPDS based LQG

compensators.

6.2.1 Relationship Between the Stability Factor α and the Minimum Phase Condition

If the stability margins associated with the loop transfer matrix $\underline{T}_3(s)$ of a given RPDS based LQG compensator (with prescribed degree of stability α) is found to be unsatisfactory, an obvious way to improve the design is to employ the robustness recovery procedure of Kwakernaak ([Kw 1] and [Kw 3]). Recall from the last section that Kwakernaak's method requires the adjustment of the state feedback gain $\underline{G}_\alpha$ for making $\underline{T}_3(s)$ appropriate the KBF transfer matrix $\underline{T}_4(s)$. This is accomplished through the introduction of a state weighting matrix of the form $\underline{Q} + \rho \underline{C}^T \underline{C}$ into the LQ Riccati equation and letting ρ go to infinity. The finite closed-loop regulator poles will then asymptotically approach the zeroes of $\underline{C}(s\underline{I} - \underline{A})^{-1} \underline{B}$ (see Theorem 4.13 of [Kw 1]). However, the LQ regulator thus obtained is no longer guaranteed to possess the same prescribed degree of stability as the original RPDS design. This is the case when some zeroes of $\underline{C}(s\underline{I} - \underline{A})^{-1} \underline{B}$ have real parts larger than $-\alpha$.

If the RPDS Riccati equation (4.59) is used as the design equation, it follows from Theorem 3.2 that the resulting regulator poles will always lie to the left of $\sigma = -\alpha$ for every value of ρ. But the asymptotic location for these finite poles may not coincide with those of $\underline{C}(s\underline{I} - \underline{A})^{-1} \underline{B}$ unless $\underline{C}(s\underline{I} - \underline{A} - \alpha\underline{I})^{-1} \underline{B}$ is also minimum phase. If $\underline{C}(s\underline{I} - \underline{A} - \alpha\underline{I})^{-1} \underline{B}$ fails to be minimum phase, the asymptotic state feedback gain will satisfy

$$\frac{1}{\sqrt{\rho}} \underline{G}_\alpha \rightarrow \underline{R}^{-1/2} \underline{W} \underline{\tilde{C}} \tag{6.6}$$

as ρ approaches infinity where $\underline{\tilde{C}} \neq \underline{C}$ and $\underline{W}$ is some orthonormal matrix (see Chapter 3 of [Kw 1]). It can be readily demonstrated with the use of elementary matrix manipulations that full state KBF loop cannot be recovered asymptotically as a result of $\underline{C} \neq \underline{\tilde{C}}$.

Defining

$$\underline{\bar{\Phi}}(s) \triangleq (s\underline{I} - \underline{A} - \underline{H}\,\underline{C})^{-1} \tag{6.7}$$

we can rewrite $\underline{T}_3(s)$ as

$$\underline{T}_3(s) = \underline{C}\,\underline{\phi}(s)\,\underline{B}\,\underline{G}_\alpha\,(\underline{\phi}^{-1}(s) + \underline{B}\,\underline{G}_\alpha + \underline{H}\,\underline{C})^{-1}\,\underline{H}$$

$$= \underline{C}\,\underline{\phi}(s)\,\underline{B}\,\underline{G}_\alpha[\underline{\bar{\Phi}}(s) - \underline{\bar{\Phi}}(s)\,\underline{B}\,(\underline{I} + \underline{G}_\alpha\,\underline{\bar{\Phi}}(s)\,\underline{B})^{-1}\,\underline{G}_\alpha\,\underline{\bar{\Phi}}(s)]\,\underline{H} \tag{6.8}$$

$$= \underline{C}\,\underline{\phi}(s)\,\underline{B}\,(\underline{I} + \underline{G}_\alpha\underline{\bar{\Phi}}(s)\,\underline{B})^{-1}\,\underline{G}_\alpha\,\underline{\bar{\Phi}}(s)\,\underline{H} \tag{6.9}$$

To go from (6.8) to (6.9), we employ the matrix inversion lemma (see for example Appendix A of [Sc 1]). As ρ approaches infinity the following approximation follows immediately from (6.6) and (6.19)

$$\underline{C}\,\phi(s)\,\underline{B}\,(\underline{I} + \underline{G}_\alpha\underline{\bar{\phi}}(s)\,\underline{B})^{-1}\,\underline{G}_\alpha\,\underline{\bar{\phi}}(s)\,\underline{H}$$

$$\rightarrow \quad \underline{C}\,\underline{\phi}(s)\,\underline{B}\,(\underline{\tilde{C}}\,\underline{\bar{\phi}}(s)\,\underline{B})^{-1}\,\underline{\tilde{C}}\,\underline{\bar{\phi}}(s)\,\underline{H} \tag{6.10}$$

It can be shown that the matrix function on the right side of (6.10) is equal to the KBF loop transfer matrix $\underline{\tilde{C}}\,\underline{\phi}(s)\,\underline{H}$ when $\underline{C} = \underline{\tilde{C}}$. If $\underline{C} \neq \underline{\tilde{C}}$, there exists no useful simplification of this matrix function and the robustness properties of the KBF loop is not recovered as a result.

The following example illustrates the effect of α on the design of LQG compensators using Kwakernaak's robustness recovery procedure.

Example 6.1 Consider the LQG problem

$$\min_{u(t)\,\epsilon\, f(y(t))} J = E\left[\lim_{t_1\to\infty} \int_0^{t_1} e^{2\alpha t}\,[\underline{x}^T(t)\,\underline{Q}\,\underline{x}(t) + \underline{u}^T(t)\,\underline{R}\,\underline{u}(t)]dt\right] \tag{6.11}$$

subject to the dynamic constraint

$$\dot{\underline{x}}(t) = \begin{bmatrix} 0 & 1 \\ -3 & 4 \end{bmatrix} \underline{x}(t) + \begin{bmatrix} 0 \\ 1 \end{bmatrix} \underline{u}(t) + \begin{bmatrix} 35 \\ -61 \end{bmatrix} \zeta(t) \tag{6.12}$$

and the observation constraint

$$y(t) = [2 \quad 1]\,\underline{x}(t) + \theta(t) \tag{6.13}$$

where

$$\underline{Q} = 80 \begin{bmatrix} \sqrt{35} \\ 1 \end{bmatrix} [\sqrt{35} \quad 1] \tag{6.14}$$

and $\zeta(t)$, $\theta(t)$ are zero mean white noise processes of spectral intensity equal to 1.0.

The plant in this example is a stable minimum phase system with transfer function given by

$$\frac{y(s)}{u(s)} = \frac{s+2}{(s+1)(S+3)} \quad . \tag{6.15}$$

Solution of the above LQG problem for $\alpha = 0$ results in a state feedback gain given by

$$\underline{G}_\alpha = [50 \quad 10] \tag{6.16}$$

and a Kalman Bucy Filter gain given by

$$\underline{H} = \begin{bmatrix} 30 \\ -50 \end{bmatrix} \tag{6.17}$$

Inspecting the Nyquist diagram of the LQG loop transfer function reveals poor stability margin (GM = (-6.75 d,b ∞) and PM = (-15°, 15°)) for the resulting LQG design. This is due to the presence of a instable pole in the LQG loop transfer function. In order to improve the robustness properties of the feedback loop, we employ the robustness recovery procedure of Kwakernaak. A new choice of the state weighting matrix given by

$$\underline{Q}_{\rho} = \underline{Q} + \rho \begin{bmatrix} 2 \\ 1 \end{bmatrix} [2 \quad 1] \tag{6.18}$$

is employed in the LQ algebraic Riccati equation

$$\underline{K} \begin{bmatrix} 0 & 1 \\ -4 & -3 \end{bmatrix} + \begin{bmatrix} 0 & -4 \\ 1 & -3 \end{bmatrix} \underline{K} - \underline{K} \begin{bmatrix} 0 \\ 1 \end{bmatrix} [0 \quad 1] \underline{K} + \underline{Q}_{\rho} = \underline{0} \tag{6.19}$$

The state feedback gains for various values of ρ are computed and the respective LQG loop transfer functions $t_3(s)$ are plotted in Fig. 6.2. It is observed that the stability margins of the resulting designs improve steadily with increasing ρ (see Table 6.1). For $\alpha > 0$ we replace equation 6.19 with the following RPDS algebraic Riccati equation

$$\underline{K}_{\alpha} \begin{bmatrix} \alpha & 1 \\ -4 & -3+\alpha \end{bmatrix} + \begin{bmatrix} \alpha & -4 \\ 1 & -3+\alpha \end{bmatrix} \underline{K}_{\alpha} - \underline{K}_{\alpha} \begin{bmatrix} 0 \\ 1 \end{bmatrix} [0 \quad 1] + \underline{Q}_{\rho} = \underline{0} \tag{6.20}$$

the resulting LQG design is always guaranteed to possess a degree of stability α. However, asymptotic recovery of the KBF loop with this modified procedure is only possible for values of α less than 2,0. This is vividly demonstrated by the Nyquist diagrams depicted in Fig. 6.3 and Fig. 6.4. When α is chosen to be 1.8 (Fig. 6.3), the stability margins of the

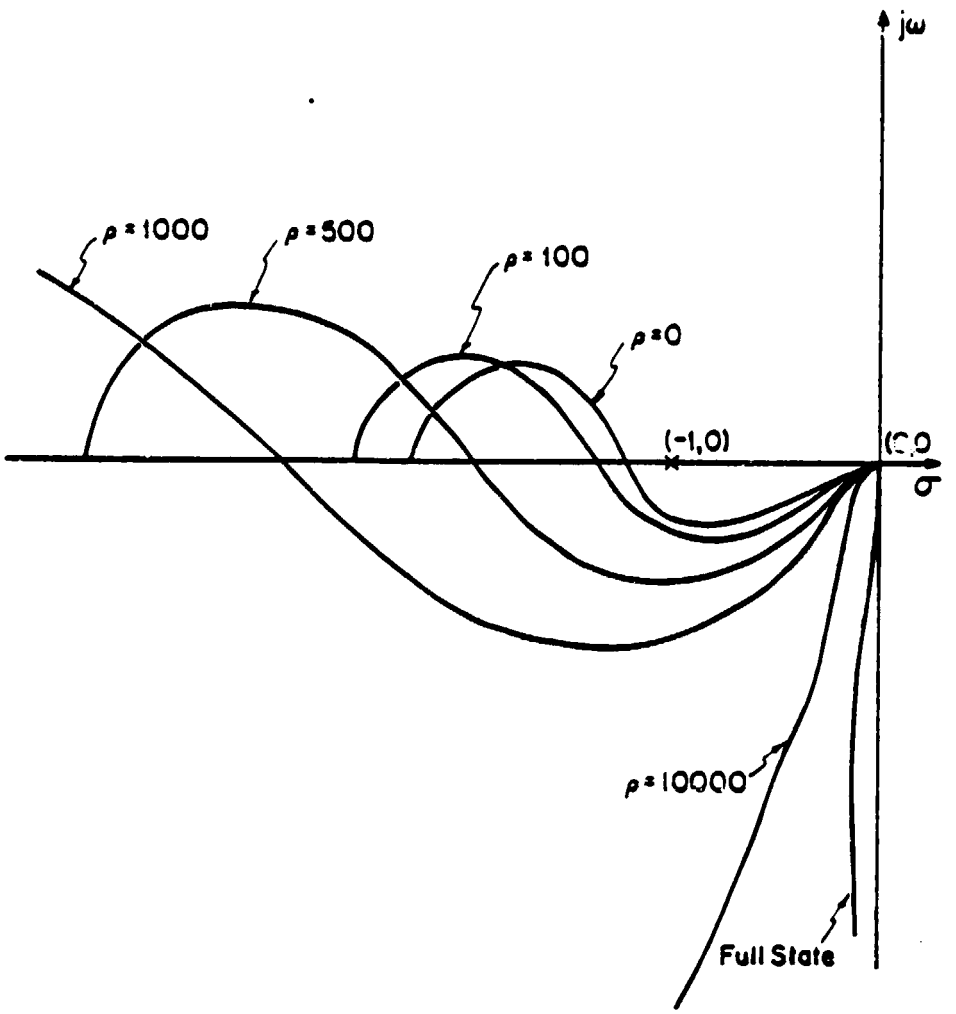

FIG. 6.2 Nyquist Diagrams for Design Iteration of RPDS Based LQG Compensators (α = 0) Using Kwakernaak's Recovery Procedure

ρ	PM[1]	GM[2]	d[3]
0	15.3°	-2.0db	0.29
100	21.8°	-2.7db	0.39
500	35°	-5.51db	0.58
1000	45.4°	-9.6db	0.9
10000	72°	-34db [4]	0.917

TABLE 6.1

Summary of Stability Margin for Design Iteration of a RPDS Based LQG Compensator (α = 4.5) in Example 6.1

[1] This is in violation of the notation introduced in Chapter IV. The angle given here corresponds to the value of θ in the definition of PM.

[2] Only the downward gain margin is given here. The upward gain margin is infinity for all cases.

[3] d is the nearest distance between the Nyquist diagram and the critical point (-1,0).

[4] The actual gain reduction margin is lower than the value indicated

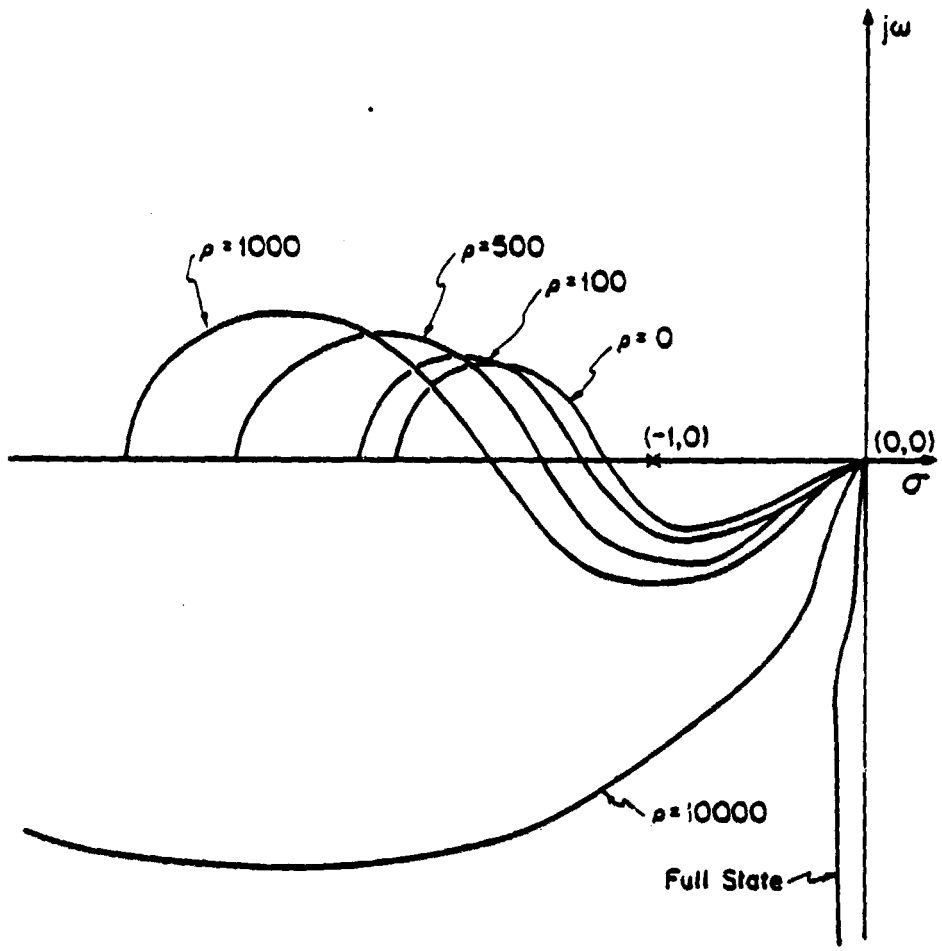

FIG. 6.3 Nyquist Diagrams for Design Iteration of RPDS Based LQG Compensator (α =1.8) Using Kwakernaak's Recovery Procedure

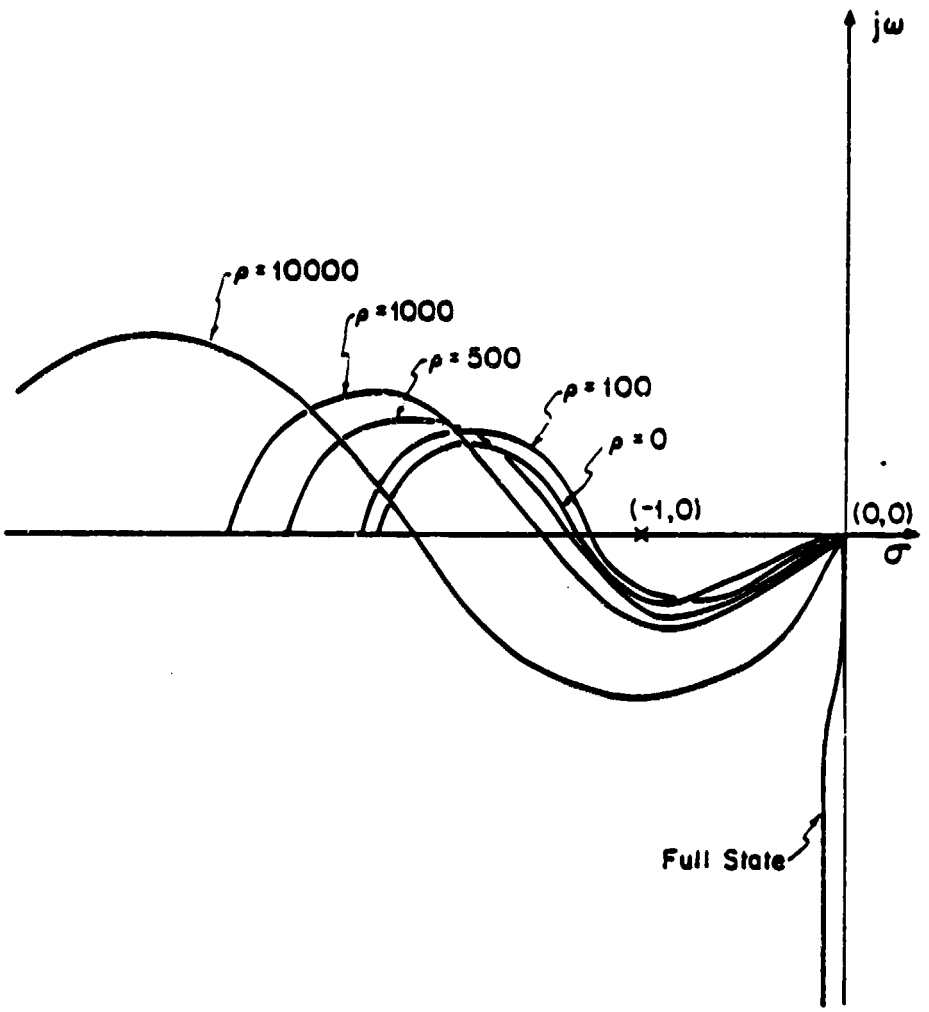

FIG. 6.4 Nyquist Diagrams for Design Interaction of a RPDS Based LQG Compensator (α = 2.2) Using Kwakernaak's Recovery Procedure

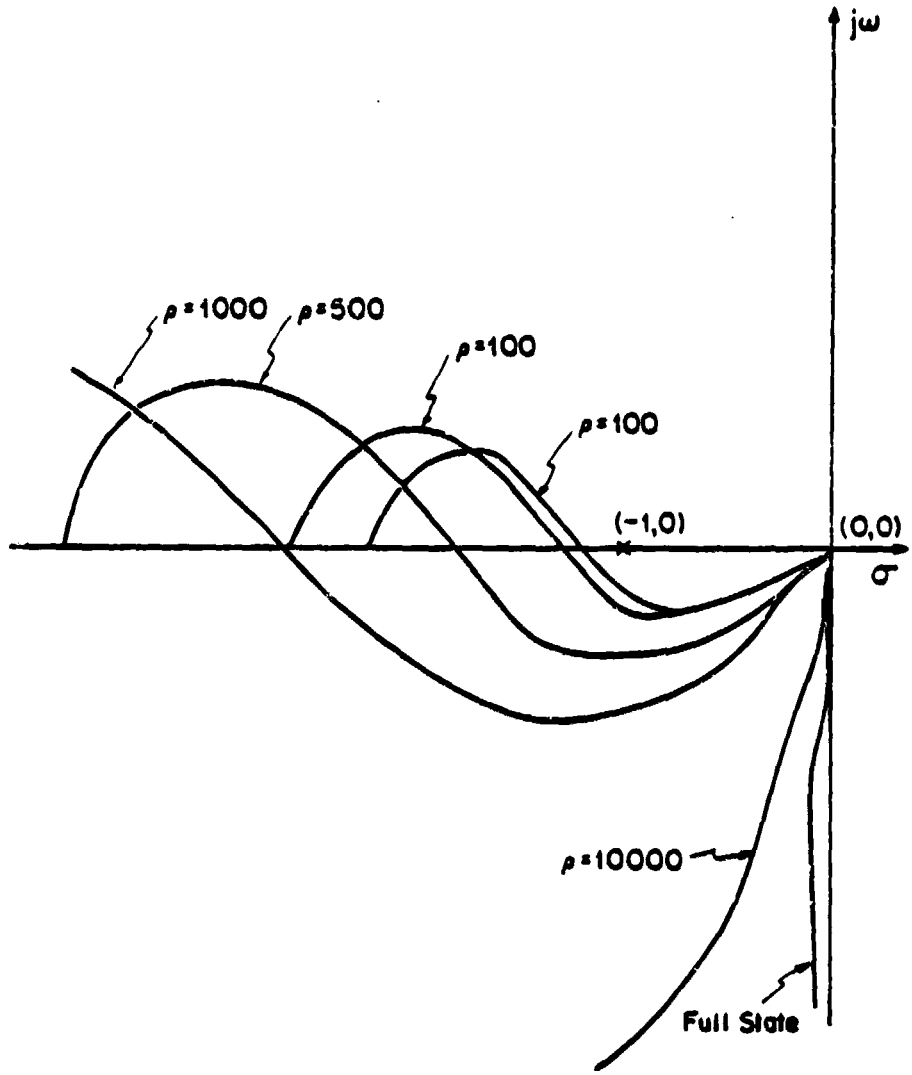

FIG. 6.5 Myquist Diagrams for Design Iteration of a RPDS Based LQG Compensator (α = 4.5) Using Doyle/Stein's Robustness Recovery Method

design improve steadily with increasing value of ρ and reasonably good stability margins are obtained for value of ρ equals to 1,000. For case where α equals 2.2 (Fig. 6.4) the stability margins of the resulting design remains unsatisfatory even when large value of ρ is employed.

The above problem is not shared by the robustness recovery procedure due to Doyle and Stein. Nyquist diagrams of the transfer functions that result from the design iterations of a RPDS based LQG compensator using Doyle/Stein's method are depicted in Fig. 6.5. The choice of α chosen for this case is 4.5. It is clear from the figure that the stability margins of the design improve as larger value of ρ is used demonstrates satisfactory improvement.

6.2.2 Rate of Robustness Recovery with Respect to the Noise Scaling Parameter

The robustness recovery method of Doyle and Stein [Do 1] requires the use of a process noise with spectral intensity of the form

$$\tilde{\Xi} = \Xi + \rho \, B \, B^T \tag{6.21}$$

and letting ρ go to infinity for asymptotic recovery of the full state RPDS stability margins. This procedure provides characterization of the LQG feedback loop as the noise scaling parameter ρ approaches infinity. It does not, however, give us any clue as to the behavior of the LQG loop when ρ varies. We shall examine in this chapter the effect of α on the rate of recovering the RPDS stability margins with respect to changes in ρ. In the SISO case, this can be simply accomplished by inspection of the respective Nyquist diagrams. In the MIMO case, the singular value

plots of the respective loop transfer matrices have to be used (For an example of this, see [Do 1]). For ease of exposition, only SISO systems will be considered in the following example.

Example 6.2 Consider the RFDS based LQG design problem defined in Example 6.1. Design iterations with noise scaling factor ρ = 0, 100, 500, 1000 and 10000 are performed for several choices of the stability factor α. The Nyquist diagrams of the LQG design with α chosen to be 0, 3, 4.5, 6 and 9 are plotted for each of the five iterations (Fig. 6.6) and the resulting stability margins tabulated (Table 6.2 and Fig. 6.7). Several interesting observations are in order.

First it is noticed that the Nyquist diagrams of the LQG designs with value of α equals to 0, 3 and 4.5 move further away from the critical point (-1,0) than those designs with α equals to 6 and 9 as the value of ρ increases. Consequently, the stability margins of the designs with α equals to 0,3 and 4.5 are superior to those with values of α equals to 6 and 9 for a fixed value of ρ (see Table 6.2 and Fig. 6.7). Secondly, the rate of robustness recovery with respect to ρ does not strictly decrease with α for the values of α under consideration. It is clear from the Nyquist diagrams in Fig. 6.6 and the data presented in Table 6.2 that the stability margins for LQG designs with α equals to 4.5, 6.0 and 9.0 decreases with increasing value of α for a fixed value of ρ. This is however not the case for designs with α equals to 0 and 3.

In view of the above observation, it does not seem likely that one can make any conclusive statement concerning the effect of α on the rate of robustness recovery. However, these observations do illuminate a potential

C-3

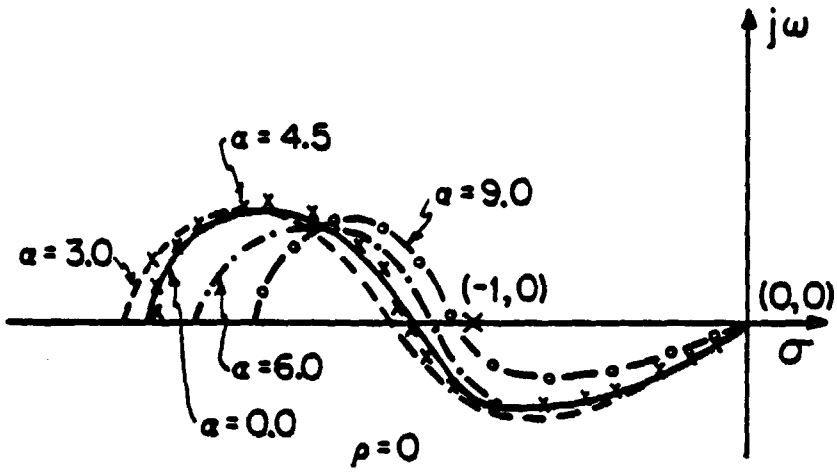

Fig. 6.6a

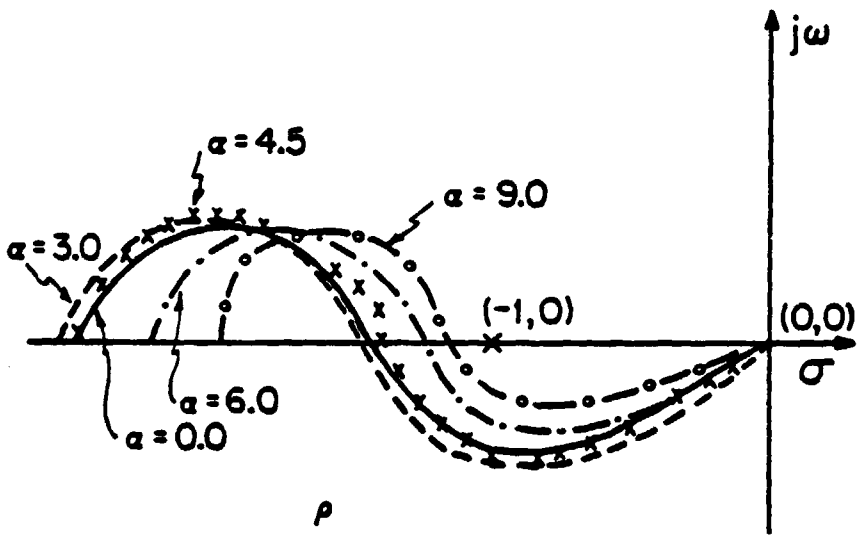

Fig 6.6b

Nyquist Diagrams for Design Iterations of RPDS Based LQG Compensators (α = 0.0, 3.0, 4.5, 6.0 and 0.0) Using Doyle/Stein Method

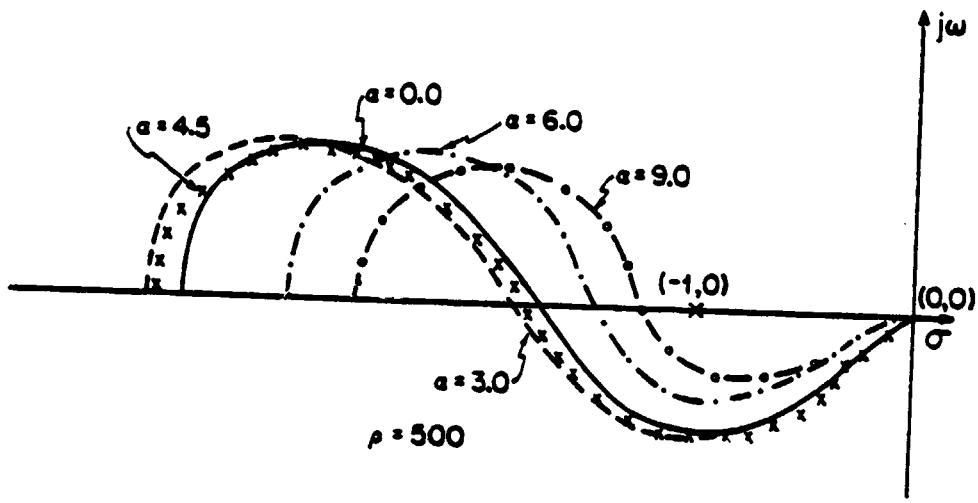

Fig. 6.6c

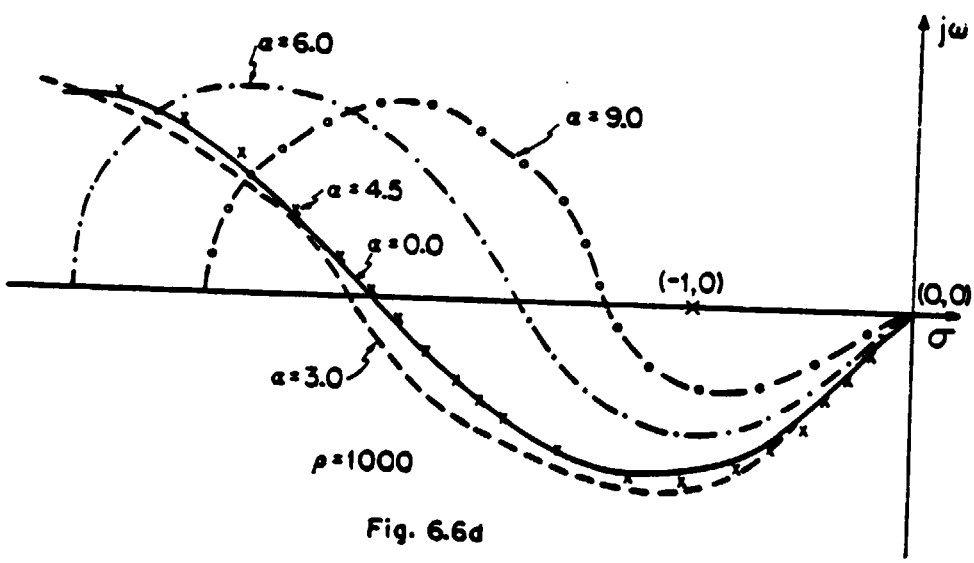

Fig. 6.6d

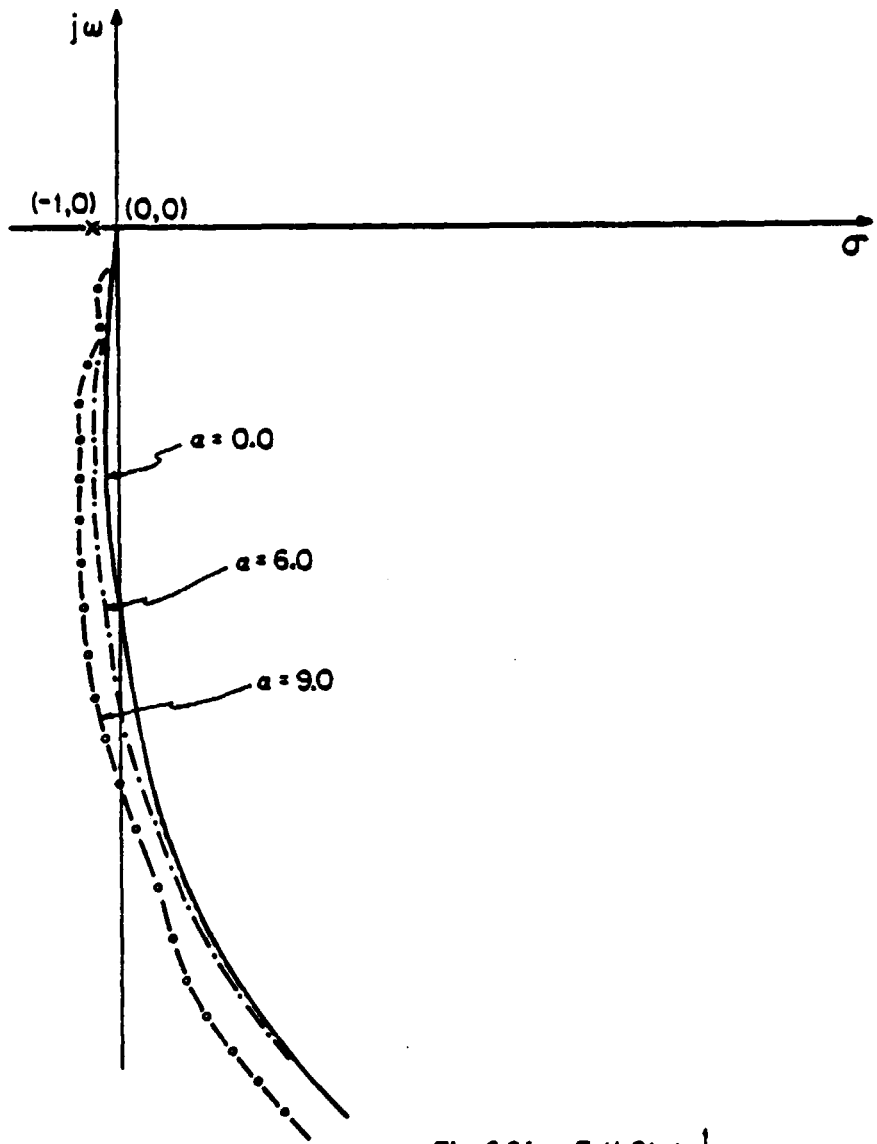

Fig. 6.6f Full State[1]

[1] Since the Nyquist Diagram of the RPDS Transfer Functions Corresponding to $\alpha = 0.0$, 0.3 and 0.45 are very closed to one another, only that of $\alpha = 0.0$ is Displayed

\α	0	3	4.5	6	9
GM[1]	-1.9db	-1.9db	-2.02db	-1.27db	-0,72db
PM[2]	16.5°	16.5°	16.5°	11.5°	8°
d[3]	0.2	0.22	0.208	0,15	0.1

$\rho = 0$

\α	0	3	4.5	6	9
GM	-2.65db	-2.83db	-2.67db	-1.25db	-1.0db
PM	21°	21°	20.6°	14.5°	11°
	0.36	0.375	0.354	0.187	0.133

$\rho = 10^2$

\α	0	3	4.5	6	9
GM	-5.0db	-5.5db	-5.32db	-3.65db	-1.9db
PM	32.5°	32°	32.5°	25.5°	16°
d	0.733	0.8	0.8	0.45	0.25

$\rho = 500$

Table 6.2 to be continued

α	0	3	4.5	6	9
GM	-8db	-8.5db	-8.3db	-5db	-3db
PM	43^{o}	42.5^{o}	43^{o}	34^{o}	21^{o}
d	0.917	0.95	0.95	0.73	0.33

$\rho = 10^{3}$

α	0	3	4.5	6	9
GM	$>-37db^{4}$	$>-43db^{4}$	$>-38db^{4}$	-28.5db	-14db
PM	75^{o}	75^{o}	75^{o}	67^{o}	56^{o}
d	0.95	0.95	0.95	0.87	0.80

$\rho = 10^{4}$

Table 6.2 to be continued

\α	0	3	4.5	6	9
GM	-∞db	-∞db	-∞db	-∞db	-∞db
PM	86.5°	89°	85.5°	87°	82°
d	1	1	1	1	1

Full state

TABLE 6.2

Summary of Stability Margins for Example 6.2

[1] This is a violation of the notation introduced in Chapter IV. The angle given here corresponds to the value of θ in the definition of PM

[2] Only the downward gain margin is given here. The upward gain margin is infinity for all cases.

[3] d is the nearest distance between the Nyquist diagram and the critical point (-1,0). The actual gain reduction margin is lower the value indicated.

[4] The actual gain reduction margin is lower than that indicated.

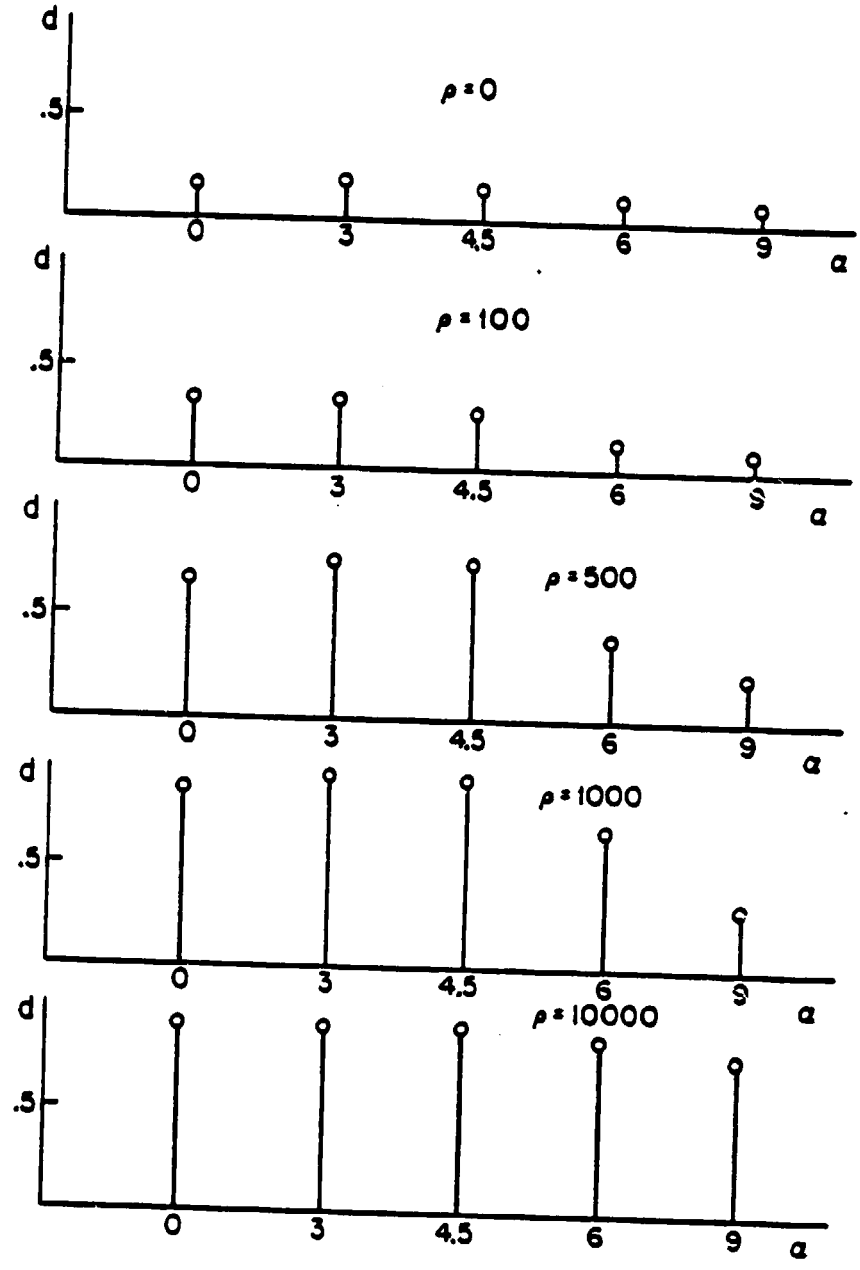

FIG. 6.7 Effect of α on the Distance from the Critical Point (-1,0) at Different Design Iteration of a RPDS Based LQG Compensator

problem that may occur in the design of RPDS based LQG compensator using robustness recovery procedures. It is apparent from this example that large values of α ($\alpha = 6,9$) may slow down the recovery of RPDS stability margins and thus necessitate the introduction of high filter gains for securing good robustness peroperties. The use of high filter gain in feedback loop often leads to degradation of observation noise rejection that is undesirable from the performance point of view. The resulting situation is one where a satisfactory compromise among the need for speed of response (as specified by the choice of α), noise rejection and stability robustness has to be made by appropriate choices of α and ρ.

6.2.3 Effect of the Stability Factor α on the Noise Rejection Properties

To conclude the discussion in this section, we examine the effect of the stability factor α on the noise rejection properties of RPDS based LQG compensators. Such effect can be characterized in terms of the behavior of the state covariance matrix (assuming zero mean for the random vector $\underline{x}(t)$

$$\underline{\Sigma}_x \triangleq E[\underline{x}(t)\ \underline{x}^T(t)] \tag{6.22}$$

with different values of α.

Recall from the definition of the state estimate error $\underline{e}(t)$ in (4.171) that

$$\underline{e}(t) = \hat{\underline{x}}(t) - \underline{x}(t) \tag{6.23}$$

It is useful to point out that $\hat{\underline{x}}(t)$ and $\underline{e}(t)$ are uncorrelated random vectors (Chapter III of [An 2] and Chapter IV of [Kw 1]). As a result of this, we can express $\underline{\Sigma}_x$ as a sum of two covariance matrices

$$\underline{\Sigma}_x = \underline{\Sigma}_{\hat{x}} + \underline{\Sigma}_e \tag{6.24}$$

where

$$\underline{\Sigma}_{\hat{x}} = E[\hat{\underline{x}}(t)\ \hat{\underline{x}}(t)^T] \tag{6.25}$$

and

$$\underline{\Sigma}_e = E[\underline{e}(t)\ \underline{e}(t)^T] \tag{6.26}$$

Moreover, the dynamics of the LQG control system can be conveniently described by using $[\underline{e}(t)^T\ \hat{\underline{x}}(t)^T]$ as a state vector. The underlying differential equation in this case is given by

$$\frac{d}{dt}\begin{bmatrix}\underline{e}(t)\\ \hat{\underline{x}}(t)\end{bmatrix} = \begin{bmatrix}\underline{A} - \underline{H}\,\underline{C} & 0\\ -\underline{H}\,\underline{C} & \underline{A} - \underline{B}\,\underline{G}_Q\end{bmatrix}\begin{bmatrix}\underline{e}(t)\\ \hat{\underline{x}}(t)\end{bmatrix} + \begin{bmatrix}-\underline{I} & \underline{H}\\ \underline{0} & \underline{H}\end{bmatrix}\begin{bmatrix}\underline{\zeta}(t)\\ \underline{\theta}(t)\end{bmatrix} \tag{6.27}$$

which can be readily derived by inspection of the block diagram in Fig. 6.1. Using the above dynamical equation, and Theorem 1.53 of [Kw 1] (which is a standard result in stochastic process theory) leads directly to the following result.

<u>Lemma 6.1</u> Given a LQG control system described by (6.27) the steady state covariance matrix

$$E\left(\begin{bmatrix}\underline{e}(t)\\ \hat{\underline{x}}(t)\end{bmatrix}\ [\underline{e}(t)^T\ \hat{\underline{x}}(t)^T]\right) = \begin{pmatrix}\underline{\Sigma}_e & 0\\ 0 & \underline{\Sigma}_{\hat{x}}\end{pmatrix} \tag{6.28}$$

satisfies the algebraic matrix equation

$$\begin{bmatrix} \underline{A} - \underline{H}\,\underline{C} & 0 \\ -\underline{H}\,\underline{C} & \underline{A} - \underline{B}\,\underline{G}_\alpha \end{bmatrix} \begin{bmatrix} \underline{\Sigma}_e & 0 \\ 0 & \underline{\Sigma}_{\hat{x}} \end{bmatrix} + \begin{bmatrix} \underline{\Sigma}_e & 0 \\ 0 & \underline{\Sigma}_{\hat{x}} \end{bmatrix} \begin{bmatrix} \underline{A} - \underline{H}\,\underline{C} & -\underline{H}\,\underline{C} \\ 0 & \underline{A} - \underline{B}\,\underline{G}_\alpha \end{bmatrix}^T$$

$$+ \begin{bmatrix} \underline{\Xi} + \underline{H}\,\underline{\Theta}\,\underline{H}^T & \underline{H}\,\underline{\Theta}\,\underline{H}^T \\ \underline{H}\,\underline{\Theta}\,\underline{H}^T & \underline{H}\,\underline{\Theta}\,\underline{H}^T \end{bmatrix} = \begin{bmatrix} 0 & 0 \\ 0 & 0 \end{bmatrix} \tag{6.29}$$

It is straightforward to show that the solution of equation 6.29 can be obtained by solving the two following decoupled matrix equations

$$(\underline{A} - \underline{H}\,\underline{C})\,\underline{\Sigma}_e + \underline{\Sigma}_e\,(\underline{A} - \underline{H}\,\underline{C})^T + (\underline{\Xi} + \underline{H}\,\underline{\Theta}\,\underline{H}^T) = \underline{0} \tag{6.30}$$

and

$$(\underline{A} - \underline{B}\,\underline{G}_\alpha)\,\underline{\Sigma}_{\hat{x}} + \underline{\Sigma}_{\hat{x}}(\underline{A} - \underline{B}\,\underline{G}_\alpha)^T + \underline{H}\,\underline{\Theta}\,\underline{H}^T = \underline{0} \tag{6.31}$$

This is a direct consequence of the fact that $\hat{\underline{x}}(t)$ and $\underline{e}(t)$ are uncorrelated. It becomes clear from (6.30) and (6.31) that the RPDS state feedback gain (and hence the stability factor α) only affects the matrix $\underline{\Sigma}_{\hat{x}}$. Differentiating both sides of (6.31) with respect to α and rearranging, we obtain

$$(\underline{A} - \underline{B}\,\underline{G}_\alpha)\,\frac{\partial \underline{\Sigma}_{\hat{x}}}{\partial \alpha} + \frac{\partial \underline{\Sigma}_{\hat{x}}}{\partial \alpha}\,(\underline{A} - \underline{B}\,\underline{G}_\alpha)^T = \underline{D} \tag{6.32}$$

where

$$\underline{D} \triangleq \underline{B}\,\underline{R}^{-1}\,\underline{B}^T\,\frac{\partial \underline{K}_\alpha}{\partial \alpha}\,\underline{\Sigma}_{\hat{x}} + \underline{\Sigma}_{\hat{x}}\,\frac{\partial \underline{K}_\alpha}{\partial \alpha}\,\underline{B}\,\underline{R}^{-1}\,\underline{B}^T \tag{6.33}$$

The matrix $\left.\frac{\partial \underline{\Sigma}_{\hat{x}}}{\partial \alpha}\right|_{\alpha=\bar{\alpha}}$ allows us to access the effect of stability factor on the noise covariance matrix $\underline{\Sigma}_{\underline{x}}$ at $\alpha = \bar{\alpha}$, If the ith diagonal

element of $\frac{\partial \Sigma_{\hat{x}}}{\partial \alpha}$ is positive, then the variance of the ith state will increase with α at $\alpha = \bar{\alpha}$. Likewise, if the ith element of $\frac{\partial \Sigma_{\hat{x}}}{\partial \alpha}\Big|_{\alpha=\bar{\alpha}}$ is negative, then the variance of the ith state will decrease with α, at $\alpha = \bar{\alpha}$. Since $(\underline{A} - \underline{B}\,\underline{G})$ is a stable matrix, we can thus conclude from the well known properties of algebraic Lyapunov equation that $\frac{\partial \Sigma_{\hat{x}}}{\partial \alpha}\Big|_{\alpha=\bar{\alpha}}$ is positive (negative) semidefinite (i.e the variance of all states increases (decreases) with α at $\alpha = \bar{\alpha}$), if the matrix $\underline{D}$ is negative (positive) semidefinite. If $\underline{D}$ turns out to be indefinite, the resulting $\frac{\partial \Sigma_{\hat{x}}}{\partial \alpha}\Big|_{\alpha=\bar{\alpha}}$ is also indefinite. In this case, the increase of α will increase the variance for some states and decrease that for others.

The following example is again based on LQG problem considered in Example 6.1. It demonstrates the behavior of $\Sigma_{\hat{x}}$ with increment of α.

Example 6.3 Consider the RPDS based LQG controller design problem in Example 6.1. The noise covariance matrix Σ_x is computed for the resulting designs at five different values of α and ρ is chosen to be 0 (see Table 6.3). It is clear from the tabulated results that the variance of the first state decreases with α while that of the second state increases with α.

6.3 Concluding Remarks

We have identified in this chapter several potential problems that may result from the use of robustness recovery procedure in design

α	$\underline{\Sigma}_{\underline{x}}$	
0	189.5 -554.9	- 554.9 1910.2
1.5	186.6 -554.9	-554.9 1930.2
4.5	177.4 -554.9	-554.9 2055.5
6.0	155.3 -554.9	-554.9 2550.1
9.0	139.7 -554.9	-554.9 3961.3

TABLE 6.3

Noise Covariance Matrices of the State Vector $\underline{x}(t)$ for Different Values of α; $\rho = 0$

of RPDS based LQG compensator. Too large a choice of the stability factor is found to prevent the recovery of the full state KBF stability margins with the Kwakernaak's procedure and slow down the rate of robustness recovery with the Doyle/Stein's procedure. However, it is important to point out that the result on rate of robustness recovery is obtained only for a particular single-input system. More practical experience with application of robustness recovery method to MIMO RPDS based LQG compensator design is needed before the nature of this problem can be fully comprehended.

CHAPTER VII

SUMMARY, CONCLUSIONS AND SUGGESTED DIRECTIONS FOR FUTURE RESEARCH

7.1 Summary

We have examined in this thesis a wide range of problems related to RPDS methodology and its applications. This includes attempts to

(i) explore the use of RPDS methodology for time-varying systems

(ii) adapt RPDS methodology for LQ regulator problem with design specifications other than prescribed degree of stability

(iii) develop methods of eigenstructure analysis for RPDS control systems

(iv) clarify the robustness properties of RPDS in the multiple-input case

(v) identify potential problems that may occur in the design of RPDS based LQG compensators.

We began our investigation in Chapter II with a formulation of the RPDS problem for linear time-varying systems. A generalized notion of 'degree of stability' that applies to all finite-dimensional linear systems is introduced. This definition has the desirable property that it reduces to characterization in terms of eigenvalues for the LTI systems. It turns out that the exponential weighting technique for solving the time-invariant RPDS problem is equally applicable to the time-varying

case. The related problem of designing Kalman Bucy filters with prescribed degree of stability (FPDS) is formulated and solved in a dual fashion. For case of LTI systems with stationary noises, the optimal filter solution admits interesting interpretations in terms of the special form of noise intensity matrices required for speeding up the error dynamics.

In Chapter III, several eigenstructure characterizations of the time-invariant RPDS are derived. The sensitivity equations for the RPDS poles are obtained in two different ways. The first approach is a direct application of the classical eigenvalue sensitivity result. The second approach utilizes the special eigenstructure properties of Hamiltonian System associated with RPDS problem. The computational requirements for these methods are briefly compared. Asymptotic behavior of the RPDS root-loci is studied next. It is shown that the properties of the RPDS root-loci can be readily derived from the optimal root-loci properties of a related LQ regulator problem. Based upon the behavior of RPDS poles as the control weighting on the states becomes vanishingly small, a novel algorithm for designing regulators with prescribed damping ratio (RPDR) is developed.

The important design issue of robustness is considered in Chapter IV. Based on the framework of frequency domain robustness analysis due to Lehtomaki [Le 1], various robustness properties of RPDS are characterized in terms of the minimum singular value of the RPDS return difference and inverse return difference matrices. In particular, the RPDS designs with $\underline{R}$ chosen to be diagonal are found to possess excellent gain and phase margins with respect to the stability and degree of stability property. However, tolerance of uncertainties for RPDS will improve

with increasing value of stability factor only for specific types of model error representation such as $\underline{E}_4(s) = (T^{-1}(s) - \tilde{\underline{T}}(s))\ \underline{T}^{-1}(s)$

Chapter V continues the discussion of Chapter IV with a multi-terminal DC/AC power system example. RPDS state feedback design for several choices of the stability factor α are applied to a 9-machine, 4 terminal DC/AC power network. Robustness properties of the closed-loop system thus obtained are evaluated in two ways. First, the closed-loop pole pattern results from change of operating points and introduction of unmodelled dynamics are studied. Second, the minimum singular value of the return difference and the inverse return difference matrices are computed and compared with the magnitude of the respective type of model errors as specified in the robustness tests of Chapter IV.

Output feedback realization of RPDS using LQG methods is considered in Chapter VI. In view of the lack of guaranteed stability margins for such compensators, only those RPDS based LQG control systems designed with the robustness recovery precedures are considered. Particularly, we examine the effect of α on the recovery of stability margins for full state feedback loop. It is found that too large a value of α may prevent the recovery of the KBF loop stability margin using Kwaakernaak's method and slow down the rate of recovering the RPDS stability margin using Doyle/Stein's method.

7.2 Conclusions

The major contributions of this thesis are basically of two categories. In the first category are results related to the extension of RPDS methodology. The classical RPDS problem formulation and its solution rechnique (due to Anderson and Moore) is found to be useful

for solving a number of RPDS related problems not previously considered in literature. These include

(i) the extension of exponential weighting technique to solution of the time-varying RPDS problem

(ii) the formulation of RPDR problem as a special case of RPDS problem

(iii) the adaptation of optimal root-loci results to RPDS root-loci

(iv) the adaptation of LQ eigenvalue sensitivity results to the respective problem of RPDS

While most of these results are of theoretical interest, those obtained for RPDS root-loci are also of importance from the design point of view. The contributions in the second category are mainly related to design implications of RPDS. While a large value of α can lead to regulators with good damping properties, other design considerations will put an upper limit on the actual value of α to be used. Some of such design considerations discussed in this thesis are

(i) effect of α on the cross-over frequency - too large a value of α may extend the cross-over frequency of RPDS well into regions dominated by unknown and/or unmodelled dynamics

(ii) effect of α on robustness properties - increasing the value of α will lead to improvement in tolerance of modelling error only in very specific context. In other words, such improvement is only valid for certain type of model error representations. For instance, we have demonstrated that the guaranteed stability margins of a RPDS may in fact deteriorate with increasing value of α.

(iii) effect of the stability factor α on robustness recovery of LQG - too large a choice of α may lead to failure in recovering the KBF loop with Kwakernaak's procedure and impede the rate of recovery of RPDS stability margin with Doyle/Stein's procedure.

To summarize, RPDS method is not merely a procedure to be used blindly for design of fast response sytems. It is clear from our discussions in Chapters IV, V and VI that a fair amount of iteration on the design of RPDS, with due regard given to various design considerations such as stability robustness and noise rejection is necessary to obtain satisfactory results.

Like the LQ regulator method of which it is a special case, the RPDS design procedure is basically a multi-loop procedure. With the aid of the various recently developed frequency domain tools (such as the singular value-based robustness tests for MIMO systems and the robustness recovery procedures), it should provide a reasonable starting place to design feedback systems with a prescribed degree of stability.

7.3 Suggestions for Future Research

Due to the lack of time, we were not able to pursue in depth the many interesting avenues of research opened up by this work. As suggestion for future research, we list the following:

(i) The effect of the stability factor on the tolerance of structured model errors

The robustness tests considered in this thesis use only the magnitude information of the error. As a result, they can be unduly conservative

in that some of the small pertubations that will theoretically destabilize the system will not occur physically. These tests can be further refined to take into account the difference between model errors that increase the stability margins of the feedback systems and those that decrease it (see [Le 1] Chapter 4). A useful avenue of research is to study the effect of α on the robustness properties of RPDS when structural information of the error $\underline{E}(s)$ (i.e. numerical relations among elements of $\underline{E}(s)$) is taken into account.

(ii) Discrete Time RPDS

The formulation and solution of discrete time RPDS problems have been considered by several authors ([Sa 2], [An 2]). In the LTI case, the corresponds to picking a state feedback gain G_α such that the quadratic performance index

$$J = \sum_{n=0}^{\infty} \alpha^{2n} [\underline{x}^T(n) \tilde{\underline{Q}} \underline{x}(n) + 2 \underline{u}^T \tilde{\underline{M}} \underline{x}(n) + \underline{u}^T(n) \tilde{\underline{R}} \underline{u}(n)] \tag{7.1}$$

is minimized subject to

$$\underline{x}(n+1) = \underline{A} \underline{x}(n) + \underline{B} \underline{u}(n) \qquad n = 0,1,2,\ldots \tag{7.2}$$

where $\tilde{\underline{Q}}$, $\tilde{\underline{M}}$, $\tilde{\underline{R}}$ are some weighting matrices having the property that $\begin{bmatrix} \tilde{\underline{Q}} & \tilde{\underline{M}}^T \\ \tilde{\underline{M}} & \tilde{\underline{R}} \end{bmatrix}$ is positive definite, and $\alpha \geq 1$ is the stability factor. Provided that the system is controllable and cost observable, then the optimal state feedback gain is given by [Sa 2]

$$G_\alpha = (\tilde{\underline{R}} + \underline{B}^T \underline{K}_\alpha \underline{B})^{-1} (\underline{B}^T \underline{K}_\alpha \underline{A} + \tilde{\underline{M}}) \tag{7.3}$$

where $\underline{K}_\alpha$ is the unique symmetric positive definite solution of the discrete RPDS Riccati equation

$$\underline{K}_\alpha = \alpha^2[\underline{A}^T \underline{K}_\alpha \underline{A} + \tilde{\underline{Q}} - (\underline{B}^T \underline{K}_\alpha \underline{A} + \tilde{\underline{M}})^T (\tilde{\underline{R}} + \underline{B}^T \underline{K}_\alpha \underline{B}) (\underline{B}^T \underline{K}_\alpha \underline{A} + \tilde{\underline{M}})] \tag{7.4}$$

The eigenstructure and robustness properties for this class of regulators have not been treated in the literature thus far. In view of the similarity in structure between the continuous time and the discrete time RPDS problem, we expect the eigenstructure characterization of discrete time RPDS to follow from that of continuous time RPDS given in Chapter III.

The generality of the framework for robustness analysis developed in [Le 1](which we have extensively applied in Chapter IV) also allows us to characterize the robustness properties of discrete time RPDS in terms of the minimum singular value of its return difference and inverse return difference matrices. The derivation of the respective robustness theorems are based on the discrete multivariable Nyquist theorem, which is essentially identical to Theorem 4.1 with the Nyquist contour replaced by the unit circle centered at the origin. Based on such a framework, the effect of α on the robustness properties of discrete time RPDS can be studied in a fashion similar to that of Chapter IV.

A significant difference between the continuous time and discrete time RPDS occurs when one tries to solve the discrete time RPDS problem using only time-invariant weighting matrices (compare with corollary 2.5). It can be readily shown by algebraic manipulation of the discrete Riccati equation (7.4) that an appropriate choice of constant matrices $\underline{Q}$, $\underline{M}$ and

$\underline{R}$ for such purpose is given by

$$\underline{Q} = \tilde{\underline{Q}}\,\alpha^2 + (\alpha^2 - 1)\underline{A}^T \underline{K}_\alpha \underline{A} \tag{7.6}$$

$$\underline{M} = \tilde{\underline{M}}\,\alpha^2 + (\alpha^2 - 1)\underline{B}^T \underline{K}_\alpha \underline{A} \tag{7.7}$$

$$\underline{R} = \tilde{\underline{R}}\,\alpha^2 + (\alpha^2 - 1)\underline{B}^T \underline{K}_\alpha \underline{B} \tag{7.8}$$

where $\underline{K}_\alpha$ is the unique positive definite solution of the algebraic Riccati equation. The intresting point to observe is the expression for $\underline{M}$ as given by (7.7). $\underline{M}$ turns out to be a nonzero matrix even if the cross-weighting matrix $\tilde{\underline{M}}$ in the time-varying cost functional (7.1) is chosen to be zero. In the dual problem of FPDS design, this implies the need to use correlated process noise and observation noise that are second order stationary. A proper explanation of the above observation is not obvious. Understanding of this problem is probably important to a better appreciation of the robustness properties of discrete time RPDS, for it is well known in the case of continuous time optimal regulators that the use of cross-weighting matrix between $\underline{u}(t)$ and $\underline{x}(t)$ can lead to deterioration of the stability margins.

(iii) Alternative formulation of the Regulators with Prescribed Damping Ratio (RPDR) problem.

In Chapter III of this report, the RPDR problem is formulated and solved as a special case of the RPDS problem. It is of interest to know if there exists a more direct approach to formulate and solve the RPDR problem.

REFERENCES

[An 1] B.D.O. Anderson and B.C. Moore, Linear Optimal Control, Englewood Cliffs, N.J., Prentice-Hall, 1971.

[An 2] B.D.O. Anderson and B.C. Moore, Optimal Filtering, Englewood Cliffs, N.J., Prentice-Hall, 1979.

[Ath 1] M. Athans, "The Role and Use of the Stochastic Linear-Quadratic-Guassian Problem in Control System Design," IEEE Trans. Auto. Control, Vol. AC-16, No. 6, pp. 529-551, Dec. 1971.

[Bo 1] H.W. Bode, Network Analysis and Feedback Amplifier Design, New York, Von Nostrand, 1945.

[Br 1] R.W. Brockett, Finite Dimensional Linear Systems, New York, Wiley, 1970.

[Ch 1] S.M. Chan, Small Signal Control of Multiterminal DC/AC Power Systems, Ph.D. Thesis, Department of Electrical Engineering and Computer Science, Massachusetts Institute of Technology, Cambridge, Mass., May 1981.

[Cha 1] S.S.L. Chang, Synthesis of Optimal Control Systems, New York, MrGraw Hill, 1961.

[De 1] C.A. Desoer and M. Vidyasagar, Feedback Systems: Input-Output Properties, New York, Academic Press, 1975.

[Do 1] J.C. Doyle and G. Stein, "Robustness with Observers," IEEE Trans. Auto. Control, Vol. AC-24, No.4, pp.607-610, Aug. 1979.

[Do 2] J.C. Doyle, "Robustness of Multi-Loop Linear Feedback Systems," in Proc. 1978 IEEE Conf. on Decision and Control, San Diego, Ca., Jan. 10-12, 1979.

[Do 3] J.C. Doyle and G. Stein, "Multivariable Feedback Design: Concepts for a Classical/Modern Synthesis," IEEE Trans. Auto.Control, Vol. AC-26, No.1, pp. 4-16, Feb. 1981.

[Do 4] J.C. Doyle, "Guaranteed Margins for LQG Regulator," IEEE Trans. Auto. Control, Vol. AC-23, pp. 756-757, Aug. 1978.

[Gr 1] C.E. Grund, R.L. Hauth, F. Nozari, J.R. Winkleman, S.M. Chan, N.A. Lehtomaki, M. Athans and N.R. Sandell, Jr., "Integration and Control of Multi-Terminal HVDC Systems Embedded in AC Networks," Topical Report, EUSED, General Electric Company, Schenectady, N.Y., 12345, April 1980.

[Ha 1] C.A. Harvey and G. Stein, "Quadratic Weights for Asymptotic Regulator Properties," IEEE Trans. Auto. Control, Vol. AC-23, No. 3, pp. 378 - 387, June 1978.

[Ho 1] J.M. Horowitz, Synthesis of Feedback Systems, New York,, Academic Press, 1963.

[Ka 1] R.E. Kalman, "When is a Linear System Optimal?", Trans. ASME Ser. D: J. Basic. Eng., Vol. 86, pp. 51-60, March 1964.

[Kw 1] H. Kwakernaak and R. Sivan, Linear Optimal Control Systems, New York, Wiley Interscience, 1972.

[Kw 2] H. Kwakernaak, "Asymptotic Root-Loci for Multivariable Linear Optimal Regulators," IEEE Trans. Auto. Control, Vol. AC-23, No. 3, June 1978.

[Kw 3] H. Kwakernaak, "Optimal Low-Sensitivity Linear Feedback Systems," Automatica, Vol. 5, May 1969.

[Le 1] N.A. Lehtomaki, Practical Robustness Measures in Multivariable Control System Analysis, Ph.D. Thesis, Dept. of Electrical Engineering and Computer Science, M.I.T., Cambridge, Ma., May 1981.

[Le 2] N.A. Lehtomaki, N.R. Sandell, Jr., and M. Athans, "Robustness Results in Linear-Quadratic-Guassian Based Multivariable Control Designs," IEEE Trans. Auto.Control, Vol. AC-26, No.1, pp.75-92, Feb. 1981.

[Nu 1] D.U. Nuzman and N.R. Sandell, Jr., "An Inequality Arising in Robustness Analysis of Multivariable Systems," IEEE Trans. Auto.Control, Vol.1,AC-24, No.3, pp. 492-493, June 1979.

[Ro 1] H.H. Rosenbrock, "Design of Multivariable Control Systems Using Inverse Nyquist Array," Proc. IEEE, Vol. 116, pp. 1929-1936, Nov. 1969.

[Sa 1] M.G. Safonov, A.J. Laub and G.L. Hartmann, "Feedback Properties of Multivariable Systems: The Role and Use of Return Difference Matrix," IEEE Trans. Auto. Control, Vol. AC-26, No.1, Feb. 1981.

[Sa 2] M.G. Safonov, Robustness and Stability Aspects of Stochastic Multivariable Feedback System Design, M.I.T. Press, 1980.

[Sa 3] M.G. Safonov and M. Athans, "Gain and Phase Margins for Multi-Loop LQG Regulators, "IEEE Trans. Auto.Control, Vol. AC-22, No. 2, pp. 94-99, April 1977.

[Sc 1] F.C. Schweppe, Uncertain Dynamic Systems, Englewood Cliffs, N.J., Prentice-Hall, 1973.

August, 1981 LIDS-TH-1129

ON REGULATORS WITH A PRESCRIBED DEGREE OF STABILITY

by

PENG-TENG PETER NG

This report is based on the unaltered thesis of Peng-Teng Peter Ng, submitted in partial fulfillment of the requirements for the degree of Master of Science at the Massachusetts Institute of Technology, July 1981. The research was conducted at the M.I.T. Laboratory for Information and Decision Systems, with support provided by the NASA Ames Research Center under grant NGL-22-009-124 and the U.S. Department of Energy under contract DOE/DE-AC01-78RA03395.

Laboratory for Information and Decision Systems
Massachusetts Institute of Technology
Cambridge, Massachusetts 02139

[So 1] O.A. Solheim, "Design of Optimal Control Systems with Prescribed Eigenvalues," Int. J. Control, Vol. 15, No.1, pp.143-160, 1972.

[St 1] G. Stein, "Generalized Quadratic Weights for Asymptotic Regulator Properties," IEEE Trans. Auto. Control, Vol. AC-25, No. 4, pp. 559-566, Aug. 1979.

[Str 1] G. Strang, Linear Algebra and Its Applications, New York, Academic Press 1976.

[Th 1] P.M. Thompson, Linear State Feedback, Quadratic Weights and Closed-Loop Eigenstructures, S.M. Thesis, Dept. of Electrical Engineering and Computer Science, M.I.T., Cambridge, MA, June 1979.